

University of Nevada, Reno

**Osmotically-Driven Membrane Processes for Water
Reuse and Energy Recovery**

A dissertation submitted in partial fulfillment of the requirements for the degree
of Doctor of Philosophy in Civil and Environmental Engineering

by
Andrea Achilli

Dr. Amy E. Childress and Dr. Eric A. Marchand / Dissertation Advisors

August 2009



THE GRADUATE SCHOOL

We recommend that the dissertation
prepared under our supervision by

ANDREA ACHILLI

entitled

Osmotically-Driven Membrane Processes For Water Reuse And Energy Recovery

be accepted in partial fulfillment of the
requirements for the degree of

DOCTOR OF PHILOSOPHY

Amy E. Childress, Ph.D., Advisor

Eric A. Marchand, Ph.D., Committee Member

Tzahi Y. Cath, Ph.D., Committee Member

Keith E. Dennett, Ph.D., Committee Member

Do-Hwan Park, Ph.D., Committee Member

Scott W. Tyler, Ph.D., Graduate School Representative

Marsha H. Read, Ph. D., Associate Dean, Graduate School

August, 2009

ABSTRACT OF THE DISSERTATION

Osmotically-Driven Membrane Processes for Water Reuse and Energy Recovery

by

Andrea Achilli

Doctor of Philosophy in Civil and Environmental Engineering

University of Nevada, Reno, 2009

Professor Amy E. Childress, Chair

Osmotically-driven membrane processes are an emerging class of membrane separation processes that utilize concentrated brines to separate liquid streams. Their versatility of application make them an attractive alternative for water reuse and energy production/recovery.

This work focused on innovative applications of osmotically-driven membrane processes.

The novel osmotic membrane bioreactor (OMBR) system for water reuse was presented. Experimental results demonstrated high sustainable flux and relatively low reverse diffusion of solutes from the draw solution into the mixed liquor. Membrane fouling was minimal and controlled with osmotic backwashing. The OMBR system was found to remove greater than 99% of organic carbon and ammonium-nitrogen.

Forward osmosis (FO) can employ different draw solution in its process. More than 500 inorganic compounds were screened as draw solution candidates, the desktop screening process resulted in 14 draw solutions suitable for FO applications. The 14 draw solutions were then tested in the laboratory to evaluate water flux and reverse salt

diffusion through the membrane. Results indicated a wide range of water flux and reverse salt diffusion depending on the draw solution utilized. Internal concentration polarization was found to lower both water flux and reverse salt diffusion by reducing the draw solution concentration at the interface between the support and dense layer of the membrane. A small group of draw solutions was found to be most suitable for FO processes with currently available FO membranes.

Another application of osmotically-driven membrane processes is pressure retarded osmosis (PRO). PRO was investigated as a viable source of renewable energy. A PRO model was developed to predict water flux and power density under specific experimental conditions. The predictive model was tested using experimental results from a bench-scale PRO system. Previous investigations of PRO were unable to verify model predictions due to the lack of suitable membranes and membrane modules. In this investigation, for the first time, the use of a custom-made laboratory-scale membrane module enabled the collection of experimental PRO data. Results obtained with a flat-sheet cellulose triacetate FO membrane and NaCl feed and draw solutions closely matched model predictions. Power density was substantially reduced due to internal concentration polarization in the asymmetric membrane and, to a lesser degree, to salt passage. External concentration polarization was found to exhibit a relatively small effect on reducing the osmotic pressure driving force. Using the predictive PRO model, optimal membrane characteristics and module configuration can be determined in order to design a system specifically tailored for PRO processes.

AKNOWLEDGEMENTS

My deepest gratitude goes to my major advisor Prof. Amy Childress for her patience and constant encouragement during these years. I am grateful to my co-advisor Prof. Eric Marchand for his guidance and his advices. I also want to thank Prof. Tzahi Cath and my other committee members, Prof. Keith Dennett, Prof. Do-Hwan Park, and Prof. Scott Tyler for their support, inspiration and constant enthusiasm for my research.

Thank you, Ryan Holloway for your friendship, for being there in the early days, and for your wise advice. Thank you, Riz Martinetti for being always there in helping and assisting in so many ways. Thank you, Mirinda Hutton for all your support. And thank you Kerri Hickenbottom for your high-quality work and dedication to the research and for all your encouragement, help, and support during these years.

TABLE OF CONTENTS

1	INTRODUCTION	1
1.1	Problem statement and significance.....	1
1.2	Membrane bioreactors	1
1.3	The novel osmotic membrane bioreactor.....	3
1.4	Draw solution selection.....	5
1.5	Pressure retarded osmosis.....	7
1.6	Objectives	8
1.6.1	OMBR.....	8
1.6.2	Draw solution selection.....	9
1.6.3	PRO.....	9
1.7	Dissertation organization	10
2	THE FORWARD OSMOSIS MEMBRANE BIOREACTOR: A LOW FOULING ALTERNATIVE TO MBR PROCESSES.....	16
2.1	Introduction.....	17
2.2	Materials and methods	21
2.2.1	FO Membranes.....	21
2.2.2	Batch abiotic experiments.....	21
2.2.3	Continuous-flow OMBR experiments	23
2.2.4	Cleaning experiments.....	25
2.2.5	Analytical Methods.....	26
2.3	Results and discussion	26
2.3.1	Batch experiments.....	26
2.3.2	Continuous-flow OMBR experiments	28
2.4	Conclusions.....	36
3	SELECTION OF INORGANIC-BASED DRAW SOLUTIONS FOR OSMOTICALLY-DRIVEN MEMBRANE PROCESSES	41
3.1	Introduction.....	42
3.2	Materials and methods	48
3.2.1	Draw solution selection criteria	48
3.2.2	FO Membrane	50
3.2.3	Solution chemistries.....	50
3.2.4	FO membrane permeability characterization.....	51
3.2.5	FO performance experiments.....	52
3.2.6	Analytical methods	55

3.2.7	RO reconcentration evaluation	55
3.3	Results and discussion	56
3.3.1	Water flux	56
3.3.2	Salt diffusion	57
3.3.3	Reverse osmosis reconcentration	61
3.3.4	Draw solution costs	62
3.3.5	Is there a best draw solution?	64
3.4	Conclusions	67
4	POWER GENERATION WITH PRESSURE RETARDED OSMOSIS:	73
4.1	Introduction	74
4.2	Theory	77
4.2.1	Osmotic processes	77
4.2.2	Salt permeability	79
4.2.3	Concentration polarization	80
4.2.4	External concentration polarization in PRO	81
4.2.5	Internal concentration polarization in PRO	82
4.2.6	Water flux in PRO	83
4.2.7	Power density in PRO	84
4.3	Experimental	85
4.3.1	Membranes	85
4.3.2	Solution chemistries	85
4.3.3	RO experiments	86
4.3.4	PRO experiments	87
4.4	Results and discussion	90
4.4.1	Determination of membrane characteristics (A and B)	90
4.4.2	Calculations of mass transport coefficient (k)	92
4.4.3	Determination of solute resistivity (K)	92
4.4.4	PRO model results	93
4.4.5	PRO experimental results	99
4.5	Conclusions	104
5	CONCLUSIONS	110
5.1	Research Synopsis	110
5.2	Summary of evaluation of OMBR	110
5.3	Summary of evaluation of inorganic-based draw solutions for forward osmosis applications	111
5.4	Summary of evaluation of pressure retarded osmosis to produce renewable energy	112
5.5	Environmental significance	113

LIST OF FIGURES

Figure 2.1	Schematic diagram of an OMBR system.....	20
Figure 2.2	Schematic diagram of the batch laboratory-scale OMBR apparatus.....	22
Figure 2.3	Schematic diagram of the continuous-flow laboratory-scale OMBR apparatus.....	23
Figure 2.4	Water flux as a function of DS concentration for batch FO experiments with three CTA membranes.....	27
Figure 2.5	Reverse salt diffusion as a function of DS concentration for batch FO experiments with three CTA membranes.....	28
Figure 2.6	Water flux through the FO membrane and salt concentration in the bioreactor as a function of time for continuous-flow experiments with membrane B. Osmotic backwashings (OBW) are indicated at 14, 21, and 28 d.....	31
Figure 2.7	Water fluxes of membrane B. Comparison between water flux for the new membrane, and before/after osmotic backwashing at 14, 21, and 28 d. The concentration of the draw solution was 50 g NaCl/L.....	32
Figure 2.8	Reverse salt diffusion through membrane B. Comparison between reverse salt diffusion for the new membrane, and before/after osmotic backwashing at 14, 21, and 28 d. The concentration of the draw solution was 50 g NaCl/L.....	33
Figure 3.1	Illustration of an asymmetric membrane with the dense layer facing the feed solution and concentration profiles across the membrane. Internal concentration polarization (ICP) is also shown. The feed concentration is DI water so no external concentration polarization occurs. The osmotic pressures corresponding to $C_{F,b}$, $C_{D,i}$, and $C_{D,b}$ are denoted as $\pi_{F,b}$, $\pi_{D,i}$, and $\pi_{D,b}$	45
Figure 3.2	Illustration of flow diagram for draw solution selection.....	49
Figure 3.3	Schematic of bench-scale FO system.....	52
Figure 4.1	Schematic of a pressure-retarded osmosis (PRO) power plant. Figure adapted from Ref. [3].....	75
Figure 4.2	Representation of solvent flow in FO, PRO, and RO. Membrane orientation is indicated in each system by the thick black line representing the membrane dense layer.....	78
Figure 4.3	Magnitude and direction of J_w for FO, PRO, and RO and magnitude of W for PRO is shown. Figure adapted from Ref. [17].....	79
Figure 4.4	Illustration of osmotic driving force profiles for an asymmetric membrane with the dense layer facing the draw solution (PRO mode). Internal and external concentration polarization are also shown.....	81

Figure 4.5	Schematic of bench-scale PRO system.....	88
Figure 4.6	Water flux (J_w) as a function of applied hydraulic pressure (ΔP) during the RO experiment performed to determine <i>A</i> . Feed solution was DI water and temperature was 25 °C.....	91
Figure 4.7	Water flux (J_w) as a function of elapsed time during the RO experiment performed to determine <i>B</i> . Feed solution was 2 g/L NaCl, hydraulic pressure was 1,035 kPa, and temperature was 25 °C.....	91
Figure 4.8	Model results for water flux (J_w) and power density (W) as a function of applied hydraulic pressure (ΔP). Draw solution concentrations are (a) 35 g/L NaCl (2,763 kPa) and (b) 60 g/L NaCl (4,882 kPa).....	94
Figure 4.9	Model results for water flux (J_w) and power density (W) as a function of applied hydraulic pressure (ΔP) for different feed and draw solution concentrations.	97
Figure 4.10	Experimental results for water flux (J_w) and power density (W) as a function of applied hydraulic pressure (ΔP) (points) compared with model results (lines) under different feed and draw solution concentrations. Temperature was 25 °C.....	101
Figure 4.11	Model results for maximum power density (W_{max}) as a function of water permeability (A), mass transfer coefficient (k), and solute resistivity (K). Results illustrates W_{max} achievable with DI water feed solution and 35 g/L NaCl draw solution concentration at a hydraulic pressure of 1300 kPa.	103
Figure 5.1	Schematic diagram of an open-loop OMBR system.....	114
Figure 5.2	Schematic diagram of a ProMBR system.	115
Figure 5.3	Experimental results for power density as a function of applied hydraulic pressure with activated sludge feed solution (points) compared with model results (line) with DI water feed solution. Draw solution concentration was 35 g/L NaCl. Activated sludge feed concentration was 5.5 g MLSS/L. Temperature was 25 °C.....	116
Figure 5.4	Experimental results for water flux as a function of time. Draw solution concentration was 35 g/L NaCl. Activated sludge feed concentration was 5.5 g MLSS/L. Temperature was 25 °C.....	117
Figure 5.5	Schematic diagram of an RO/ProMBR system.	117

LIST OF TABLES

Table 2.1	TOC and NH_4^+ -N concentrations at various locations in the OMBR system.	29
Table 2.2	TOC and NH_4^+ -N removal efficiencies at various stages of the OMBR system.	29
Table 2.3	Operation comparison between conventional MBRs and the OMBR process.....	35
Table 2.4	TOC removal efficiencies of conventional MBR membranes and the FO membrane in the OMBR system.....	36
Table 3.1	Aqueous solution osmotic pressure (π_{DS}), concentration (C_{DS}), solubility, and diffusion coefficient (D).....	54
Table 3.2	Water flux (J_w), solute resistivity (K), and structural characteristic of the membrane support layer ($t\tau/\epsilon$) for each draw solution tested.....	58
Table 3.3	Reverse salt diffusion (J_s), water flux (J_w), effective osmotic pressure ($\pi_{D,i}$), effective draw solution concentration ($C_{D,i}$), ratio between reverse salt diffusion and effective draw solution concentration ($J_s/C_{D,i}$), and ratio between reverse solute diffusion and water flux (J_s/J_w).....	60
Table 3.4	Calculated RO permeate water concentrations using ROSA and IMSDesign software. Average RO permeate water concentrations are also reported.	62
Table 3.5	Draw solute specific cost. Specific cost is defined as the cost of solute needed to produce 1 L of draw solution with an osmotic pressure of 2800 kPa.....	63
Table 3.6	Draw solute replenishment cost. Replenishment cost is the product between the specific salt diffusion and the draw solution cost for FO and between the permeate concentration and the draw solution cost for RO. Total cost is the sum of the two.	63
Table 3.7	Ratios between the best draw solution and the draw solution itself for each of the five parameters investigated. Each draw solution was evaluated at an osmotic pressure of 2800 kPa.	65
Table 4.1	NaCl aqueous solution characteristics	86
Table 4.2	PRO experiment conditions	90
Table 4.3	Mass transfer coefficient (k) at various draw solution concentrations	92
Table 4.4	Solute resistivity (K) at various draw solution concentrations with DI water as feed solution.....	93
Table 4.5	Solute resistivity (K) at various feed solution concentrations	93

Table 4.6	Comparison between power density results from the literature and from the current study.....	102
-----------	--	-----

Chapter 1

1 INTRODUCTION

1.1 Problem statement and significance

Water scarcity and environmental impacts of energy use are issues rapidly growing in today's world [1]. Water and energy are intrinsically linked; both are required to maintain adequate standard of living. Water sustainability is essential for meeting human needs for drinking water and sanitation in both developing and developed countries. High-quality reuse, supplemental decentralization, and low energy consumption are key objectives to achieving sustainability in wastewater treatment [2]. In terms of energy, the continuous dependence on fossil fuel combustion is accelerating changes in our climate toward dangerous long-term effects. Sustainable sources of energy production must be studied as many of the currently available alternatives are inadequate to replace current and future fossil fuel use [3].

1.2 Membrane bioreactors

Consideration of water sustainability has led to the development of new and adapted technologies in order to balance societal needs with the protection of natural systems. Membrane bioreactors (MBRs) are one such technology and they are attractive for domestic wastewater treatment as they have the potential to produce high quality effluent with low energy consumption [2, 4, 5]. In a submerged MBR, microporous (microfiltration (MF) or ultrafiltration (UF)) membranes are immersed in a bioreactor and water is filtered through the membranes using vacuum; suspended solids are retained in the system and high levels of treatment (including nutrient removal) can be achieved [6]. The MBR replaces the two stages of the conventional activated sludge process

(biotreatment and clarification) with a single, integrated process. MBR effluent may be suitable for use as irrigation water, process water, or a source of potable water. For potable reuse (e.g., indirect reuse through aquifer recharge), advanced treatment (e.g., reverse osmosis (RO), nanofiltration (NF), or chemical oxidation) is necessary after the MBR [7]. The advantages of MBRs over conventional treatment have been thoroughly reviewed [5] and they include product water consistency, reduced footprint, reduced sludge production due to a high biomass concentration in the bioreactor, and essentially complete suspended solids removal from the effluent. The main problem associated with MBRs is membrane fouling. Fouling reduces permeate flux and increases the frequency of membrane cleaning and replacement [8]. Membrane fouling can occur in the MBR itself, and also in the downstream RO system [9]. Specifically, high concentrations of dissolved organic compounds in the MBR effluent can cause severe fouling of RO membranes; this leads to reduction of water flux and deterioration of treated water quality [10].

In order to operate conventional MBRs at constant flux, physical membrane cleaning techniques are utilized; they include backwashing, relaxation, or a combination of the two, depending on the membrane configuration (flat-sheet or tubular). Chemicals are often added to enhance physical cleaning [11]. During backwashing, the permeate is pumped in the opposite direction through the membrane to effectively remove most of the reversible fouling due to pore blocking. The efficiency of backwashing has been studied in detail and the key parameters have been found to be frequency, duration, and intensity [12-14]. During membrane relaxation, permeate suction is stopped and the back-transport of foulants is naturally enhanced as reversibly attached foulants diffuse away

from the membrane surface due to the concentration gradient. Tubular and hollow fibers membranes undergo regular backwashing and sometimes relaxation [12-16]. Flat-sheet membranes cannot be backwashed due to their inability to withstand pressure in the opposite direction of the operating flow; for this reason, relaxation is used to control the fouling of these membranes [8]. Membrane cleaning markedly affects energy requirements, operational and capital costs, system productivity, and membrane integrity of MBR systems [11].

1.3 The novel osmotic membrane bioreactor

The osmotic membrane bioreactor (OMBR) is a novel hybrid process that utilizes a submerged forward osmosis (FO) membrane in the bioreactor. In an OMBR system (OMBR followed by RO) the high rejection of the FO membrane will result in an RO influent with lower fouling propensity and may lead to a higher quality RO product water compared to a conventional MBR followed by RO. Also, the FO-followed-by-RO treatment scheme represents a dual osmotic barrier system. This is particularly important when low molecular weight organics are present. These organics typically have 40-60% rejection rates through osmotic (e.g., RO) membranes. For this reason, the industry standard is to follow the RO process with advanced oxidation. However, it is possible that the removal of these organics in the OMBR system (which includes two osmotic membrane barriers (FO and RO)) will make the use of a subsequent advanced oxidation process unnecessary. Furthermore, in FO membrane processes, osmotic backwashing can be performed to remove foulants from the surface of the membrane. During osmotic backwashing, water flows from the support side of the membrane to the active side,

thereby reversing the direction of flow through the FO membrane and potentially removing foulants [17, 18]. Compared to conventional membrane cleaning and relaxation technologies, osmotic backwashing may reduce energy requirements and costs, and improve system productivity.

In order to understand the OMBR process, it is helpful to first understand FO. FO is the engineered application of osmosis [19-23]. In FO, impaired water is in contact with the active side of the membrane and a highly concentrated draw solution is in contact with the support side of the membrane. During the process, the impaired water is concentrated and the draw solution is diluted. A desalination process (e.g., RO or distillation) can be used to reconcentrate the draw solution and thus supply draw solution at constant concentration to the FO process and simultaneously produce high-quality product water. Thus, in most water treatment applications, FO is not the ultimate process but rather a high-level pretreatment step before an ultimate reconcentration/desalination process. The main advantage of FO is that it operates at very low hydraulic pressure, it has high rejection of a wide array of contaminants, and it may have lower fouling propensity than pressure-driven membrane processes [17, 24, 25].

In an OMBR system, wastewater is fed into a reactor which is continuously aerated to supply oxygen for the biomass and to scour the membrane. Through osmosis, water diffuses from the bioreactor, across a semi-permeable membrane, and into a lower water chemical potential draw solution. The FO membrane acts as a barrier to solute diffusion and provides high rejection of the contaminants in the wastewater stream [21, 24, 26]. The diluted draw solution is sent to a reconcentration process (e.g., RO or distillation) which reconcentrates the draw solution and generates a high-quality product

water.

1.4 Draw solution selection

A key consideration in optimizing an OMBR system is selection of the best draw solution [22]. The main criterion is that the draw solution has a higher osmotic pressure than the feed solution. Another important criterion in some FO applications is the availability of a suitable process for reconcentration of the draw solution after it has been diluted in the FO process. The reconcentration process should achieve high recovery of the draw solution to minimize losses, be affordable, and be able to produce high-quality product water. For example, when considering FO for production of potable water, it is important that draw solution solutes not be present in the final product water, and if trace concentrations are present, they should be below the drinking water maximum contaminant level. Other considerations for selection of suitable draw solution are that it is not toxic, it can be safely handled, and that the cost of the draw solution is low enough to ensure economic-viability of the process.

Often NaCl solutions are used as the draw solution in FO investigations [17, 21, 25-27]. NaCl is highly soluble, not toxic at low concentrations, and relatively easy to reconcentrate to high concentrations using conventional desalination processes (e.g., RO or distillation) without risk of scaling [22]. Other chemicals (e.g., CaCl_2 or $\text{Ca}(\text{NO}_3)_2$) have also been suggested and tested as draw solutes [17, 19, 21, 25-30]. For all the draw solutions tested, concentration polarization is also an important consideration.

Concentration polarization is the accumulation or depletion of solutes near the membrane surface. In FO, when water diffuses through the membrane, feed solution solutes are concentrated on the feed/dense surface of the membrane and draw solution solutes are

diluted on the permeate/support surface of the membrane. Thus, concentration polarization occurs externally on the active layer side and internally in the support layer side of the membrane.

Recent investigations have established that internal concentration polarization is a major factor in limiting water flux in osmotically-driven membrane processes [31-34]. There is agreement that internal concentration polarization is influenced by the structure (thickness, tortuosity, and porosity) of the membrane support layer and by the diffusion coefficient of the draw solution. However, there is not unanimous agreement as to whether internal concentration polarization is influenced by the diffusion coefficient of the draw solution. McCutcheon et al. [31] present a model developed by Lee et al. [34] in which the membrane support layer characteristics and the solution diffusion coefficient contribute to internal concentration polarization, while Tan and Ng [32] suggest that internal concentration polarization is influenced by the membrane characteristics only. In these investigations, NaCl was the only draw solution evaluated.

Membranes for osmotically-driven processes are also prone to reverse salt diffusion, where a small amount of salt permeates the membrane from the draw solution to the feed solution [35]. Reverse salt diffusion is expected to occur because of the large difference in solute concentration between the draw solution and the feed solution. Internal concentration polarization may influence the rate of reverse salt diffusion by lowering the effective solute concentration at the interface between the dense and the support layer of the membrane, reducing the solute diffusion driving force [35]. In the OMBR process, reverse salt diffusion will result in accumulation of salt inside the

bioreactor and, depending on its concentration, may inhibit or have toxic effects on the microbial community in the reactor.

1.5 Pressure retarded osmosis

Pressure retarded osmosis (PRO) is an engineered osmotic process that, as a viable source of renewable energy [43-45], can contribute to a more sustainable energy future. In a PRO system, water from a low salinity feed solution (e.g., fresh water) permeates through a membrane into a pressurized, high salinity brine/draw solution (e.g., seawater); power is obtained by depressurizing a portion of the diluted seawater through a hydroturbine [36]. It is estimated that the global energy production potential of PRO is on the order of 2,000 TWh per year [37], while the estimated global energy production from all renewable sources is approaching 10,000 TWh per year [38].

The concept of harvesting energy generated during mixing of fresh and salt water was developed in the mid 1950s [39]. Following the 1973 oil crisis, the interest in PRO for power generation spiked and led to several investigations of the technical [40-42] and economic feasibility [42, 43] of PRO. Loeb and coworkers began publishing results from PRO experiments in 1976 [44]. They utilized hollow-fiber seawater RO membranes enclosed in a “minipermeator” (Permasep B-10). A pressurized brine flowed on the shell side of the bundle of hollow-fiber membranes and the fresh water flowed through the bore. Further investigations of Loeb and Mehta [45], Mehta and Loeb [46, 47], and Jellinek and Masuda [48] revealed power outputs far below the expected outputs; likely due to the use of RO membranes and membrane modules that were designed for seawater desalination. It was determined that seawater RO membranes were not suitable for FO

and PRO applications due to their hydrophobicity and thick support layer [49]. Furthermore, it was found that existing membrane modules did not allow for high cross-flow velocity on the membrane surface [31]. Thus, the lack of suitable membranes and modules hindered the efforts to establish this technology [50]. Also, during this time, a few models were proposed to predict flux and pressure behavior in PRO [34, 45, 47]; however, it was difficult to validate these models because of the lack of suitable membranes and membrane modules. For example, Lee and coworkers [34] were only able to validate their model under FO and RO conditions.

1.6 Objectives

The overall goal of this research was to explore the use of osmotically-driven membrane processes for water reuse and energy production. The use of forward osmosis in conjunction with a bioreactor and the feasibility of pressure retarded osmosis were investigated.

1.6.1 OMBR

The overall goal of the OMBR investigation was to evaluate the feasibility of the OMBR system to treat domestic wastewater. The specific objectives were to present the novel OMBR system and to report the results of preliminary experiments focused on water flux, reverse salt diffusion, fouling propensity, and nutrient removal. Furthermore, the operation of the OMBR process was compared to conventional MBR processes in terms of filtration time, backwashing time, net flux, and removal efficiencies.

1.6.2 Draw solution selection

The objective of the draw solution investigation was to develop a protocol for the selection of optimal draw solutions for an FO process/application. More than 500 inorganic compounds were screened, and at the end of the screening process, selected draw solutions were tested in the laboratory to evaluate water flux and reverse salt diffusion. RO reconcentration and rejection of the draw solutions was evaluated using RO system design software [51, 52]. Analysis of experimental data and model results, combined with considerations of the costs associated with the FO and RO processes, provided guidance for selection of the most appropriate draw solution for FO applications. Furthermore, the large draw solution matrix (in terms of both constituents and concentrations) enabled insight into the role of membrane characteristics and solution characteristics on water flux and reverse salt diffusion. Specifically, the influence of concentration polarization on water flux and reverse salt diffusion was elucidated.

1.6.3 PRO

The objective of the PRO investigation was to evaluate the contribution of membrane characteristics and operating conditions on water flux and subsequently, on power density. Concentration polarization is expected to severely reduce water flux and power density in PRO; however, the causes and effects of concentration polarization have not been investigated nearly as much for FO and PRO processes [28, 31] as for RO processes [53, 54]. In the current investigation, a predictive PRO model that includes the influence of draw solution, feed solution, concentration polarization, and hydraulic pressure on water flux and subsequent power output was developed. The model was

tested using experimental results. Experiments were conducted using current-generation FO membranes and a well-established draw solution (NaCl). In this investigation, for the first time, experimental PRO results were compared with model predictions.

Furthermore, power density were evaluated under different operating conditions. With the availability of a PRO model, power density can be predicted for variable membrane characteristics, membrane structure, and module configuration. The optimization of these parameters will contribute to the design of membranes and membrane modules specifically tailored for PRO processes.

1.7 Dissertation organization

This dissertation is a compilation of papers written over the course of the dissertation research. Chapter 2 is an entire paper published in *Desalination* and is reprinted with permission from Elsevier Science B.V. Chapter 3 is a paper that has been submitted for publication in the *Journal of Membrane Science*. Chapter 4 is an entire paper that has been accepted for publication in the *Journal of Membrane Science*.

References

- [1] M. Elimelech, The global challenge for adequate and safe water, *Journal of water supply research and technology-AQUA* 55 (2006) 3-10.
- [2] A.G. Fane and S.A. Fane, The role of membrane technology in sustainable decentralized wastewater systems, *Water Science and Technology*, 51 (2005) 317-325.
- [3] M. Parry, J. Palutikof, P. Vanderlinden and C. Hanson, *Climate Change 2007: Impacts, Adaptation and Vulnerability. Contribution of Working Group II to the Fourth Assessment Report of the Intergovernmental Panel on Climate Change*, Cambridge University Press, Cambridge, UK, 2007.

- [4] A. Fane, Sustainability and membrane processing of wastewater for reuse, *Desalination*, 202 (2007) 53-58.
- [5] T. Stephenson, S. Judd, B. Jefferson and K. Brindle, *Membrane bioreactors for wastewater treatment*, IWA Publishing, 2000.
- [6] S. Judd, *The MBR Book: Principles and applications of membrane bioreactors in water and wastewater treatment*, Elsevier, 2006.
- [7] P. Lawrence, S. Adham and L. Barro, Ensuring water re-use projects succeed - institutional and technical issues for treated wastewater re-use, *Desalination*, 152 (2002) 291-298.
- [8] P. Le-Clech, V. Chen and T.A.G. Fane, Fouling in membrane bioreactors used in wastewater treatment, *Journal of Membrane Science*, 284 (2006) 17-53.
- [9] J.S. Vrouwenvelder and D. van der Kooij, Diagnosis, prediction and prevention of biofouling of NF and RO membranes, *Desalination*, 139 (2001) 65-71.
- [10] M. Barger and R.P. Carnahan, Fouling prediction in reverse osmosis process, *Desalination*, 83 (1991) 3-31.
- [11] P. Le-Clech, A. Fane, G. Leslie and A. Childress, MBR focus: the operators' perspective, *Filtration + Separation*, 42 (2005) 20-23.
- [12] El H. Bouhabila, R. Ben-Aim and H. Buisson, Fouling characterisation in membrane bioreactors, *Separation and Purification Technology*, 22-23 (2001) 123-132.
- [13] C. Psoch and S. Schiewer, Critical flux aspect of air sparging and backflushing on membrane bioreactors, *Desalination*, 175 (2005) 61-71.
- [14] C. Psoch and S. Schiewer, Resistance analysis for enhanced wastewater membrane filtration, *Journal of Membrane Science*, 280 (2006) 284-297.
- [15] S.P. Hong, T.H. Bae, T.M. Tak, S. Hong and A. Randall, Fouling control in activated sludge submerged hollow fiber membrane bioreactors, *Desalination*, 143 (2002) 219-228.
- [16] P. J. Smith, S. Vigneswaran, H. Hao Ngo, R. Ben-Aim and H. Nguyen, Design of a generic control system for optimising back flush durations in a submerged membrane hybrid reactor, *Journal of Membrane Science*, 255 (2005) 99-106.

- [17] R.W. Holloway, A.E. Childress, K. E. Dennett and T.Y. Cath, Forward osmosis for concentration of anaerobic digester centrate, *Water Research*, 41 (2007) 4005-4014.
- [18] A. Sagiv and R. Semiat, Backwash of RO spiral wound membranes, *Desalination*, 179 (2005) 1-9.
- [19] J.R. McCutcheon, R.L. McGinnis and M. Elimelech, A novel ammonia--carbon dioxide forward (direct) osmosis desalination process, *Desalination*, 174 (2005) 1-11.
- [20] C.D. Moody and J.O. Kessler, Forward osmosis extractors, *Desalination*, 18 (1976) 283-295.
- [21] R.J. York, R.S. Thiel and E.G. Beaudry, Full-scale experience of direct osmosis concentration applied to leachate management, *Seventh International Waste Management and Landfill Symposium (Sardinia '99)*, Cagliari, Italy, 1999.
- [22] T.Y. Cath, A.E. Childress and M. Elimelech, Forward osmosis: Principles, applications, and recent developments, *Journal of Membrane Science*, 281 (2006) 70-87.
- [23] R.E. Kravath and J.A. Davis, Desalination of seawater by direct osmosis, *Desalination*, 16 (1975) 151-155.
- [24] J.L. Cartinella, T.Y. Cath, M.T. Flynn, G.C. Miller, K. W. Hunter and A.E. Childress, Removal of natural steroid hormones from wastewater using membrane contactor processes, *Environmental Science and Technology*, 40 (2006) 7381-7386.
- [25] A. Achilli, T.Y. Cath, E.A. Marchand and A.E. Childress, The forward osmosis membrane bioreactor: A low fouling alternative to MBR processes, *Desalination*, 239 (2009) 10-21.
- [26] T.Y. Cath, S. Gormly, E.G. Beaudry, M.T. Flynn, V.D. Adams and A.E. Childress, Membrane contactor processes for wastewater reclamation in space. I. Direct osmotic concentration as pretreatment for reverse osmosis, *Journal of Membrane Science*, 257 (2005) 85-98.
- [27] C.R. Martinetti, A.E. Childress and T.Y. Cath, High recovery of concentrated RO brines using forward osmosis and membrane distillation, *Journal of Membrane Science*, 331 (2009) 31-39.
- [28] J.R. McCutcheon, R.L. McGinnis and M. Elimelech, Desalination by ammonia--carbon dioxide forward osmosis: Influence of draw and feed solution

- concentrations on process performance, *Journal of Membrane Science*, 278 (2006) 114–123.
- [29] K.B. Petrotos, P.C. Quantick and H. Petropakis, A study of the direct osmotic concentration of tomato juice in tubular membrane-module configuration. I. The effect of certain basic process parameters on the process performance, *Journal of Membrane Science*, 150 (1998) 99-110.
- [30] K.B. Petrotos, P.C. Quantick and H. Petropakis, Direct osmotic concentration of tomato juice in tubular membrane-module configuration. II. The effect of using clarified tomato juice on the process performance, *Journal of Membrane Science*, 160 (1999) 171-177.
- [31] J.R. McCutcheon and M. Elimelech, Influence of concentrative and dilutive internal concentration polarization on flux behavior in forward osmosis, *Journal of Membrane Science*, 284 (2006) 237-247.
- [32] C.H. Tan and H.Y. Ng, Modified models to predict flux behavior in forward osmosis in consideration of external and internal concentration polarizations, *Journal of Membrane Science*, 324 (2008) 209-219.
- [33] A. Achilli, T.Y. Cath and A.E. Childress, Power generation with pressure retarded osmosis: an experimental and theoretical investigation, *Journal of Membrane Science*, In press (2009)
- [34] K.L. Lee, R.W. Baker and H.K. Lonsdale, Membrane for power generation by pressure retarded osmosis, *Journal of Membrane Science*, 8 (1981) 141-171.
- [35] N.T. Hancock and T.Y. Cath, Novel performance modeling of forward osmosis - reverse osmosis integrated system, American Water Works Association 2009 Membrane Technology Conference, Memphis, Tennessee, 2009.
- [36] S. Loeb, Large-scale power production by pressure-retarded osmosis, using river water and sea water passing through spiral modules, *Desalination*, 143 (2002) 115-122.
- [37] R.J. Aaberg, Osmotic Power. A new and powerful renewable energy source?, *Refocus*, 4 (2003) 48-50.
- [38] The Energy Information Administration, <http://www.eia.doe.gov/>
- [39] R.E. Pattle, Production of electric power by mixing fresh and salt water in the hydroelectric pile, *Nature*, 174 (1954) 660.

- [40] R.S. Norman, Water salination: a source of energy, *Science*, 186 (1974) 350-352.
- [41] O. Levenspiel and N. de Nevers, The osmotic pump, *Science*, 183 (1974) 157-160.
- [42] S. Loeb, Production of energy from concentrated brines by pressure-retarded osmosis, I. Preliminary technical and economic correlations, *Journal of Membrane Science*, 1 (1976) 49-63.
- [43] S. Loeb and R.S. Norman, Osmotic power plants, *Science*, 189 (1975) 654-655.
- [44] S. Loeb, F. Van Hessen and D. Shahaf, Production of energy from concentrated brines by pressure-retarded osmosis, II. Experimental results and projected energy costs, *Journal of Membrane Science*, 1 (1976) 249-269.
- [45] S. Loeb and G.D Mehta, A Two coefficient water transport equation for pressure-retarded osmosis, *Journal of Membrane Science*, 4 (1979) 351-362.
- [46] G.D Mehta and S. Loeb, Performance of permasep B-9 and B-10 membranes in various osmotic regions and at high osmotic pressures, *Journal of Membrane Science*, 4 (1979) 335-349.
- [47] G.D. Mehta and S. Loeb, Internal polarization in the porous substructure of a semipermeable membrane under pressure-retarded osmosis, *Journal of Membrane Science*, 4 (1978) 261-265.
- [48] H.H. Jellinek and H. Masuda, Osmo-power. Theory and performance of an osmo-power pilot plant, *Ocean Engineering*, 8 (1981) 103-128.
- [49] J.R. McCutcheon and M. Elimelech, Influence of membrane support layer hydrophobicity on water flux in osmotically driven membrane processes, *Journal of Membrane Science*, 318 (2008) 458-466.
- [50] K. Gerstandt, K.-V. Peinemann, S.E. Skilhagen, T. Thorsen and T. Holt, Membrane processes in energy supply for an osmotic power plant, *Desalination*, 224 (2008) 64-70.
- [51] IMSDesign, Hydranautics, Oceanside, CA.
- [52] Reverse Osmosis System Analysis (ROSA), Dow Filmtec, Midland, MI.
- [53] M. Elimelech and S. Bhattacharjee, A novel approach for modeling concentration polarization in crossflow membrane filtration based on the equivalence of osmotic pressure model and filtration theory, *Journal of Membrane Science*, 145 (1998) 223-241.

- [54] S.S. Sablani, M.F.A. Goosen, R. Al-Belushi and M. Wilf, Concentration polarization in ultrafiltration and reverse osmosis: a critical review, *Desalination*, 141 (2001) 269-289.

Chapter 2

2 THE FORWARD OSMOSIS MEMBRANE BIOREACTOR: A LOW FOULING ALTERNATIVE TO MBR PROCESSES

(Reprinted with permission from Desalination, © 2009 Elsevier Science B.V.)

Abstract

A novel submerged osmotic membrane bioreactor (OMBR) is presented. The system utilizes a forward osmosis (FO) membrane module inside a bioreactor. Through osmosis, water is transported from the mixed liquor across a semi-permeable membrane, and into a draw solution (DS) with a higher osmotic pressure. To produce potable water, the diluted DS is treated in a reverse osmosis (RO) unit; the byproduct is a reconcentrated DS for reuse in the FO process. Preliminary results from experiments conducted with a flat-sheet cellulose triacetate FO membrane demonstrated high sustainable flux and relatively low reverse diffusion of solutes from the DS into the mixed liquor. Membrane fouling was controlled with osmotic backwashing. The FO membrane was found to reject 98% of organic carbon and 90% of ammonium-nitrogen; the OMBR process (bioreactor and FO membrane) was found to remove greater than 99% of organic carbon and 98% of ammonium-nitrogen, respectively; suggesting a better compatibility of the OMBR with downstream RO systems than conventional membrane bioreactors.

Keywords: Osmotic membrane bioreactor, Forward osmosis, Membrane fouling, Wastewater treatment, Nutrient removal

2.1 Introduction

More stringent regulations and the potential to produce high quality effluent make membrane bioreactors (MBRs) an attractive process for domestic wastewater treatment [1]. In a submerged MBR, microporous (microfiltration (MF) or ultrafiltration (UF)) membranes are immersed in a bioreactor and water is filtered through the membranes using vacuum; suspended solids are retained in the system and high levels of treatment (including nutrient removal) can be achieved [2]. The MBR replaces the two stages of the conventional activated sludge process (biotreatment and clarification) with a single, integrated process. MBR effluent may be suitable for use as irrigation water, process water, or a source of potable water. For potable reuse (e.g., indirect reuse through aquifer recharge), advanced treatment (e.g., reverse osmosis (RO), nanofiltration (NF), or chemical oxidation) is necessary after the MBR [3]. The advantages of MBRs over conventional treatment have been thoroughly reviewed [1] and they include product water consistency, reduced footprint, reduced sludge production due to a high biomass concentration in the bioreactor, and essentially complete suspended solids removal from the effluent. The main problem associated with MBRs is membrane fouling. Fouling reduces permeate flux and increases the frequency of membrane cleaning and replacement [4]. Membrane fouling can occur in the MBR itself, and also in the downstream RO system [5]. Specifically, high concentrations of dissolved organic compounds in the MBR effluent can cause severe fouling of RO membranes; this leads to reduction of water flux and deterioration of treated water quality [6].

In order to operate conventional MBRs at constant flux, physical membrane cleaning techniques are utilized; they include backwashing, relaxation, or a combination

of the two, depending on the membrane configuration (flat-sheet or tubular). Chemicals are often added to enhance physical cleaning [7]. During backwashing, the permeate is pumped in the opposite direction through the membrane. Backwashing effectively removes most of the reversible fouling due to pore blocking. The efficiency of backwashing has been studied in detail and the key parameters have been found to be frequency, duration, and intensity [8-10]. During membrane relaxation, permeate suction is stopped and the back-transport of foulants is naturally enhanced as reversibly attached foulants diffuse away from the membrane surface due to the concentration gradient. Tubular and hollow fibers membranes undergo regular backwashing and sometimes relaxation [8-12]. Flat-sheet membranes cannot be backwashed due to their inability to withstand pressure in the opposite direction of the operating flow; for this reason, relaxation is used to control the fouling of these membranes [4].

A novel MBR system that utilizes a submerged forward osmosis (FO) membrane in the bioreactor is investigated in the current study. FO, or simply osmosis, is the transport of water across a selectively permeable membrane from a solution of higher water chemical potential (low osmotic pressure) to a solution of lower water chemical potential (higher osmotic pressure). Typically, the FO process results in concentration of the feed stream and dilution of a highly concentrated stream (referred to as the draw solution (DS)) [13]. In an osmotic MBR (OMBR) system (Figure 2.1), wastewater is fed into a reactor which is continuously aerated to supply oxygen for the biomass and to scour the membrane. Through osmosis, water diffuses from the bioreactor, across a semi-permeable membrane, and into a lower water chemical potential DS. The FO membrane acts as a barrier to solute diffusion and provides high rejection of the contaminants in the

wastewater stream [14-16]. The diluted DS is sent to a reconcentration process (e.g., RO or distillation) which reconcentrates the DS and generates a high-quality product water. Thus, in most wastewater treatment applications, FO is not the ultimate process but rather a high-level pretreatment step before an ultimate reconcentration process. Compared to the MF or UF process in a conventional MBR, the FO process in the OMBR offers the advantages of much higher rejection (semi-permeable membrane versus microporous membrane) at a lower hydraulic pressure. FO is also likely to have lower fouling propensity than pressure-driven systems [13], and therefore, require less frequent backwashing. When comparing an OMBR system (OMBR followed by RO) with a conventional MBR followed by RO, the high rejection of the FO membrane will result in an RO influent with lower fouling propensity and may lead to a higher quality RO product water. Furthermore, the FO followed by RO treatment scheme represents a dual barrier purification system. In FO membrane processes, osmotic backwashing can be performed to remove foulants from the surface of the membrane. During osmotic backwashing, water flows from the support side of the membrane to the active side, thereby reversing the direction of flow through the FO membrane and potentially removing foulants [17, 18].

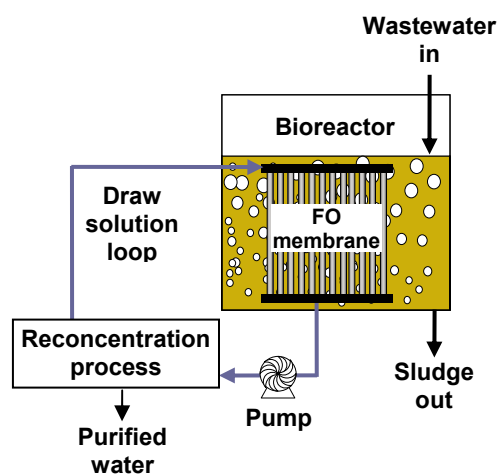


Figure 2.1 Schematic diagram of an OMBR system.

A key consideration in developing an OMBR system is selection of an appropriate DS [13]. The main criterion is that the DS has a higher osmotic pressure than the feed solution. Another important criterion in some FO applications is the availability of a suitable process for reconcentrating the draw solution after it has been diluted in the FO process. Very often a NaCl solution is selected because it has high solubility and is relatively easy to reconcentrate to high concentrations using a conventional desalination process (e.g., RO or distillation) without risk of scaling [13].

Diffusion of the draw solute (e.g., Na^+ or Cl^- ions) into the bioreactor through the membrane must also be considered in the OMBR process. This “reverse salt diffusion” is expected to occur because of the difference in solute concentration between the DS and the reactor solution. Reverse salt diffusion from the DS not only results in a reduced driving force, but may also have inhibitory or toxic effects on the microbial community inside the reactor.

In this paper, the feasibility of the OMBR system to treat domestic wastewater is evaluated. The specific objectives of this paper are to present the novel OMBR system and to report the results of preliminary experiments focused on water flux, reverse salt diffusion, fouling propensity, and nutrient removal. Furthermore, the operation of the OMBR process is compared to conventional MBR processes in terms of filtration time, backwashing time, net flux, and TOC removal efficiencies.

2.2 Materials and methods

2.2.1 FO Membranes

Three flat-sheet cellulose triacetate (CTA) FO membranes (Hydration Technologies, Inc., Albany, OR), designated membranes A, B, and C, were used in the experiments. These membranes are unique compared to other semi-permeable membranes (e.g., RO membranes), and have been determined to be the best available membranes for current FO applications [13, 19]. These membranes have different selectivities and permeabilities; however, specific differences are proprietary.

2.2.2 Batch abiotic experiments

An abiotic batch apparatus was used to characterize the water flux and reverse salt diffusion of the three membranes (Figure 2.2). In this apparatus, a unique plate-and-frame FO membrane module was immersed in a 14 L reactor containing doubly deionized water (DDW). In the FO membrane module, two flat-sheet membranes were held in place by frames bolted to an inner plate. The DS flowed between the membranes through inlet and outlet channels located on opposite sides of the plate. The membranes were oriented with

their active sides facing the reactor and their support sides facing the DS. The total membrane surface area was 0.0173 m^2 . Mesh spacers were placed between the membrane and the central unit to both support the membrane and increase the turbulence of the DS as it passed through the membrane module. An aerator was placed at the bottom of the reactor to continuously agitate the reactor contents.

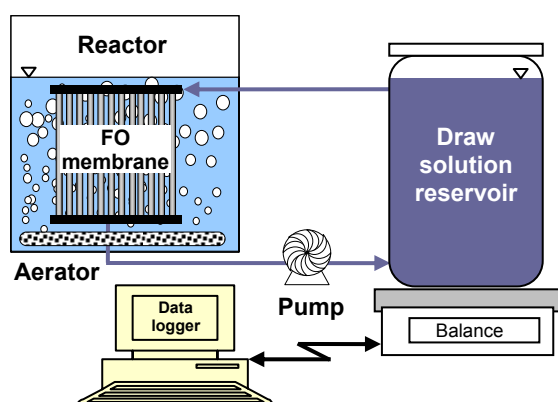


Figure 2.2 Schematic diagram of the batch laboratory-scale OMBR apparatus.

The DS reservoir was placed on an analytical balance (PB5001-S, Mettler-Toledo, Columbus, OH) linked to a computer; a variable-speed gear pump (Cole-Palmer, Vernon Hills, IL) was used to recirculate the DS at 1.5 L/min. The DS concentration was allowed to decrease from 70 to 30 g NaCl/L as water diffused through the membrane from the reactor to the DS reservoir. Flux through the membrane was calculated based on the change of weight of the DS. The conductivity of the reactor solution was continuously monitored (Accumet Basic, Fisher Scientific, Hampton, NH) and recorded to calculate the reverse salt diffusion.

The three CTA membranes were tested under the same conditions and using NaCl as the DS. The temperature was held constant at $23 \pm 1^\circ\text{C}$.

2.2.3 Continuous-flow OMBR experiments

A continuous-flow apparatus was used to evaluate the OMBR system under continuous feed and constant DS conditions (Figure 2.3). Water flux, reverse salt diffusion, and removal efficiencies of the biological process, the FO process, and the RO process were investigated.

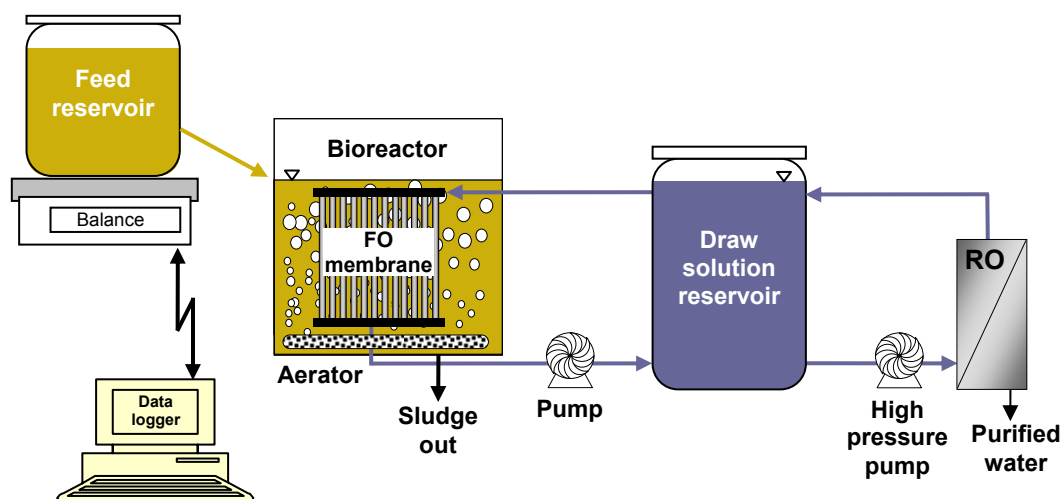


Figure 2.3 Schematic diagram of the continuous-flow laboratory-scale OMBR apparatus.

The reactor was continuously fed from a stock solution feed reservoir. The synthetic feed solution consisted of 5 g/L meat extract, 1 g/L $C_6H_{12}O_6$, 0.6 g/L $(NH_4)_2SO_4$, and 0.14 g/L K_2HPO_4 . Between 1 and 2 g/L $NaHCO_3$ was also added to maintain neutral pH. This solution had a chemical oxygen demand (COD) of 4.5 ± 0.2 g/L, a C:N:P ratio of 100:5:1, and a food-to-microorganism (F/M) ratio of 0.25 kg COD/(kg

MLSS·d). Due to the large volume of the bioreactor (14 L) and the associated large hydraulic retention time (HRT) of the system (3.5 d), the feed concentrations were higher than those found in typical domestic wastewaters. These concentrations were necessary to keep the F/M ratio within the range of 0.10 to 0.40 kg COD/(kg MLSS·d), a range that is typical for MBR treatment processes [1]. Similar to the batch apparatus, the plate-and-frame FO membrane module was immersed in a 14 L reactor. However, in the continuous-flow apparatus, the reactor was filled with 5.5 g mixed liquor suspended solids per liter (g MLSS/L) that were collected from the aeration basin of a conventional wastewater treatment facility (Truckee Meadows Water Reclamation Facility, Reno, Nevada). The mixed liquor was acclimated to the new feed for a period of 2 weeks prior to being added to the OMBR system. The mixed liquor level in the reactor was held constant by a float valve. The aerator placed at the bottom of the reactor agitated the solution, provided oxygen to the microbial community, and lightly scoured the membrane surface.

The feed reservoir was placed on an analytical balance linked to a computer. Flux through the membrane was calculated based on the change of weight of the feed solution transferred to the reactor. A variable-speed gear pump was used to recirculate the DS at 1.5 L/min. The conductivity of the mixed liquor was monitored and recorded in order to calculate the reverse salt diffusion and the total accumulation of salt in the bioreactor.

The DS concentration was held constant at 50 ± 1 g NaCl/L by continuous reconcentration with an RO system. The RO system was comprised of a SEPA-CF membrane cell (GE Osmonics, Minnetonka, MN), utilizing an SW30HR membrane

(Dow Chemical Company, Midland, MI), and driven by a high pressure positive displacement pump (Hydracell M03, Wanner Eng., Minneapolis, MN).

The continuous-flow experiments were conducted utilizing membrane B as the FO membrane. The solids retention time (SRT) of the OMBR was 15 days, thus guaranteeing the development of nitrifying bacteria [20]; the SRT was maintained by daily wasting of excess sludge. The temperature was held constant at $23\pm 1^\circ\text{C}$.

2.2.4 Cleaning experiments

After 14, 21, and 28 days of continuous operation, the membrane module was removed from the continuous-flow apparatus and placed in the batch apparatus. An abiotic batch experiment was performed for approximately 8 h in order to quantify the water flux loss due to fouling only. Reverse salt diffusion was also measured. Water flux loss in the continuous system is expected to be caused by a combination of fouling and reduced driving force due to the salt accumulated in the bioreactor through reverse salt diffusion. Because DDW is used as the reactor solution in the batch abiotic experiments, and the experiment duration was only 8 h, the reverse salt diffusion over the duration of the experiments did not result in substantial salt accumulation in the bioreactor (approximately 100 mg NaCl/L at the end of the experiment). Considering this, and also considering that fouling does not occur in the abiotic experiments, flux decline due to only the membrane fouling that occurred in the continuous-flow experiments can be isolated. The batch cleaning experiments were designed to mirror the abiotic batch experiments that were used to initially characterize the flux and rejection of the membranes; the experiments lasted as long as it took for the DS concentration to decrease

from 70 to 30 g NaCl/L (approximately 8 h). After 8 h, an osmotic backwash was performed in batch mode for 1 h. The osmotic backwash was accomplished by filling the reactor with a 5 g NaCl/L solution, filling the DS reservoir with DDW, and recirculating the DDW through the membrane module at a flow rate of 1.5 L/min with a variable-speed gear pump. Following the osmotic backwash and prior to returning the membrane module to the continuous system, the membrane was operated in abiotic batch mode for an additional 8 h (as the DS again decreased from 70 to 30 g NaCl/L). This step isolated the effect of osmotic backwashing on water flux and reverse salt diffusion.

2.2.5 Analytical Methods

Daily grab samples were collected from the feed reservoir, the reactor, the DS reservoir, and the product water. The samples were first centrifuged (Centrifuge 5415C, Eppendorf AG, Hamburg, Germany) at 9,000 rpm for 15 min to separate the biomass from the solution. The supernatant was then filtered through a 0.22 μm filter to remove the fine particles and biomass residuals. Samples from the DS and product water were tested without centrifugation. The samples were analyzed for ammonium nitrogen (NH_4^+ -N) according to Standard Methods (APHA, 1999) and for total organic carbon (TOC) using a TOC analyzer (TOC-Vcsh, Shimadzu Corp., Kyoto, Japan).

2.3 Results and discussion

2.3.1 Batch experiments

Water flux as a function of DS concentration is illustrated in Figure 2.4 for the three membranes tested in this study. For all three membranes, water flux decreases as

DS concentration decreases because of the decreasing osmotic pressure difference between the DS and the reactor solution. Water flux through membrane A is at least 29% greater than the water flux through membrane B, and water flux through membrane B is at least 71% greater than the water flux through membrane C. Thus, it appears that membrane A is the loosest, membrane B is in the middle, and membrane C is the tightest membrane.

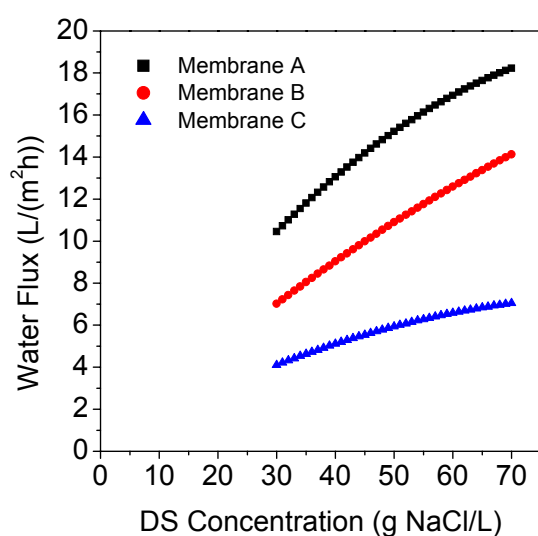


Figure 2.4 Water flux as a function of DS concentration for batch FO experiments with three CTA membranes.

The rate of reverse salt diffusion as a function of DS concentration is depicted in Figure 2.5. For all three membranes, reverse salt diffusion decreases linearly as the DS concentration decreases. The magnitude of reverse salt diffusion for membrane A is at least 2.2 times greater than that for membrane B and the reverse salt diffusion for membrane B is at least 7.3 times greater than that for membrane C. Thus, the membrane with the highest water flux (membrane A) also showed the highest reverse salt diffusion

and the membrane with the lowest water flux (membrane C) showed the lowest reverse salt diffusion. These results are expected as the loosest membrane matrix would be expected to have the advantage of high water flux and the disadvantage of high reverse salt diffusion. Membrane B was selected for the continuous flow experiments because it exhibited a favorable water flux while maintaining a reverse salt diffusion rate that would not lead to a salt concentration inside the bioreactor high enough to adversely affect the biological process.

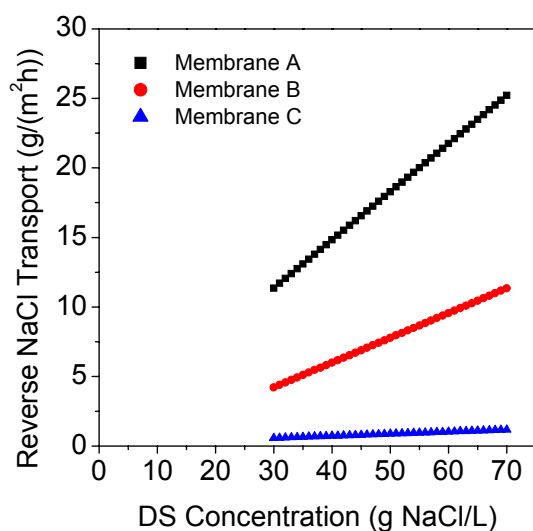


Figure 2.5 Reverse salt diffusion as a function of DS concentration for batch FO experiments with three CTA membranes.

2.3.2 Continuous-flow OMBR experiments

TOC and $\text{NH}_4^+\text{-N}$ concentrations at various locations in the OMBR system are summarized in Table 2.1. The difference between the feed solution concentrations and the bioreactor concentrations represents the effect of both biological degradation and the FO process. Biological degradation reduces the TOC and $\text{NH}_4^+\text{-N}$ concentrations in the

bioreactor, while the FO process increases these constituents, as the semi-permeable membrane rejects and retains TOC and $\text{NH}_4^+\text{-N}$ inside the bioreactor. The data in Table 2.1 reveal that biological degradation works to greatly reduce the concentrations of TOC and $\text{NH}_4^+\text{-N}$, substantially overcoming the concentration process of the FO membrane. In the DS and in the product water, TOC and $\text{NH}_4^+\text{-N}$ concentrations further decrease due to the FO and RO membrane rejection, respectively.

Table 2.1 TOC and $\text{NH}_4^+\text{-N}$ concentrations at various locations in the OMBR system.

	Feed Solution	Bioreactor	Draw Solution	Product Water
TOC (mg/L)	1,325 ± 25	140 ± 5	3 ± 0.5	2.5 ± 0.5
$\text{NH}_4^+\text{-N}$ (mg/L)	65 ± 5	15 ± 2	1.5 ± 0.5	0.4 ± 0.1

Removal efficiencies of the FO membrane, the OMBR process (bioreactor and FO membrane), and the overall system (OMBR followed by RO) are summarized in Table 2.2. For removal only by the FO membrane, both the TOC and $\text{NH}_4^+\text{-N}$ rejections are comparable to published results for semi-permeable membranes [17, 21]. For the OMBR process (bioreactor and FO membrane), the TOC and $\text{NH}_4^+\text{-N}$ removals are substantially higher than those obtained in conventional MBRs, where removals up to 95% are typical [2]. For the OMBR system (OMBR followed by RO), greater than 99% removal is achieved for both TOC and $\text{NH}_4^+\text{-N}$.

Table 2.2 TOC and $\text{NH}_4^+\text{-N}$ removal efficiencies at various stages of the OMBR system.

	% Rejection of FO membrane	% Removal of OMBR process (bioreactor + FO)	% Removal of overall system (OMBR + RO)
TOC (mg/L)	97.9	99.8	99.8
$\text{NH}_4^+\text{-N}$ (mg/L)	90.0	97.7	99.4

Water flux and salt concentration in the OMBR are illustrated in Figure 2.6. The average water flux during the experiment was approximately $9 \text{ L}/(\text{m}^2 \cdot \text{h})$. This flux value was approximately 18% lower than the pure water flux observed in the batch experiments ($11 \text{ L}/(\text{m}^2 \cdot \text{h})$ at $50 \text{ g NaCl}/\text{L}$). These results confirm the lower fouling propensity of the FO process compared to pressure-driven membrane processes, where severe fouling causes the operating water flux to be a small percent of the initial water flux (75% lower than the initial flux in one investigation ([11])). The likely cause of flux decline is increased hydraulic resistance caused by foulants deposited on the membrane surface. In order to determine how much of the 18% flux decline is due to membrane fouling and how much is due to increasing salinity in the reactor, the NaCl concentration in the OMBR must be considered. As can be seen in Figure 2.6, the salt concentration in the bioreactor steadily increases due to reverse salt diffusion over the first 14 d. This reduces the net difference between the DS concentration and the reactor salt concentration and results in a lower driving force. Eventually it is expected that the reactor salt concentration will reach a constant value depending on the operating SRT. The operating SRT determines the amount of daily sludge wasting and hence, the removal of salt from the bioreactor. NaCl that enters the bioreactor due to reverse salt diffusion will only be removed from the bioreactor by sludge wasting; thus the SRT regulates its concentration inside the bioreactor. From Figure 2.6, it appears that the salt concentration in the bioreactor stabilized at approximately $4 \text{ g}/\text{L}$ around 14 d of operation. Thus, reverse salt diffusion plays a substantial role in flux decline over the first 14 d. After that time, when the salt concentration in the reactor remains relatively constant, observed flux decline is

likely due to membrane fouling only. It is also worth noting that the level of salinity observed in the reactor is not a concern in terms of inhibition or toxic effects on the biological processes [22].

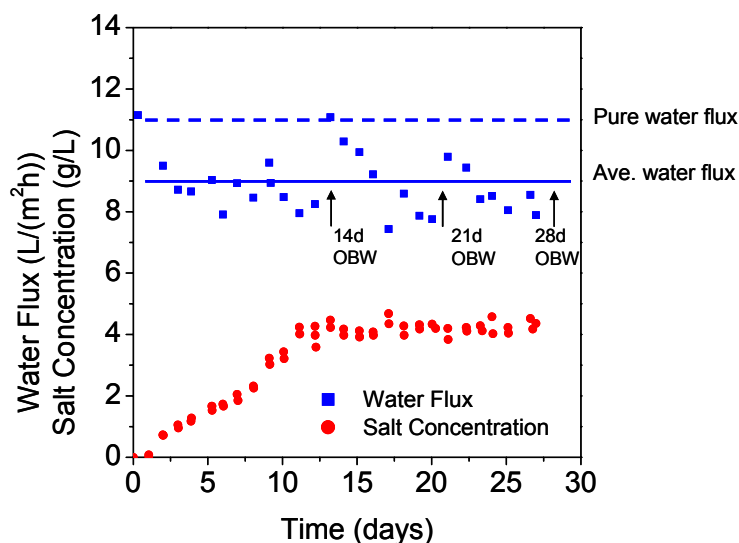


Figure 2.6 Water flux through the FO membrane and salt concentration in the bioreactor as a function of time for continuous-flow experiments with membrane B. Osmotic backwashings (OBW) are indicated at 14, 21, and 28 d.

The arrows at 14, 21, and 28 d in Figure 6 indicate times when osmotic backwashing was performed. Figure 2.7 and 8 summarize the results of the offline batch experiments performed to study membrane fouling and backwashing at 14, 21, and 28 d. In Figure 2.7, the left and right bars of each pair depict the effects of membrane fouling and osmotic backwashing on water flux, respectively. After 14 d of operation, the water flux decreased by approximately 20% from the initial flux of the new membrane. Osmotic backwashing was able to restore approximately 50% of this flux loss, leaving an overall 10% lower flux due to irreversible fouling. Similar trends were observed after 21 and 28 d. This suggests that after an initial phase of irreversible fouling (occurring in the

first 14 days), later phases of fouling are more reversible and the water flux can be maintained at a constant value over time. This reinforced the earlier observation (in Figure 2.6) of the low fouling effects of the OMBR process. Additionally, these preliminary results indicate that osmotic backwashing is an effective way to control membrane fouling. Comparing Figure 2.7 with Figure 2.6, it is worth noting that the values of water fluxes taken from the continuous experiments at the end of each cycle (the points just before each arrow in Figure 2.6) match with the water fluxes of the abiotic batch experiments prior to osmotic backwashing (the left bars in Figure 2.7), showing that no unintentional cleaning occurred during the abiotic batch experiments, and that the cleaning was in effect due to the osmotic backwashing.

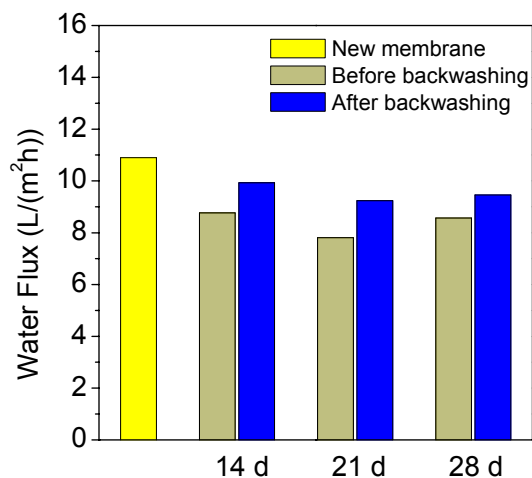


Figure 2.7 Water fluxes of membrane B. Comparison between water flux for the new membrane, and before/after osmotic backwashing at 14, 21, and 28 d. The concentration of the draw solution was 50 g NaCl/L.

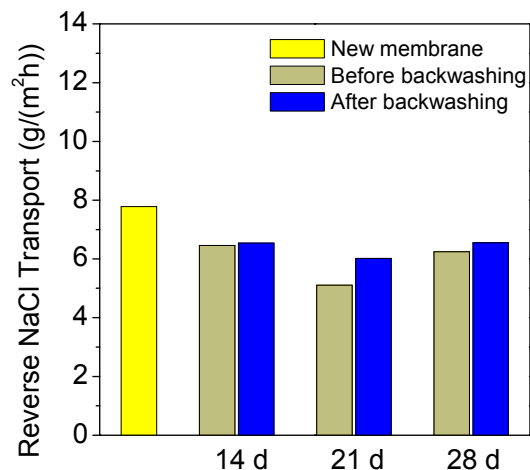


Figure 2.8 Reverse salt diffusion through membrane B. Comparison between reverse salt diffusion for the new membrane, and before/after osmotic backwashing at 14, 21, and 28 d. The concentration of the draw solution was 50 g NaCl/L.

Furthermore, integrating the results of the offline batch experiments, the resulting average water flux is 9.4 L/(m²·h), approximately 15% lower than the pure water flux observed in the batch experiments (11 L/(m²·h) at 50 g NaCl/L). This is the hypothetical average water flux influenced by membrane fouling only. Comparing this to the flux loss due to membrane fouling and salt concentration in the bioreactor (18% from Figure 6), the flux loss is almost completely due to membrane fouling; only minimal flux decline is attributed to the reduced driving force resulting from salt accumulation in the bioreactor.

The effects of fouling and osmotic backwashing on reverse salt diffusion are illustrated in Figure 2.8. The reverse salt diffusion of the used membrane is approximately 16% less than that of the new membrane, and it remains fairly constant (between 5 and 6.5 g/(m²·h)) over the duration of the experiment. Generally, there is no obvious effect of membrane backwashing on the reverse salt diffusion in the process; and

as would be expected, the limited fouling that occurs at the membrane surface has a beneficial effect of reducing the reverse salt diffusion from approximately $7.7 \text{ g}/(\text{m}^2\cdot\text{h})$ for the new membrane to approximately $6.4 \text{ g}/(\text{m}^2\cdot\text{h})$ for the used membrane.

The operation of the novel OMBR process is compared to conventional MBR processes in Table 2.3. In microporous MBR systems, the length of the filtration-cleaning cycle varies between 4 and 90 min and the cycles repeat between 24 and 274 times per day depending on the membrane configuration and operating conditions. During the experiments reported here, the OMBR process required substantially fewer backwashing cycles (once per week) than the conventional MBR process. In the osmotically-driven MBR, the lack of hydraulic pressure across the membrane means that chemical or particulate foulants are not forced onto the membrane surface. Because cleaning duration and intervals markedly affect energy requirements, operational costs, system productivity, and membrane integrity [7], the need for less frequent backwashing is a substantial benefit of the OMBR process. The net flux of conventional MBRs is greatly influenced by the downtime caused by cleaning procedures, with a reduction up to 50% from the instantaneous flux (e.g., a net flux of $11 \text{ L}/(\text{m}^2\cdot\text{h})$ compared to an instantaneous flux of $22 \text{ L}/(\text{m}^2\cdot\text{h})$ in Table 2.3). The fewer backwashing cycles required by the OMBR process leads to a net flux essentially equal to its instantaneous flux, and in some cases, greater than the net flux of conventional MBRs.

Table 2.3 Operation comparison between conventional MBRs and the OMBR process.

Membrane	Material	Pore size μm	Flux $\text{L}/(\text{m}^2\cdot\text{h})$	Filtration-Cleaning cycle		Cycles/day	Net flux ^a $\text{L}/(\text{m}^2\cdot\text{h})$	Ref.
				Filtration (min)	Backwashing (min)			
Hollow fiber	Polyethylene – Polysulfone	0.1	20	5-45	0.25-15 ^b	24-274	15-18	[8, 11, 12]
Tubular	Polypropylene	0.2	8-22	30	0.25	48	– ^c	[9, 10]
Flat sheet	C-PVC – Stainless steel	0.2-0.4	17-22	3-8	1-4 ^b	120	8.7-11	[23, 24]
OMBR	CTA	– ^d	9.0	10,020	60	0.14	8.95	This study

^a Net flux is either reported by the authors of the articles or calculated based on the information contained in the articles. Calculations are based on relaxation time, backwashing time, and backwashing water flux. In the case of relaxation only, the net flux value is calculated by multiplying the flux by the ratio between the filtration time and the total cycle time. In the case of backwashing, the net flux value is calculated by subtracting the backwashing flux times the backwashing time from the filtration flux where the filtration flux is calculated the same as the relaxation flux

^b Relaxation time

^c Data not available. The authors of the articles did not report the net flux, nor the flux during backwashing

^d The CTA is a semi-permeable membrane

A further advantage of the OMBR process (bioreactor and FO) compared to a conventional MBR is the higher TOC removal efficiencies that can be achieved by an FO membrane compared to a microporous membrane (Table 2.4). Soluble organic matter is responsible for most of the fouling of RO membranes downstream of conventional MBRs [5, 6]. Microporous membranes do not reject soluble matter due to their porous nature, but due to the formation of a cake layer on their surface, the membrane plus cake layer system can typically retain 28-87% of soluble organic matter. The semi-permeable FO membrane has been shown to reject 98% of TOC, due to its non-porous composition.

Table 2.4 TOC removal efficiencies of conventional MBR membranes and the FO membrane in the OMBR system.

Membrane	Material	Pore size μm	Removal %	Ref.
Hollow fiber	Polyethylene	0.1	75	[12]
Hollow fiber	Polysulfone	0.1	68 ^a	[25]
Flat sheet	Stainless steel	0.2	58 ^a	[24]
Flat sheet	C-PVC	0.4	28-79 ^a	[26]
Flat sheet	Polyethylene	0.4	87 ^a	[27]
OMBR	CTA	– ^b	98	This study

^a Based on COD

^b The CTA is a semi-permeable membrane

2.4 Conclusions

A novel submerged OMBR system was presented. Long-term water fluxes for experiments with activated sludge operated at a solids concentration of 5.5 g MLSS/L were only 18% lower than water fluxes for experiments using DDW. Most of the reduction in water flux was due to membrane fouling; only a small part was due to increased salt concentration inside the bioreactor due to reverse salt diffusion.

Osmotic backwashing was conducted once per week to restore water flux to approximately 90% of the initial water flux. Compared to a conventional MBR, this system required substantially less backwashing. OMBR process removal efficiencies for TOC and NH_4^+ -N were greater than 99% and 98%, respectively, suggesting a better compatibility of the OMBR with downstream RO systems than conventional MBRs.

Acknowledgments

The authors acknowledge the support of the Department of Energy, Grant No. DE-FG02-05ER64143 and Hydration Technology Innovations (Albany, OR) for donating the FO membrane.

List of Abbreviations

COD	Chemical oxygen demand
CTA	Cellulose triacetate
DDW	Doubly deionized water
DS	Draw solution
FO	Forward osmosis
F/M	Food to microorganism ratio
HRT	Hydraulic retention time
MBR	Membrane bioreactor
MF	Microfiltration
MLSS	Mixed liquor suspended solids
OMBRO	Osmotic membrane bioreactor

RO	Reverse osmosis
SRT	Solids retention time
TOC	Total organic carbon
UF	Ultrafiltration

References

- [1] T. Stephenson, S. Judd, B. Jefferson and K. Brindle, Membrane bioreactors for wastewater treatment, IWA Publishing, 2000.
- [2] S. Judd, The MBR Book: Principles and applications of membrane bioreactors in water and wastewater treatment, Elsevier, 2006.
- [3] P. Lawrence, S. Adham and L. Barro, Ensuring water re-use projects succeed - institutional and technical issues for treated wastewater re-use, *Desalination*, 152 (2002) 291-298.
- [4] P. Le-Clech, V. Chen and T.A.G. Fane, Fouling in membrane bioreactors used in wastewater treatment, *Journal of Membrane Science*, 284 (2006) 17-53.
- [5] J.S. Vrouwenvelder and D. van der Kooij, Diagnosis, prediction and prevention of biofouling of NF and RO membranes, *Desalination*, 139 (2001) 65-71.
- [6] M. Barger and R.P. Carnahan, Fouling prediction in reverse osmosis process, *Desalination*, 83 (1991) 3-31.
- [7] P. Le-Clech, A. Fane, G. Leslie and A. Childress, MBR focus: the operators' perspective, *Filtration + Separation*, 42 (2005) 20-23.
- [8] El H. Bouhabila, R. Ben-Aim and H. Buisson, Fouling characterisation in membrane bioreactors, *Separation and Purification Technology*, 22-23 (2001) 123-132.
- [9] C. Psoch and S. Schiewer, Critical flux aspect of air sparging and backflushing on membrane bioreactors, *Desalination*, 175 (2005) 61-71.
- [10] C. Psoch and S. Schiewer, Resistance analysis for enhanced wastewater membrane filtration, *Journal of Membrane Science*, 280 (2006) 284-297.

- [11] S.P. Hong, T.H. Bae, T.M. Tak, S. Hong and A. Randall, Fouling control in activated sludge submerged hollow fiber membrane bioreactors, *Desalination*, 143 (2002) 219-228.
- [12] P. J. Smith, S. Vigneswaran, H. Hao Ngo, R. Ben-Aim and H. Nguyen, Design of a generic control system for optimising back flush durations in a submerged membrane hybrid reactor, *Journal of Membrane Science*, 255 (2005) 99-106.
- [13] T.Y. Cath, A.E. Childress and M. Elimelech, Forward osmosis: Principles, applications, and recent developments, *Journal of Membrane Science*, 281 (2006) 70-87.
- [14] R.J. York, R.S. Thiel and E.G. Beaudry, Full-scale experience of direct osmosis concentration applied to leachate management, *Seventh International Waste Management and Landfill Symposium (Sardinia '99)*, Cagliari, Italy, 1999.
- [15] T.Y. Cath, S. Gormly, E.G. Beaudry, M.T. Flynn, V.D. Adams and A.E. Childress, Membrane contactor processes for wastewater reclamation in space. I. Direct osmotic concentration as pretreatment for reverse osmosis, *Journal of Membrane Science*, 257 (2005) 85-98.
- [16] J.L. Cartinella, T.Y. Cath, M.T. Flynn, G.C. Miller, K. W. Hunter and A.E. Childress, Removal of natural steroid hormones from wastewater using membrane contactor processes, *Environmental Science and Technology*, 40 (2006) 7381-7386.
- [17] R.W. Holloway, A.E. Childress, K. E. Dennett and T.Y. Cath, Forward osmosis for concentration of anaerobic digester centrate, *Water Research*, 41 (2007) 4005-4014.
- [18] A. Sagiv and R. Semiat, Backwash of RO spiral wound membranes, *Desalination*, 179 (2005) 1-9.
- [19] J.R. McCutcheon, R.L. McGinnis and M. Elimelech, Desalination by ammonia-carbon dioxide forward osmosis: Influence of draw and feed solution concentrations on process performance, *Journal of Membrane Science*, 278 (2006) 114-123.
- [20] B.E. Rittmann and P.L. McCarty, *Environmental Biotechnology: principles and applications*, McGraw-Hill, New York, 2001.
- [21] J.E. Drewes, M.Reinhard and P. Fox, Comparing microfiltration-reverse osmosis and soil-aquifer treatment for indirect potable reuse of water, *Water Research*, 37 (2003) 3612-3621.

- [22] O. Lefebvre and R. Moletta, Treatment of organic pollution in industrial saline wastewater: a literature review, *Water Research*, 40 (2006) 3671-3682.
- [23] H.C. Chua, T.C. Arnot and J.A. Howell, Controlling fouling in membrane bioreactors operated with a variable throughput, *Desalination*, 149 (2002) 225-229.
- [24] S. Zhang, Y. Qu, Y. Liu, F. Yang, X. Zhang, K. Furukawa and Y. Yamada, Experimental study of domestic sewage treatment with a metal membrane bioreactor, *Desalination*, 173 (2005) 83-93.
- [25] M.E. Hernandez Rojas, R. Van Kaam, S. Schetrite and C. Albasi, Role and variations of supernatant compounds in submerged membrane bioreactor fouling, *Desalination*, 179 (2005) 95-107.
- [26] N. Jang, X. Ren, G. Kim, C. Ahn, J. Cho and I.S. Kim, Characteristics of soluble microbial products and extracellular polymeric substances in the membrane bioreactor for water reuse, *Desalination*, 202 (2007) 90-98.
- [27] S.F. Aquino, A.Y. Hu, A. Akramand and D.C. Stuckey, Characterization of dissolved compounds in submerged anaerobic membrane bioreactors (SAMBRs), *Journal of Chemical Technology and Biotechnology*, 81 (2006) 1894–1904.

Chapter 3

**3 SELECTION OF INORGANIC-BASED DRAW SOLUTIONS FOR
OSMOTICALLY-DRIVEN MEMBRANE PROCESSES**

(Submitted for publication in the *Journal of Membrane Science*)

Abstract

Osmotically-driven membrane processes use hypertonic draw solutions to induce mass transport of solvents (i.e., water) through semipermeable membranes. More than 500 inorganic compounds were screened as draw solution candidates by taking into consideration water solubility, phase, hazard, osmotic pressure, and cost. The desktop screening process resulted in 14 draw solutions suitable for forward osmosis applications. The 14 draw solutions were then tested in the laboratory to evaluate water flux and reverse salt flux through the membrane. Each of the draw solutions were tested at the same osmotic pressure difference across the membrane. Results indicated a wide range of water flux and reverse salt flux depending on the draw solution utilized. Internal concentration polarization was found to lower both water flux and reverse salt flux by reducing the draw solution concentration at the interface between the support and dense layer of the membrane. A small group of draw solutions was found to be most suitable for FO processes. With currently available FO membranes, MgCl_2 was found to be the best inorganic compound to make a draw solution; NaCl , NaHCO_3 , and Na_2SO_4 were the next best alternatives.

Keywords: Forward osmosis, Draw solution, Inorganic compound, Concentration polarization, Reverse salt diffusion

3.1 Introduction

Osmosis is the net diffusive transport of water through a selectively permeable membrane from a solution of low solute concentration (low osmotic pressure) to a draw solution of high solute concentration (high osmotic pressure). Draw solutions are typically made from low molecular weight salts [1]. In osmosis, the membrane allows passage of water, but rejects almost all solute molecules and/or ions.

From the mid 1970s there has been growing interest in engineered applications of osmosis [2-5], which is now referred to as forward osmosis (FO). In FO, impaired water is in contact with the dense side of the membrane and a highly concentrated draw solution is in contact with the support side of the membrane. Through osmosis, relatively pure water is withdrawn from the impaired water into the draw solution, the impaired water becomes concentrated and the draw solution becomes diluted. A desalination process (e.g., reverse osmosis (RO) or distillation) can be used to reconcentrate the draw solution and simultaneously produce high-quality product water. Thus, in most water treatment applications, FO is not the ultimate process but rather a high-level pretreatment step before an ultimate reconcentration/desalination process.

FO has been evaluated as an alternative method for seawater and brackish water desalination [1-5], wastewater concentration and reclamation [5-8], and food concentration [9-11]. FO can also be employed in conjunction with biological processes for wastewater reuse in osmotic membrane bioreactors (OMBRs) [12, 13]. The main

advantage of FO is that it operates at very low hydraulic pressure, it has high rejection of a broad range of contaminants, and it may have lower fouling propensity than pressure-driven membrane processes [8, 12, 14].

One key component for successful development of FO technologies is the selection of an appropriate draw solution. The main criterion is that the draw solution has a higher osmotic pressure than the feed solution. The osmotic pressure difference drives the process and can be substantially reduced by concentration polarization. Concentration polarization is the accumulation or depletion of solutes near the membrane surface. Because FO membranes are comprised of an dense layer on top of a porous support layer, concentration polarization occurs externally at the feed-membrane and draw solution-membrane interfaces, and internally in the porous support layer of the membrane. Concentration polarization results in the solute being concentrated on the feed side of the membrane and being diluted inside the support layer of the membrane (Fig 1).

Water flux (J_w) in FO is described by:

$$J_w = A(\pi_{D,b} - \pi_{F,b}) \quad (1)$$

where $\pi_{D,b}$ is the bulk osmotic pressure of the draw solution and $\pi_{F,b}$ is the bulk osmotic pressure of the feed solution. This equation, however, describes water flux only in the absence of concentration polarization. However, even when ultrapure water is used as the feed solution ($\pi_{F,b}=0$), internal concentration occurs and dilutes the solute concentration in the support layer of the membrane. McCutcheon et al. [15] derived an expression that modifies eq. (1) to include the effect of internal concentration polarization in FO applications.

$$J_w = A(\pi_{D,b} \exp(-J_w K)) \quad (2)$$

The exponent term in equation (2) is defined as the dilutive internal concentration polarization modulus:

$$\exp(-J_w K) = \frac{\pi_{D,i}}{\pi_{D,b}} \quad (3)$$

where $\pi_{D,i}$ is the osmotic pressure of the draw solution at the interface between the dense and support layer of the membrane, referred to as the effective draw solution osmotic pressure. Similarly, the effective draw solution concentration is the concentration at the interface between the dense and support layer of the membrane ($C_{D,i}$ in Figure 3.1) and is calculated utilizing eq. (3) assuming that $C_{D,i} / C_{D,b} = \pi_{D,i} / \pi_{D,b}$ [16]. The solute resistivity for diffusion within the porous support layer (K) is defined by:

$$K = \frac{t\tau}{D\varepsilon} \quad (4)$$

where t , τ , and ε are the thickness, tortuosity, and porosity of the support layer, respectively, and D is the diffusion coefficient of the draw solution.

Recent investigations have established that internal concentration polarization is a major factor in limiting water flux in osmotically-driven membrane processes [15, 17-19]. There is agreement that internal concentration polarization is influenced by the structure (thickness, tortuosity, and porosity) of the membrane support layer and by the diffusion coefficient of the draw solution [15, 17]. However, there is not unanimous agreement as to whether internal concentration polarization is influenced by the diffusion coefficient of the draw solution. McCutcheon et al. [15] present a model that was initially developed by Lee et al. [19] in which the membrane support layer characteristics and the

solution diffusion coefficient contribute to internal concentration polarization, while Tan and Ng [17] suggest that internal concentration polarization is influenced by the membrane characteristics only. In these investigations, NaCl was the only draw solution evaluated.

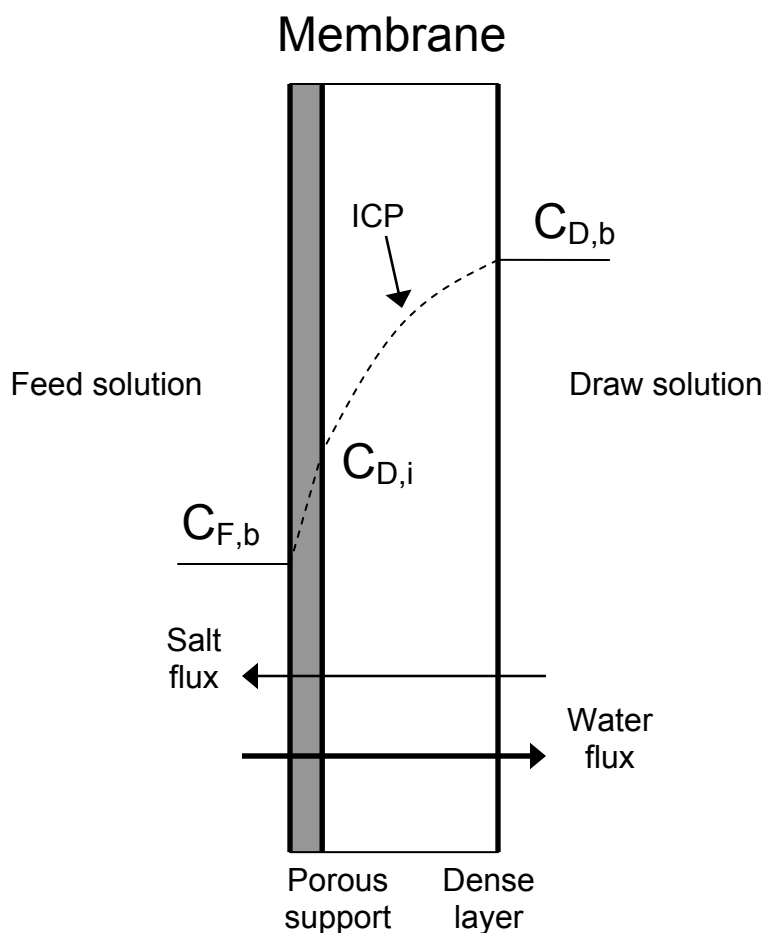


Figure 3.1 Illustration of an asymmetric membrane with the dense layer facing the feed solution and concentration profiles across the membrane. Internal concentration polarization (ICP) is also shown. The feed concentration is DI water so no external concentration polarization occurs. The osmotic pressures corresponding to $C_{F,b}$, $C_{D,i}$, and $C_{D,b}$ are denoted as $\pi_{F,b}$, $\pi_{D,i}$, and $\pi_{D,b}$.

Similar to RO, trace quantities of salts will diffuse from the feed solution into the draw solution. However, in osmotically-driven membrane processes, salts also diffuse through the membrane from the draw solution into the feed solution [20]. Reverse salt diffusion is expected to occur because of the large difference in solute concentration between the draw solution and the feed solution. The diffusion of solutes (J_s) through a semi-permeable membranes is described by Fick's Law [21]:

$$J_s = B \Delta C \quad (5)$$

where B is the solute permeability coefficient and ΔC is the solute concentration differential across the membrane. Internal concentration polarization decreases the rate of reverse salt diffusion by lowering the effective solute concentration at the interface between the dense and support layers of the membrane ($C_{D,i}$ in Figure 3.1) .

Reverse salt diffusion may also contaminate the feed solution. When FO is used to concentrate food, it can deteriorate the quality of the concentrated product, and when FO is used as alternative method for desalination, reverse salt diffusion may have an impact on the disposal of the concentrated feed solution. In the OMBR process, reverse salt diffusion may inhibit or have toxic effects on the microbial community in the reactor [12]. While numerous FO investigations have focused on the attainable water fluxes as a function of the draw solution composition and concentration, there is limited data on reverse salt diffusion into the feed solution and its dependence on membrane characteristics and draw solution composition [12, 13, 22].

Another important criterion in some FO applications is the availability of a suitable process for reconcentration of the draw solution after it has been diluted in the FO process. The reconcentration process should achieve high recovery of the draw

solution to minimize losses, be affordable, and be able to produce high-quality product water. When FO is used for production of potable water, it is important that draw solution solutes not be present in the final product water, and if trace concentrations are present, they must be below the drinking water maximum contaminant level. Other considerations for selection of suitable draw solutions are that the solute is water soluble, it is solid at ambient temperature and pressure, it is not toxic, it can be safely handled, exhibit relatively high osmotic pressure, and that the cost of the draw solution is low to ensure economically-viable process.

Very often an NaCl solution is used as the draw solution because it is highly soluble, it is not toxic at low concentrations, and it is relatively easy to reconcentrate to high concentrations using conventional desalination processes (e.g., RO or distillation) without risk of scaling [5, 6, 8, 12, 23]. Other chemicals have also been suggested and tested as draw solutes. McCutcheon et al. [3, 24] report a method for seawater desalination using a proprietary draw solution based on ammonium and carbon dioxide and Petrotos et al. [9, 11] investigate the concentration of tomato juice with FO using CaCl_2 , $\text{Ca}(\text{NO}_3)_2$, and NaCl.

The objective of this investigation was to develop a protocol for the selection of optimal draw solutions for an FO process/application. More than 500 inorganic compounds were screened, and at the end of the screening process, selected draw solutions were tested in the laboratory to evaluate water flux and reverse salt diffusion. RO reconcentration and rejection of the draw solutions was evaluated using RO system design software [25, 26]. Analysis of experimental data and model results, combined with

considerations of the costs associated with the FO and RO processes, provided guidelines for selection of the most appropriate draw solution for FO applications.

Furthermore, the large draw solution matrix in terms of both constituents and concentrations enabled insight into the role of membrane characteristics and solution characteristics on water flux and reverse salt diffusion. Specifically, the influence of concentration polarization on water flux and reverse salt diffusion was elucidated.

3.2 Materials and methods

3.2.1 Draw solution selection criteria

A flow diagram that describes the draw solution selection process is illustrated in Figure 3.2. More than 500 inorganic compounds were initially considered. The list was first shortened by eliminating compounds that are not soluble in water and that are not solid at ambient temperature and pressure. Then, the Hazardous Materials Identification System (HMIS) codes [27] of the remaining compounds were examined. The HMIS defines the health, flammability, and physical hazards of a chemical on a scale of 0 to 4, with 0 representing minimal hazard and 4 representing severe hazard. Candidate compounds with a ranking greater than 2 (moderate hazard) in at least one category were eliminated. Next, OLI Stream AnalyzerTM (OLI Systems, Inc., Morris Plains, NJ) was used to obtain the osmotic pressure of the draw solution candidates as a function of solution concentration. Solutions with an osmotic pressure less than 1000 kPa (145 psi) at saturation concentration were eliminated. And last, procurement costs of the compounds were evaluated. Draw solution costs were evaluated based on Fisher Scientific unit prices [28]. The specific cost of each draw solution was determined by calculating the cost of

solute needed to produce one liter of draw solution with an osmotic pressure of 2800 kPa (406 psi). Solutions with a specific cost greater than \$10/L were eliminated. At the end of the selection process, 14 inorganic compounds remained on the list.

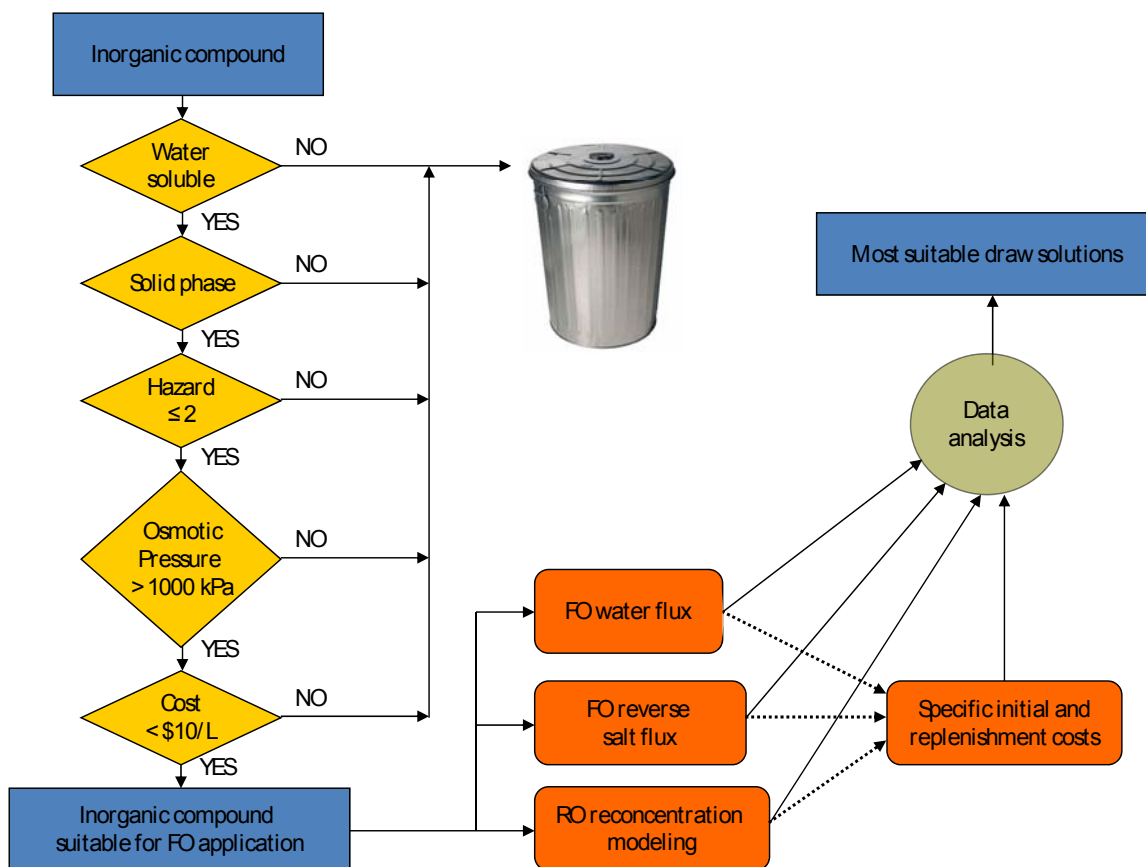


Figure 3.2 Illustration of flow diagram for draw solution selection.

The selected draw solutions were then investigated experimentally under FO conditions and theoretically under RO re-concentration conditions. FO experiments were performed to quantify the water flux and reverse salt diffusion. RO modeling was performed to evaluate RO re-concentration of the draw solution and permeate water quality. The replenishment cost of the draw solution due to reverse salt diffusion through the FO membrane and solute passage through the RO membrane was also calculated. The

replenishment cost is an important consideration in differentiating the draw solute candidates; the operating costs of all the candidates should be identical because all the draw solutions were tested at the same osmotic pressure. Testing at the same osmotic pressure ensures that the RO reconcentration process (the energy intense part of the process) operates at the same hydraulic pressure and has the same power requirements.

3.2.2 *FO Membrane*

A flat-sheet cellulose triacetate (CTA) membrane (membrane B in Ref. [12]) (Hydration Technologies, Inc., Albany, OR) was used in all FO experiments. The physical characteristics of this specific CTA membrane are unique compared with other commercially-available semi-permeable membranes and the CTA membrane has been determined to be the best available membrane in most FO investigations for various applications [1, 8].

3.2.3 *Solution chemistries*

Certified ACS-grade salts (Fisher Scientific, Pittsburg, PA) were used to make the draw solutions. These include CaCl_2 , $\text{Ca}(\text{NO}_2)_3$, KBr , KCl , KHCO_3 , K_2SO_4 , MgCl_2 , MgSO_4 , NaCl , NaHCO_3 , Na_2SO_4 , NH_4Cl , NH_4HCO_3 , and $(\text{NH}_4)_2\text{SO}_4$. Ultrapure water was used as the feed solution in all experiments. For each draw solution tested, three osmotic pressures (1400, 2800, and 4200 kPa (203, 406, and 609 psi)) were evaluated. For a few of the draw solutions (K_2SO_4 , MgSO_4 , and NaHCO_3), it was not possible to reach an osmotic pressure of 4200 kPa due to their lower solubility. The concentrations of each draw solution for each of the three osmotic pressures, together with the solubility of each

solution, were determined using OLI Stream AnalyzerTM (OLI Systems, Inc., Morris Plains, NJ). Diffusion coefficients of the draw solutions were calculated according to Lobo [29], Mullin and Nienow [30], and Albright et al. [31]. All of the values are summarized in Table 3.1 for each of the salt concentrations tested.

3.2.4 FO membrane permeability characterization

A flat-sheet, bench-scale RO test unit was used to determine the water permeability coefficient (A) of the FO membrane. The CTA membrane was installed in a SEPA cell (GE Osmonics, Minnetonka, MN) with the dense layer of the membrane facing the feed solution (RO mode). The effective membrane surface area was 139 cm². Mesh spacers placed in the feed channel enhanced the turbulence of the ultrapure water feed stream. A high-pressure positive displacement pump (Wanner Engineering Inc., Minneapolis, MN) was used to recirculate the feed solution at 1.5 L/min.

The FO membrane water permeability coefficient (A) was determined using:

$$A = \frac{J_w}{\Delta\pi - \Delta P} \quad (6)$$

where $\Delta\pi$ is the osmotic pressure differential across the membrane and ΔP is the hydraulic pressure differential across the membrane. Because ultrapure water was used as the feed solution, $\Delta\pi$ was zero during the experiments. Pressure was increased in 345-kPa (50-psi) increments from 345 to 1,035 kPa (50 to 150 psi). Pressure was held constant at each increment for a duration of 3 h. Flux through the membrane was calculated based on the change of weight of the permeate water. The temperature was held constant at 25 °C.

3.2.5 FO performance experiments

FO performance was evaluated using a flat-sheet bench-scale system (Figure 3.3). The CTA membrane was installed in a modified SEPA cell (GE Osmonics, Minnetonka, MN) that has symmetric channels on both sides of the membrane. This allowed for both the feed and draw solutions to flow tangential to the membrane.

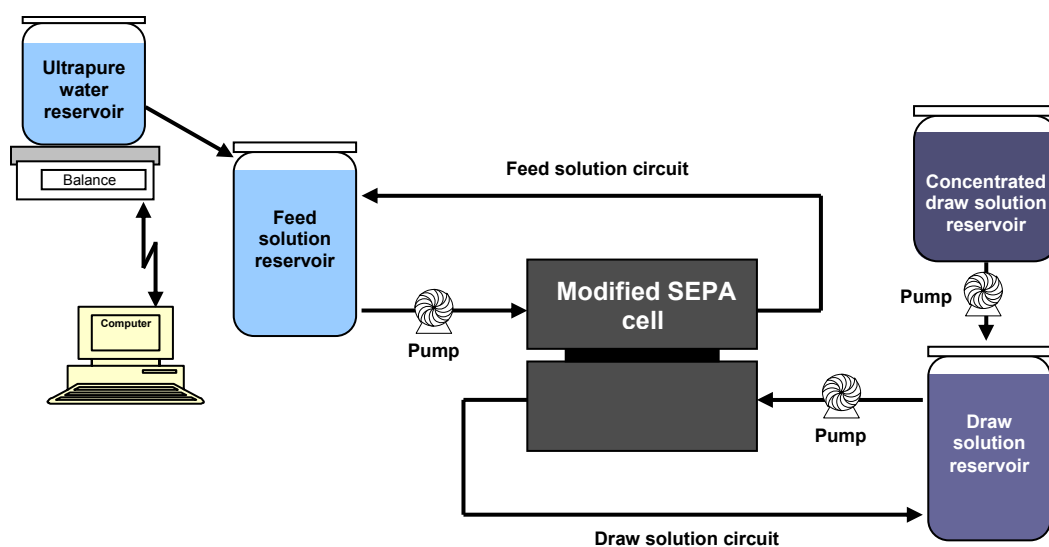


Figure 3.3 Schematic of bench-scale FO system.

The dense layer of the membrane was facing the feed solution (FO mode). The effective membrane surface area was 139 cm^2 . Mesh spacers placed in the feed and draw solution channels supported the membrane and enhanced mixing. Two variable-speed gear pumps (Cole-Palmer, Vernon Hills, IL) were used to recirculate the feed and draw solutions on the opposite sides of the membrane at 1.5 L/min . The temperatures of the feed and draw solutions were monitored with thermocouples installed at the inlets of the SEPA cell. The temperature was held constant at $25 \text{ }^\circ\text{C}$. The ultrapure water feed was contained in a 5.4-

L constant-level reservoir; the volume was held constant by continuous replenishment of the water that crossed the membrane by ultrapure water from an ultrapure water reservoir. The ultrapure water reservoir was placed on an analytical balance linked to a computer. The draw solution was contained in a 10-L reservoir. The draw solution concentration was held constant by continuous addition of concentrated draw solution from a concentrated draw solution reservoir. The pH and conductivity of the feed and draw solutions were monitored with probes placed in the feed and draw solution reservoirs.

The FO performance for each draw solution was evaluated by determining the water flux and reverse salt diffusion. The first two columns in Table 3.1 represent the matrix of experiments that were performed with ultrapure water as the feed solution. For each draw solution tested, three concentrations were evaluated. Each experiment was carried out for 24 h. Flux through the membrane was calculated based on the change of weight of the ultrapure water in the reservoir. At the end of the experiment, a grab sample of the feed solution was analyzed for ion composition. This analysis was used to quantify reverse salt diffusion. The temperature of the system was held constant at 25 °C.

Table 3.1 Aqueous solution osmotic pressure (π_{DS}), concentration (C_{DS}), solubility, and diffusion coefficient (D).

DS	π_{DS} kPa	C_{DS} g/L	Solubility at 25 °C g/L	D $10^{-9} \text{ m}^2/\text{s}$
CaCl ₂	1400	24.3	821	1.11
	2800	43.8		1.13
	4200	62.3		1.15
Ca(NO ₃) ₂	1400	42.6	1209	n.a. ^a
	2800	87.2		n.a.
	4200	131.2		n.a.
KBr	1400	37.9	536	1.87
	2800	71.3		1.9
	4200	104.7		1.95
KCl	1400	23.4	313	1.84
	2800	47.0		1.86
	4200	70.3		1.89
KHCO ₃	1400	32.0	200	1.26
	2800	65.5		1.20
	4200	99.0		1.15
K ₂ SO ₄	1400	49.4	105	1.11
	2800	101.4		1.10
MgCl ₂	1400	20.0	466	1.04
	2800	34.2		1.05
	4200	47.6		1.06
MgSO ₄	1400	73.8	342	0.43
	2800	141.3		0.37
NaCl	1400	17.9	315	1.48
	2800	35.2		1.47
	4200	51.8		1.48
NaHCO ₃	1400	30.3	101	1.01
	2800	63.9		0.96
Na ₂ SO ₄	1400	41.0	256	0.88
	2800	84.7		0.76
	4200	127.3		0.67
NH ₄ Cl	1400	17.0	305	1.84
	2800	32.6		1.87
	4200	48.2		1.91
NH ₄ HCO ₃	1400	25.2	232	n.a.
	2800	52.8		n.a.
	4200	83.4		n.a.
(NH ₄) ₂ SO ₄	1400	39.4	542	0.89
	2800	74.3		0.95
	4200	109.1		0.99

^a Values not available in the literature

3.2.6 *Analytical methods*

The ion compositions of the feed solutions were analyzed using different methods. Calcium, magnesium, potassium, and sodium were analyzed using inductively coupled plasma spectrophotometry (Perkin Elmer, Norwalk, CT); bromide, chloride, and sulfate, using ion chromatography (Dionex, Sunnyvale, CA); bicarbonate using total organic carbon analysis (Shidmadzu, Columbia, CO); and ammonium and nitrate using a nitrogen flow injection analysis system (Lachat, Loveland, CO).

3.2.7 *RO reconcentration evaluation*

The ability to reconcentrate each draw solution was evaluated by determining RO permeate water concentrations using RO system design software. Reverse Osmosis System Analysis (ROSA) (Dow Filmtec, Midland, MI) [26] was used to simulate draw solution reconcentration with an SW30HRLE-4040 membrane element and IMSDesign (Hydranautics, Oceanside, CA) [25] was used to simulate reconcentration with an SWC5-4040 membrane element. These membranes are the tightest RO membranes for the two manufacturers and were selected so to achieve the lowest permeate concentration and the highest draw solution retention in the system. All simulations were performed using five RO membrane elements in series, at a feed flowrate of 3.0 m³/h (13 gpm), and with a system recovery of 35%. The draw solutions were tested at a feed osmotic pressure of 2800 kPa (406 psi) and a temperature of 25 °C. All of the draw solutions were tested with the exception of KBr because neither software included bromide in their database.

3.3 Results and discussion

3.3.1 Water flux

Water flux results for each draw solution tested are summarized in Table 3.2. Draw solutions in Table 3.2 are ordered from the highest flux to the lowest flux using water flux at a draw solution osmotic pressure of 2800 kPa (the middle value). For the osmotic driving force of 2800 kPa, water fluxes ranged from 3.02×10^{-6} m/s (10.9 L/m²h) for KCl to 1.54×10^{-6} m/s (5.5 L/m²h) for MgSO₄. As anticipated, for each draw solution, water flux increases with increasing draw solution osmotic pressure. The difference in water fluxes achieved by the different draw solutions tested is solely due to internal concentration polarization effects because all the draw solutions were tested at a concentration that resulted in the same bulk osmotic pressure. Internal concentration polarization reduces the effective osmotic pressure difference across the dense layer of the membrane, and therefore, reduces water flux (eq. (3)). The internal concentration polarization modulus (K) is a function of the support layer characteristics (t , τ , and ε) and D (eq. (4)). Calculated values of K are also shown in Table 3.2. The term $t\tau/\varepsilon$ was calculated for each experimental condition; this term represents the structural characteristic of the membrane support layer, and therefore, should be constant for a given membrane. Results in Table 3.2 indicate that the term $t\tau/\varepsilon$ remains fairly constant under the different experimental conditions. The average $t\tau/\varepsilon$ was 4.27×10^{-4} m with a standard deviation of 0.69×10^{-4} m; an acceptable value considering the uncertainties in calculating D [29]. Because the same membrane was used for all the experiments, this reveals that internal concentration polarization is strongly dependent on D . Therefore, knowing the diffusion coefficient of a draw solution and the membrane support layer

characteristics, together with the membrane water permeability, would enable prediction of water flux of an FO system.

3.3.2 *Salt diffusion*

Water flux and reverse salt diffusion (J_s) are summarized in Table 3.3 for different experimental conditions. Draw solutions are ordered in Table 3.3 by magnitude of reverse salt diffusion – from the lowest to the highest solute diffusion at a draw solution osmotic pressure of 2800 kPa. For a bulk osmotic pressure of 2800 kPa, reverse salt diffusion ranged from 1.2 g/m²h for MgSO₄ to 22.0 g/m²h for KBr. As anticipated, reverse salt diffusion decreases with decreasing draw solution concentration. Draw solutions containing divalent ions (i.e., CaCl₂, Ca(NO₃)₂, MgCl₂, and MgSO₄) generally showed lower reverse salt diffusion than draw solutions containing monovalent ions. The lower reverse salt diffusion is attributed to the higher hydrated radius of divalent than monovalent ions [32]. In particular, both potassium and bromide have relatively small hydrated radii (approximately 300 pm), compared to the other ions tested [32-34], and result in greater rates of reverse salt diffusion. NH₄HCO₃ also showed one of the highest rates of reverse salt diffusion; this behavior suggests a specific affinity of the combination of the NH₄⁺ and HCO₃⁻ ions to the CTA membrane. This behavior is not observed when only ammonium or bicarbonate is present in a draw solution (i.e., KHCO₃, NaHCO₃, NH₄Cl, and (NH₄)₂SO₄), suggesting that in these cases, ammonium and bicarbonate diffuse more slowly through the membrane to maintain draw solution electroneutrality. Similar rates of reverse NH₄HCO₃ diffusion are reported elsewhere [22].

Table 3.2 Water flux (J_w), solute resistivity (K), and structural characteristic of the membrane support layer ($t\tau/\varepsilon$) for each draw solution tested.

DS	C_{DS} g/L	π_{DS} kPa	J_w 10^{-6} m/s	K 10^5 s/m	$t\tau/\varepsilon$ 10^{-4} m
KCl	70.3	4200	3.74	2.37	4.48
	47.0	2800	3.02	2.3	4.28
	23.4	1400	1.87	2.56	4.71
NH ₄ Cl	48.2	4200	3.61	2.56	4.88
	32.6	2800	2.90	2.53	4.74
	17.0	1400	1.88	2.52	4.65
KBr	104.7	4200	3.59	2.58	5.03
	71.3	2800	2.84	2.67	5.07
	37.9	1400	1.84	2.72	5.08
NaCl	50.8	4200	3.38	2.92	4.32
	35.2	2800	2.68	3.05	4.49
	17.9	1400	1.73	3.25	4.8
CaCl ₂	62.3	4200	3.22	3.22	3.69
	43.8	2800	2.64	3.15	3.55
	24.3	1400	1.75	3.11	3.46
K ₂ SO ₄	101.4	2800	2.52	3.47	3.82
	49.4	1400	1.74	3.19	3.54
	NaHCO ₃	63.9	2800	2.47	3.62
Ca(NO ₃) ₂	30.3	1400	1.68	3.53	3.56
	131.2	4200	2.97	n.a. ^a	n.a.
	87.2	2800	2.46	n.a.	n.a.
MgCl ₂	42.6	1400	1.66	n.a.	n.a.
	47.6	4200	2.70	4.48	4.75
	33.8	2800	2.33	4.08	4.28
(NH ₄) ₂ SO ₄	20.0	1400	1.58	4.09	4.25
	109.1	4200	2.74	4.36	4.34
	74.3	2800	2.28	4.29	4.08
KHCO ₃	39.4	1400	1.65	3.82	3.41
	99.0	4200	2.80	4.2	4.85
	65.5	2800	2.25	4.4	5.27
Na ₂ SO ₄	32.0	1400	1.48	4.85	6.1
	127.3	4200	2.56	4.93	3.32
	84.7	2800	2.14	4.87	3.7
NH ₄ HCO ₃	41.0	1400	1.48	4.84	4.26
	83.4	4200	2.85	n.a.	n.a.
	52.8	2800	2.04	n.a.	n.a.
MgSO ₄	25.2	1400	1.52	n.a.	n.a.
	141.3	2800	1.54	8.92	3.34
	73.8	1400	1.18	7.93	3.44
Average					4.27

^a Values not calculated because the diffusion coefficient (D) is not available.

For each draw solution tested, the ratio between reverse salt diffusion and effective draw solution concentration was calculated. The role of internal concentration polarization in reverse salt diffusion is to reduce the effective solute concentration at the interface between the dense and support layers of the membrane ($C_{D,i}$), thus reducing the diffusion driving force. Results in Table 3.3 indicate that for each draw solution, the ratio between reverse salt diffusion and effective draw solution concentration is relatively similar for the three different osmotic pressures tested, suggesting that the reverse salt diffusion through the membrane is directly proportional to the draw solution concentration difference across the membrane dense layer and not to the difference between bulk concentrations. This behavior is in accordance with the solute transport mechanism in nonporous membranes [21].

The ratio between reverse salt diffusion and water flux was calculated and it is shown in the rightmost column in Table 3.3. The ratio between reverse salt diffusion and water flux is a useful tool to estimate how much salt is lost during FO operation; thus, estimating the efficiency of the process. For example, for each liter of water recovered through the currently tested FO membrane, 0.2 g of KHCO_3 diffuses through the membrane compared to 2.26 g of KBr . These values were used in calculating the economic viability of the FO with different DS as they directly impact the replenishment costs (further discussed in Section 3.3.4).

Table 3.3 Reverse salt diffusion (J_s), water flux (J_w), effective osmotic pressure ($\pi_{D,i}$), effective draw solution concentration ($C_{D,i}$), ratio between reverse salt diffusion and effective draw solution concentration ($J_s/C_{D,i}$), and ratio between reverse solute diffusion and water flux (J_s/J_w).

DS	C_{DS} g/L	π_{DS} kPa	J_s g/m ² h	J_w m/s	$\pi_{D,i}$ kPa	EC _{DS} g/L	$J_s/C_{D,i}$ (g/m ² h)/(g/L)	J_s/J_w g/L
MgSO ₄	141.3	2800	1.2	1.54	711	37.2	0.03	0.21
	73.8	1400	0.9	1.18	548	28.2	0.03	0.22
KHCO ₃	99.0	4200	2.0	2.80	1296	29.5	0.07	0.20
	65.5	2800	1.4	2.25	1042	23.5	0.06	0.17
	32.0	1400	0.8	1.48	684	14.9	0.05	0.14
NaHCO ₃	63.9	2800	1.7	2.47	1145	24.2	0.07	0.19
	30.3	1400	0.9	1.68	776	15.4	0.06	0.16
Na ₂ SO ₄	127.3	4200	3.1	2.56	1187	34.2	0.09	0.33
	84.7	2800	2.7	2.14	989	27.9	0.10	0.36
	41.0	1400	1.9	1.48	684	18.2	0.11	0.36
(NH ₄) ₂ SO ₄	109.1	4200	3.6	2.74	1270	36.1	0.10	0.36
	74.3	2800	3.3	2.28	1054	23.6	0.14	0.40
	39.4	1400	2.5	1.65	765	30.8	0.08	0.43
K ₂ SO ₄	101.4	2800	3.7	2.52	1167	40.8	0.09	0.40
	49.4	1400	2.3	1.74	804	27.3	0.09	0.37
MgCl ₂	47.6	4200	5.6	2.70	1252	18.4	0.30	0.58
	33.8	2800	4.8	2.33	1081	16.7	0.29	0.57
Ca(NO ₃) ₂	20.0	1400	3.4	1.58	733	13.0	0.26	0.59
	131.2	4200	6.6	2.97	1374	41.8	0.16	0.62
	87.2	2800	6.0	2.46	1138	34.2	0.17	0.67
NaCl	42.6	1400	3.7	1.66	767	22.2	0.17	0.63
	50.8	4200	9.1	3.38	1565	19.9	0.46	0.75
	35.2	2800	7.2	2.68	1239	15.8	0.45	0.74
NH ₄ Cl	17.9	1400	4.6	1.73	799	10.2	0.45	0.74
	48.2	4200	10.2	3.61	1670	20.0	0.51	0.79
	32.6	2800	7.6	2.90	1343	16.4	0.47	0.73
CaCl ₂	17.0	1400	5.3	1.88	871	11.1	0.48	0.79
	62.3	4200	9.5	3.22	1491	25.6	0.37	0.82
	43.8	2800	7.9	2.64	1221	21.8	0.36	0.83
KCl	24.3	1400	4.8	1.75	812	15.9	0.30	0.76
	70.3	4200	15.3	3.74	1734	29.1	0.53	1.14
	47.0	2800	12.3	3.02	1397	23.4	0.52	1.13
NH ₄ HCO ₃	23.4	1400	6.8	1.87	867	14.4	0.47	1.01
	83.4	4200	20.6	2.85	1318	23.7	0.87	2.01
	52.8	2800	18.2	2.04	944	16.9	1.08	2.48
KBr	25.2	1400	11.7	1.52	702	12.6	0.93	2.14
	104.7	4200	29.2	3.59	1662	44.2	0.66	2.26
	71.3	2800	22.0	2.84	1313	35.9	0.61	2.15
	37.9	1400	12.3	1.84	850	24.8	0.50	1.86

3.3.3 *Reverse osmosis reconcentration*

The concentrations of RO permeate water modeled with ROSA and IMSDesign computer programs, along with average permeate concentrations are summarized in Table 3.4. Average permeate concentrations were then used to evaluate the replenishment costs. Permeate concentration was used in evaluating the RO reconcentration process. For all the draw solutions, permeate concentrations were lower utilizing ROSA compared to IMSDesign. The main difference between the two software outputs was when treating compounds containing sulfates and nitrates; in these cases, IMSDesign predicted higher permeate concentrations of these compounds, suggesting that the SWC5-4040 membrane might have higher permeability to nitrates and sulfates. However, as expected, both simulations showed high rejection of divalent draw solutions (CaCl_2 , MgCl_2 , and MgSO_4) and relatively poor rejection of solution containing bicarbonate (KHCO_3 , NaHCO_3 , and NH_4HCO_3). It is worth noting that in the case of the NH_4HCO_3 draw solution another reconcentration process can be utilized [3]. Utilizing this reconcentration method it is possible to achieve a permeate concentration lower than 1 ppm [35].

Table 3.4 Calculated RO permeate water concentrations using ROSA and IMSDesign software. Average RO permeate water concentrations are also reported.

DS	C_{DS}	C_P (ROSA)	C_P (IMS)	C_P Average
	g/L	mg/L	mg/L	mg/L
CaCl ₂	43.8	62.1	132.2	97.1
Ca(NO ₃) ₂	87.2	129.4	1135.7	632.6
KCl	47.0	187.9	257.4	222.7
KHCO ₃	65.5	255.0	374.8	314.9
K ₂ SO ₄	101.4	50.7	307.6	179.1
MgCl ₂	33.8	53.8	111.5	82.6
MgSO ₄	141.3	39.5	106.4	72.9
NaCl	35.2	127.3	179.0	153.2
NaHCO ₃	63.9	199.0	291.6	245.3
Na ₂ SO ₄	84.7	40.6	213.0	126.8
NH ₄ Cl	32.6	155.0	184.8	169.9
NH ₄ HCO ₃	52.8	242.0	302.4	272.2
(NH ₄) ₂ SO ₄	74.3	40.2	240.6	140.4

3.3.4 Draw solution costs

Specific draw solution cost ranges from 0.53 to 7.35 \$/L for a draw solution having an osmotic pressure of 2800 kPa (Table 3.5). This cost can be considered as an initial capital investment cost, because the draw solution is continuously circulated between the FO and RO systems. Another, more important cost item associated with the draw solution is the operating cost of replenishing the draw solution due to reverse salt diffusion through the FO membrane (Table 3.3) and solute diffusion through the RO membrane (Table 3.4). Draw solution replenishment costs per liter of water that crosses the membrane are summarized in Table 3.6. In general, FO replenishment costs are higher than RO replenishment costs, due to the lower rejection of FO membranes compared to RO membranes.

Table 3.5 Draw solute specific cost. Specific cost is defined as the cost of solute needed to produce 1 L of draw solution with an osmotic pressure of 2800 kPa.

DS	Cost	Specific cost
	\$/kg	\$/L
CaCl ₂	35	1.53
Ca(NO ₃) ₂	70	6.10
KBr	80	5.70
KCl	37	1.74
KHCO ₃	32	2.10
K ₂ SO ₄	53	5.38
MgCl ₂	28	0.96
MgSO ₄	52	7.35
NaCl	15	0.53
NaHCO ₃	20	1.28
Na ₂ SO ₄	8	1.28
NH ₄ Cl	26	0.85
NH ₄ HCO ₃	45	2.38
(NH ₄) ₂ SO ₄	60	4.46

Table 3.6 Draw solute replenishment cost. Replenishment cost is the product between the specific salt diffusion and the draw solution cost for FO and between the permeate concentration and the draw solution cost for RO. Total cost is the sum of the two.

DS	FO cost	RO cost	Total cost
	\$/L	\$/L	\$/L
CaCl ₂	0.029	0.003	0.032
Ca(NO ₃) ₂	0.047	0.044	0.091
KBr	0.172	n.a.	0.172
KCl	0.042	0.008	0.050
KHCO ₃	0.005	0.010	0.015
K ₂ SO ₄	0.021	0.009	0.031
MgCl ₂	0.016	0.002	0.018
MgSO ₄	0.011	0.004	0.015
NaCl	0.011	0.002	0.013
NaHCO ₃	0.004	0.005	0.009
Na ₂ SO ₄	0.003	0.001	0.004
NH ₄ Cl	0.019	0.004	0.023
NH ₄ HCO ₃	0.111	0.012	0.124
(NH ₄) ₂ SO ₄	0.024	0.008	0.033

The total replenishment costs for the tested FO membrane and commercial seawater RO membranes (FO + RO) range from 0.004 \$ to 0.172 \$ per liter of water produced. It is worth noting that this cost estimation is based on the purchasing cost of chemicals for laboratory use, purchasing of bulk quantities of salts would likely reduce the replenishment costs. It is also needed to point out that the purchasing cost of chemical are those found at the time the article was prepared, it is therefore recommended to consider the actual purchasing cost of chemical for future selection of draw solutions.

3.3.5 Is there a best draw solution?

Five parameters were used for an overall evaluation of the draw solutions tested. Water flux, reverse salt diffusion, RO permeate concentration, draw solution initial cost, and draw solution replenishment cost were each normalized to the best value obtained for that individual parameter (Table 3.7).

Table 3.7 Ratios between the best draw solution and the draw solution itself for each of the five parameters investigated. Each draw solution was evaluated at an osmotic pressure of 2800 kPa.

DS	Water flux	Solute reverse diffusion	RO permeate concentration	Initial cost	Replenishment cost
	$\frac{J_w}{(J_w)_{KCl}}$	$\frac{(J_s)_{KHCO_3}}{J_s}$	$\frac{(C_{P,RO})_{MgCl_2}}{C_{P,RO}}$	$\frac{(\text{Initial cost})_{NaCl}}{\text{Initial cost}}$	$\frac{(\text{Replenishment cost})_{Na_2SO_4}}{\text{Replenishment cost}}$
CaCl ₂	0.87	0.20	0.75	0.35	0.12
Ca(NO ₃) ₂	0.81	0.25	0.12	0.09	0.04
KBr	0.94	0.08	n.a.	0.09	0.02
KCl	1.00	0.15	0.33	0.30	0.08
KHCO ₃	0.75	1.00	0.23	0.25	0.25
K ₂ SO ₄	0.84	0.41	0.41	0.10	0.13
MgCl ₂	0.77	0.29	0.88	0.55	0.21
MgSO ₄	0.51	0.78	1.00	0.07	0.26
NaCl	0.89	0.18	0.48	1.00	0.29
NaHCO ₃	0.82	0.87	0.30	0.41	0.44
Na ₂ SO ₄	0.71	0.47	0.58	0.41	1.00
NH ₄ Cl	0.96	0.23	0.43	0.62	0.16
NH ₄ HCO ₃	0.68	0.07	0.27	0.22	0.03
(NH ₄) ₂ SO ₄	0.75	0.41	0.52	0.12	0.12

For example, the highest water flux was achieved with a KCl draw solution, so, the ratio $J_w/(J_w)_{KCl}$ was calculated for each draw solution. Similar calculations were performed for the other parameters. This procedure enabled the ranking of each draw solution for each parameter investigated.

While the draw solution initial cost does not have an impact on the long-term operation of an FO process, the draw solution replenishment cost may be a useful parameter to evaluate the economic viability of the FO system. For the FO process, the replenishment cost is calculated as the product between the specific reverse salt diffusion and the unit cost of the solute; therefore, it implicitly considers water flux and reverse salt diffusion. Similarly, in the RO process, the replenishment cost is calculated as the

product between the RO permeate concentration and the unit cost of the solute. Under these conditions, the three draw solutions that ranked highest were NaCl, NaHCO₃, and Na₂SO₄; NaCl mainly because of its high water flux, NaHCO₃ mainly because of its low reverse salt diffusion, and Na₂SO₄ mainly because of its low cost.

It is also worthwhile to consider the rank of the draw solutions regardless of their cost. Analyzing water flux, reverse salt diffusion, and RO permeate concentration (Table 3.7), five draw solutions rank particularly high in two of the three parameters: they are CaCl₂, KHCO₃, MgCl₂, MgSO₄, and NaHCO₃. CaCl₂ and MgCl₂ rank high because of their relatively high water flux and low RO permeate concentration; KHCO₃ and NaHCO₃ because of their relatively high water flux and low reverse salt diffusion; and MgSO₄ because of its relatively low reverse salt diffusion and RO permeate concentration. The different features of these draw solutions highlight the importance of considering the specific application and membrane being used prior to selecting the most appropriate draw solution. Furthermore, depending on the constituents in the feed water, the use of draw solutions containing calcium, magnesium, sulfate, or bicarbonate may lead to the formation of scaling on the membrane surface [36, 37]. It is worth noting, however, that Mg(OH)₂ (milk of magnesia), one of the main precipitates of magnesium, can be formed only at pHs greater than 9, while CaCO₃ (calcite) and CaSO₄ (gypsum) can be formed within a wider pH range [37]. This condition would allow using MgCl₂ in most FO applications without the risk of scaling.

3.4 Conclusions

The fourteen draw solutions that were investigated were sorted based on water flux, reverse salt diffusion, permeate water concentration after RO reconcentration, and cost. The large draw solution matrix in terms of both constituents and concentrations highlighted the influence of internal concentration polarization on water flux and reverse salt diffusion. Internal concentration polarization influences water flux and was found to be strongly dependent on the diffusion coefficient of the draw solution. Also, internal concentration polarization influences the rate of reverse salt diffusion by lowering the draw solute concentration at the interface between the support and the dense layer of the membrane.

The most suitable draw solution depends on the specific FO application and membrane used; however, a small group of draw solutes (CaCl_2 , KHCO_3 , MgCl_2 , MgSO_4 , NaCl , NaHCO_3 , and Na_2SO_4) appeared to be the most suitable to be employed in FO processes with currently available FO membranes. From the literature, the most widely employed draw solutions for FO investigations are CaCl_2 , $\text{Ca}(\text{NO}_3)_2$, NaCl , and a proprietary draw solution based on ammonium and carbon dioxide, similar to NH_4HCO_3 [3, 5, 6, 8, 9, 11, 12, 23]. From this investigation it is apparent that a broader range of draw solutes should be considered for future FO applications.

Acknowledgments

The authors acknowledge the support of the Department of Energy, Grant No. DE-FG02-05ER64143 and Hydration Technology Innovations (Albany, OR) for donating the FO membrane.

Nomenclature

ΔC	Concentration differential across the membrane (g/L)
ΔP	Hydraulic pressure differential (kPa)
$\Delta \pi$	Osmotic pressure differential (kPa)
ε	Porosity
$\pi_{D,b}$	Osmotic pressure of the bulk draw solution (kPa)
$\pi_{D,m}$	Osmotic pressure of the draw solution at the membrane surface (kPa)
$\pi_{F,b}$	Osmotic pressure of the bulk feed solution (kPa)
π_{DS}	Osmotic pressure of the draw solution (kPa)
τ	Tortuosity
A	Water permeability coefficient ((m/s)/kPa)
B	Salt permeability coefficient (m/s)
$C_{D,b}$	Salt concentration of the bulk draw solution (g/L)
$C_{D,m}$	Salt concentration of the draw solution at the membrane surface (g/L)
C_{DS}	Salt concentration of the draw solution (g/L)
$C_{F,b}$	Salt concentration of the bulk feed solution (g/L)
C_P	Salt concentration in RO permeate solution (g/L)
D	Salt diffusion coefficient (m ² /s)

DS	Draw solution
J_w	Water flux (m/s)
J_s	Salt diffusion ($\text{g/m}^2 \text{ h}$)
K	Internal concentration polarization mass transfer coefficient (s/m)
t	Thickness (m)

References

- [1] T.Y. Cath, A.E. Childress and M. Elimelech, Forward osmosis: Principles, applications, and recent developments, *Journal of Membrane Science*, 281 (2006) 70-87.
- [2] R.E. Kravath and J.A. Davis, Desalination of seawater by direct osmosis, *Desalination*, 16 (1975) 151-155.
- [3] J.R. McCutcheon, R.L. McGinnis and M. Elimelech, A novel ammonia--carbon dioxide forward (direct) osmosis desalination process, *Desalination*, 174 (2005) 1-11.
- [4] C.D. Moody and J.O. Kessler, Forward osmosis extractors, *Desalination*, 18 (1976) 283-295.
- [5] R.J. York, R.S. Thiel and E.G. Beaudry, Full-scale experience of direct osmosis concentration applied to leachate management, *Seventh International Waste Management and Landfill Symposium (Sardinia '99)*, Cagliari, Italy, 1999.
- [6] T.Y. Cath, S. Gormly, E.G. Beaudry, M.T. Flynn, V.D. Adams and A.E. Childress, Membrane contactor processes for wastewater reclamation in space. I. Direct osmotic concentration as pretreatment for reverse osmosis, *Journal of Membrane Science*, 257 (2005) 85-98.
- [7] T.Y. Cath, V.D. Adams and A.E. Childress, Membrane contactor processes for wastewater reclamation in space. II. Combined direct osmosis, osmotic distillation, and membrane distillation for treatment of metabolic wastewater, *Journal of Membrane Science*, 257 (2005) 111-119.
- [8] R.W. Holloway, A.E. Childress, K. E. Dennett and T.Y. Cath, Forward osmosis for concentration of anaerobic digester centrate, *Water Research*, 41 (2007) 4005-4014.

- [9] K.B. Petrotos, P.C. Quantick and H. Petropakis, Direct osmotic concentration of tomato juice in tubular membrane-module configuration. II. The effect of using clarified tomato juice on the process performance, *Journal of Membrane Science*, 160 (1999) 171-177.
- [10] B. Jiao, A. Cassano and E. Drioli, Recent advances on membrane processes for the concentration of fruit juices: a review, *Journal of Food Engineering*, 63 (2004) 303-324.
- [11] K.B. Petrotos, P.C. Quantick and H. Petropakis, A study of the direct osmotic concentration of tomato juice in tubular membrane-module configuration. I. The effect of certain basic process parameters on the process performance, *Journal of Membrane Science*, 150 (1998) 99-110.
- [12] A. Achilli, T.Y. Cath, E.A. Marchand and A.E. Childress, The forward osmosis membrane bioreactor: A low fouling alternative to MBR processes, *Desalination*, 239 (2009) 10-21.
- [13] E.R. Cornelissen, D. Harmsen, K.F. de Korte, C.J. Ruiken, Jian-Jun Qin, H. Oo and L.P. Wessels, Membrane fouling and process performance of forward osmosis membranes on activated sludge, *Journal of Membrane Science*, 319 (2008) 158-168.
- [14] J.L. Cartinella, T.Y. Cath, M.T. Flynn, G.C. Miller, K. W. Hunter and A.E. Childress, Removal of natural steroid hormones from wastewater using membrane contactor processes, *Environmental Science and Technology*, 40 (2006) 7381-7386.
- [15] J.R. McCutcheon and M. Elimelech, Influence of concentrative and dilutive internal concentration polarization on flux behavior in forward osmosis, *Journal of Membrane Science*, 284 (2006) 237-247.
- [16] S. Loeb, L. Titelman, E. Korngold and J. Freiman, Effect of porous support fabric on osmosis through a Loeb-Sourirajan type asymmetric membrane, *Journal of Membrane Science*, 129 (1997)
- [17] C.H. Tan and H.Y. Ng, Modified models to predict flux behavior in forward osmosis in consideration of external and internal concentration polarizations, *Journal of Membrane Science*, 324 (2008) 209-219.
- [18] A. Achilli, T.Y. Cath and A.E. Childress, Power generation with pressure retarded osmosis: an experimental and theoretical investigation, *Journal of Membrane Science*, In press (2009)

- [19] K.L. Lee, R.W. Baker and H.K. Lonsdale, Membrane for power generation by pressure retarded osmosis, *Journal of Membrane Science*, 8 (1981) 141-171.
- [20] N.T. Hancock and T.Y. Cath, Novel performance modeling of forward osmosis - reverse osmosis integrated system, American Water Works Association 2009 Membrane Technology Conference, Memphis, Tennessee, 2009.
- [21] M. Mulder, Basic principles of membrane technology, Kluwer Academic Publishers, Dordrecht, The Netherlands, 1991.
- [22] N.H. Hancock and T.Y. Cath, Solute coupled diffusion in osmotically driven processes, *Environmental Science and Technology*, (2009) In press.
- [23] C.R. Martinetti, A.E. Childress and T.Y. Cath, High recovery of concentrated RO brines using forward osmosis and membrane distillation, *Journal of Membrane Science*, 331 (2009) 31-39.
- [24] J.R. McCutcheon, R.L. McGinnis and M. Elimelech, Desalination by ammonia-carbon dioxide forward osmosis: Influence of draw and feed solution concentrations on process performance, *Journal of Membrane Science*, 278 (2006) 114-123.
- [25] IMSDesign, Hydranautics, Oceanside, CA.
- [26] Reverse Osmosis System Analysis (ROSA), Dow Filmtec, Midland, MI.
- [27] National Paint and Coating Association, <http://www.paint.org/hmis/index.cfm>
- [28] Fisher Scientific, Fisher Scientific, 2009, <http://www.fishersci.com/wps/portal/HOME>
- [29] V. Lobo, Mutual diffusion coefficients in aqueous electrolyte solutions, *Pure and Applied Chemistry*, 65 (1993) 2613-2640.
- [30] J.W. Mullin and A.W. Nienow, Diffusion Coefficients of Potassium Sulfate in Water, *Journal of Chemical and Engineering Data*, 9 (1964) 526-527.
- [31] J.G. Albright, R. Mathew and D.G. Miller, Measurement of binary and ternary mutual diffusion coefficients of aqueous sodium and potassium bicarbonate solutions at 25 degree C, *Journal of Physical Chemistry*, 91 (1987) 210-215.
- [32] B. Tansel, J. Sager, T. Rector, J. Garland, R.F. Strayer, L. Levine, M. Roberts, M. Hummerick and J. Bauer, Significance of hydrated radius and hydration shells on

ionic permeability during nanofiltration in dead end and cross flow modes, *Separation and Purification Technology*, 51 (2006) 40-47.

- [33] J. Kielland, Individual activity coefficients of ions in aqueous solutions, *Journal of the Chemical American Society*, 59 (1937) 1675-1678.
- [34] J. Sarapuk, H. Kleszczynska and B. Rozycka-Roszak, The role of counterions in the interaction of bifunctional surface active compounds with model membranes, *Biochemistry and Molecular Biology International*, 44 (1998)
- [35] R.L. McGinnis, J.R. McCutcheon and M. Elimelech, A novel ammonia-carbon dioxide osmotic heat engine for power generation, *Journal of Membrane Science*, 305 (2007) 13-19.
- [36] C. Fritzmann, J. Lowenberg, T. Wintgens and T. Melin, State-of-the-art of reverse osmosis desalination, *Desalination*, 216 (2007) 1-76.
- [37] A. Rahardianto, J. Gao, C.J. Gabelich, M.D. Williams and Y. Cohen, High recovery membrane desalting of low-salinity brackish water: Integration of accelerated precipitation softening with membrane RO, *Journal of Membrane Science*, 289 (2007) 123-137.

Chapter 4

**4 POWER GENERATION WITH PRESSURE RETARDED OSMOSIS:
AN EXPERIMENTAL AND THEORETICAL INVESTIGATION**

(Accepted for publication in the *Journal of Membrane Science*)

Abstract

Pressure retarded osmosis (PRO) was investigated as a viable source of renewable energy. In PRO, water from a low salinity feed solution permeates through a membrane into a pressurized, high salinity draw solution; power is obtained by depressurizing the permeate through a hydroturbine. A PRO model was developed to predict water flux and power density under specific experimental conditions. The model relies on experimental determination of the membrane water permeability coefficient (A), the membrane salt permeability coefficient (B), and the solute resistivity (K). A and B were determined under reverse osmosis conditions, while K was determined under forward osmosis (FO) conditions. The model was tested using experimental results from a bench-scale PRO system. Previous investigations of PRO were unable to verify model predictions due to the lack of suitable membranes and membrane modules. In this investigation, the use of a custom-made laboratory-scale membrane module enabled the collection of experimental PRO data. Results obtained with a flat-sheet cellulose triacetate (CTA) FO membrane and NaCl feed and draw solutions closely matched model predictions. Maximum power densities of 2.7 and 5.1 W/m² were observed for 35 and 60 g/L NaCl draw solutions, respectively, at 970 kPa of hydraulic pressure. Power density was substantially reduced

due to internal concentration polarization in the asymmetric CTA membranes and, to a lesser degree, to salt passage. External concentration polarization was found to exhibit a relatively small effect on reducing the osmotic pressure driving force. Using the predictive PRO model, optimal membrane characteristics and module configuration can be determined in order to design a system specifically tailored for PRO processes.

Keywords: Forward osmosis, Pressure retarded osmosis, Salinity power, Power density, Concentration polarization

4.1 Introduction

Pressure retarded osmosis (PRO) could be a viable source of renewable energy [1, 2]. In a PRO system, water from a low salinity feed solution (e.g., fresh water) permeates through a membrane into a pressurized, high salinity brine/draw solution (e.g., seawater); power is obtained by depressurizing a portion of the diluted seawater through a hydroturbine (Figure 4.1) [3].

It is estimated that the global energy production potential of PRO is on the order of 2,000 TWh per year [4], while the estimated global energy production from all renewable sources is approaching 10,000 TWh per year [5].

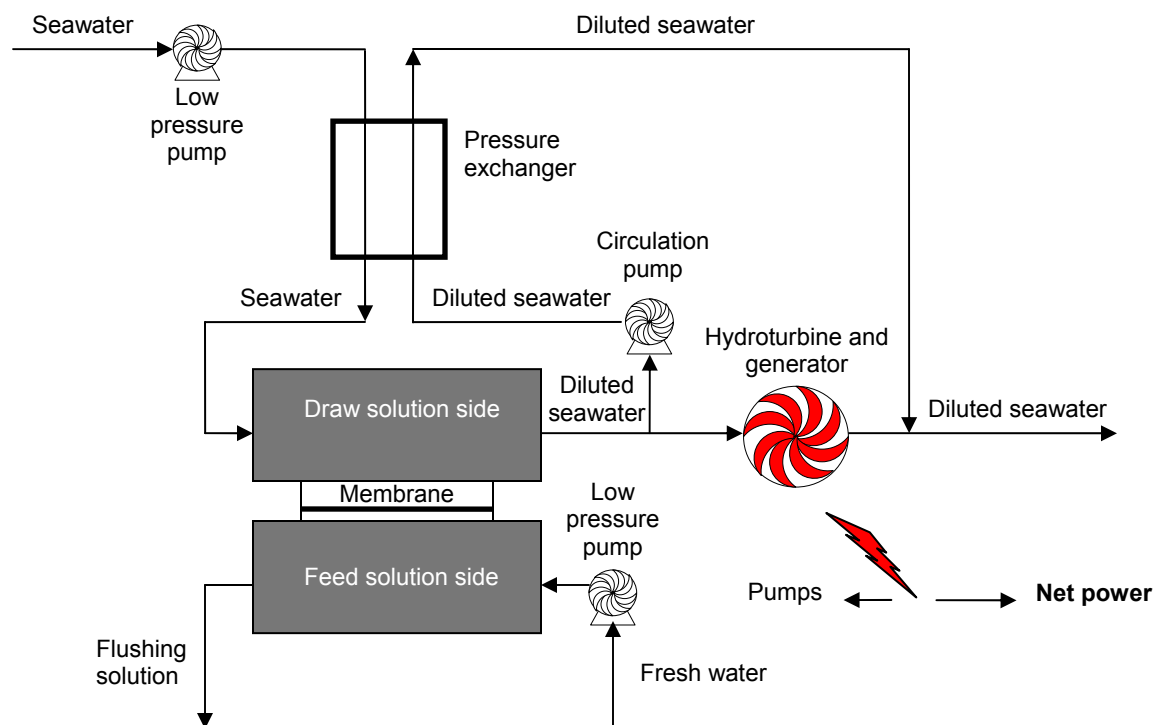


Figure 4.1 Schematic of a pressure-retarded osmosis (PRO) power plant. Figure adapted from Ref. [3].

The concept of harvesting energy generated during mixing of fresh and salt water was developed in the mid-1950s [6]. Following the 1973 oil crisis, the interest in PRO for power generation spiked and led to several investigations of the technical [2, 7, 8] and economic feasibility [1, 2] of PRO. Loeb et al. began publishing results from PRO experiments in 1976 [9]. They utilized hollow-fiber seawater reverse osmosis (RO) membranes enclosed in a “minipermeator” (Permasep B-10). A pressurized brine flowed on the shell side of the bundle of hollow-fiber membranes and the fresh water flowed through the bore. Further investigations of Loeb and Mehta [10], Mehta and Loeb [11, 12], and Jellinek and Masuda [13] revealed power outputs far below the expected outputs, likely due to the use of RO membranes and membrane modules that were

designed for seawater desalination. It was determined that seawater RO membranes were not suitable for forward osmosis (FO) and PRO applications due to their hydrophobicity and thick support layer [14]. Furthermore, it was found that existing membrane modules did not allow for high cross-flow velocity on the membrane surface [15]. Thus, the lack of suitable membranes and modules hindered the efforts to establish this technology [16]. Also, during this time, a few models were proposed to predict flux and pressure behavior in PRO [10, 12, 17]; however, it was difficult to validate these models because of the lack of suitable membranes and membrane modules. For example, Lee et al. [17] were only able to validate their model under FO and RO conditions.

In the current investigation, for the first time, experimental PRO results were compared with model predictions. The objective of this investigation was to evaluate the contributions of membrane characteristics and operating conditions to water flux and subsequently, to power density. Concentration polarization may severely reduce water flux and power density in PRO; however, the causes and effects of concentration polarization have not been investigated nearly as much for FO and PRO processes [15, 18] as for RO processes [19, 20]. In the current investigation, a predictive PRO model that includes the influence of draw solution, feed solution, concentration polarization, and hydraulic pressure on water flux and subsequent power output was developed. The model was tested using experimental results. Experiments were conducted using current-generation FO membranes and a well-established draw solution (NaCl). Water flux and power density were evaluated under different operating conditions.

With the availability of a PRO model, power density can be predicted for variable membrane characteristics, membrane structure, and module configuration. The

optimization of these parameters would contribute to the design of membranes and membrane modules specifically tailored for PRO processes.

4.2 Theory

4.2.1 Osmotic processes

Osmosis is the transport of water across a selectively permeable membrane from a solution of higher water chemical potential (lower osmotic pressure) to a solution of lower water chemical potential (higher osmotic pressure). It is driven by a difference in solute molar concentrations across a membrane that allows passage of water, but rejects most solute molecules and ions. The osmotic pressure differential ($\Delta\pi$) is the pressure which, if applied as a hydraulic pressure (ΔP) to the more concentrated solution, would prevent net transport of water across the membrane. FO uses the $\Delta\pi$ across the membrane, rather than a ΔP (as in RO), as the driving force for transport of water through the membrane. The FO process results in concentration of a feed stream and dilution of a highly concentrated stream (referred to as the draw solution). Flux in FO is in the opposite direction of RO. PRO can be viewed as an intermediate process between FO and RO, hydraulic pressure is applied to the draw solution (similar to RO) but the net water flux is still in the direction of the concentrated draw solution (similar to FO). The general equation describing water transport in FO, RO, and PRO is:

$$J_w = A(\Delta\pi - \Delta P) \quad (1)$$

where J_w is the water flux and A is the water permeability coefficient of the membrane. For FO, ΔP is zero; for RO, $\Delta P > \Delta\pi$; and for PRO, $\Delta P < \Delta\pi$. The flux directions of the

permeating water in FO, PRO, and RO are illustrated in Figure 4.2. Also in Figure 4.2, the orientation of an asymmetric membrane is indicated; in FO, the dense layer of the membrane faces the feed solution and in RO and PRO, the dense layer faces the draw solution.

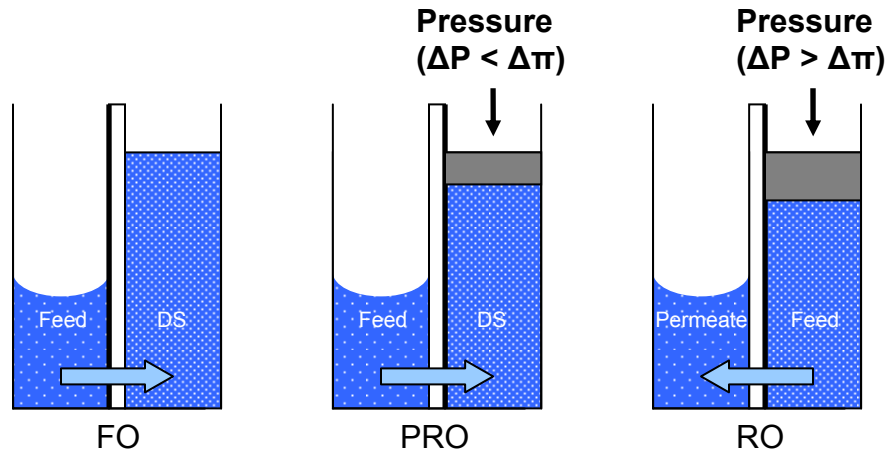


Figure 4.2 Representation of solvent flow in FO, PRO, and RO. Membrane orientation is indicated in each system by the thick black line representing the membrane dense layer.

In PRO, the power that can be generated per unit membrane area (i.e., the power density) is equal to the product of the water flux and the hydraulic pressure differential across the membrane:

$$W = J_w \Delta P = A(\Delta\pi - \Delta P)\Delta P \quad (2)$$

By differentiating eq. (2) with respect to ΔP , it can be shown that W reaches a maximum when $\Delta P = \Delta\pi/2$ (Fig. 3). Substituting this value for ΔP in eq. (2) yields:

$$W_{\max} = A \frac{\Delta\pi^2}{4} \quad (3)$$

J_w as a function of ΔP is illustrated in Figure 4.3 for both real and ideal conditions. The FO point (at $\Delta P=0$), the PRO zone (where $\Delta P < \Delta\pi$), and the RO zone (where $\Delta P > \Delta\pi$) are indicated. The flux reversal point occurs where $\Delta P = \Delta\pi$. Fig. 3 also illustrates W and W_{max} in the PRO zone.

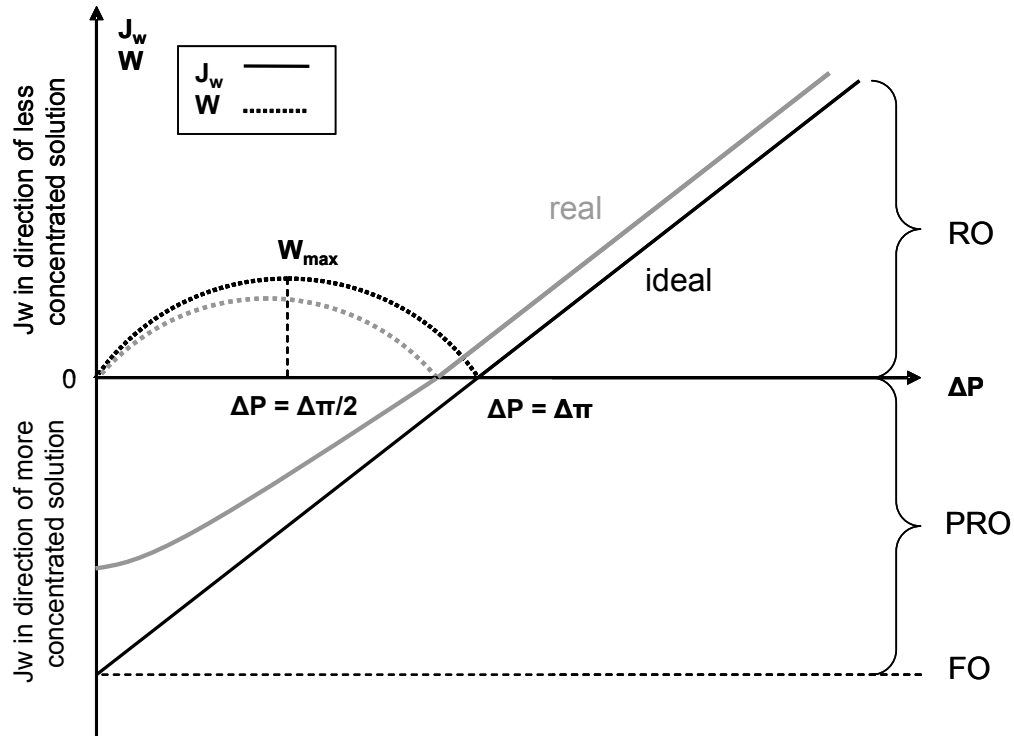


Figure 4.3 Magnitude and direction of J_w for FO, PRO, and RO and magnitude of W for PRO is shown. Figure adapted from Ref. [17].

4.2.2 Salt permeability

Membranes for osmotically-driven processes are susceptible to reverse salt diffusion, where a small amount of salt permeates the membrane from the draw solution to the feed solution due to the concentration gradient across the membrane [21]. Reverse salt diffusion reduces the effective osmotic pressure difference across the membrane. The

salt permeability coefficient of a semi-permeable membrane can be obtained from RO experiments [17] and is given by:

$$B = \frac{A(1-R)(\Delta P - \Delta \pi)}{R} \quad (4)$$

where B is the salt permeability coefficient and R is salt rejection. R is defined as:

$$R = 1 - \frac{C_P}{C_F} \quad (5)$$

where C_P is the salt concentration in the permeate solution and C_F is the salt concentration in the feed solution.

4.2.3 Concentration polarization

Another, more severe phenomenon, which also reduces the effective osmotic pressure difference across the membrane, is concentration polarization [15].

Concentration polarization is the accumulation or depletion of solutes near an interface. As a result of water crossing the membrane, the solute is concentrated on the feed side of the membrane surface and diluted on the permeate side of the membrane surface.

Because the membranes used for osmotic processes are typically asymmetric [22] (comprised of a thin dense layer on top of a porous support layer), concentration polarization occurs externally on the dense layer side and internally in the support layer side. In PRO applications, the dense layer of the membrane faces the draw solution and the porous support layer faces the feed solution (Figure 4.2). This configuration is necessary to ensure that the membrane can sustain the hydraulic pressure induced on the

draw solution side [12, 17, 23]. In this configuration, both dilutive external concentration polarization and concentrative internal concentration polarization occur (Figure 4.4).

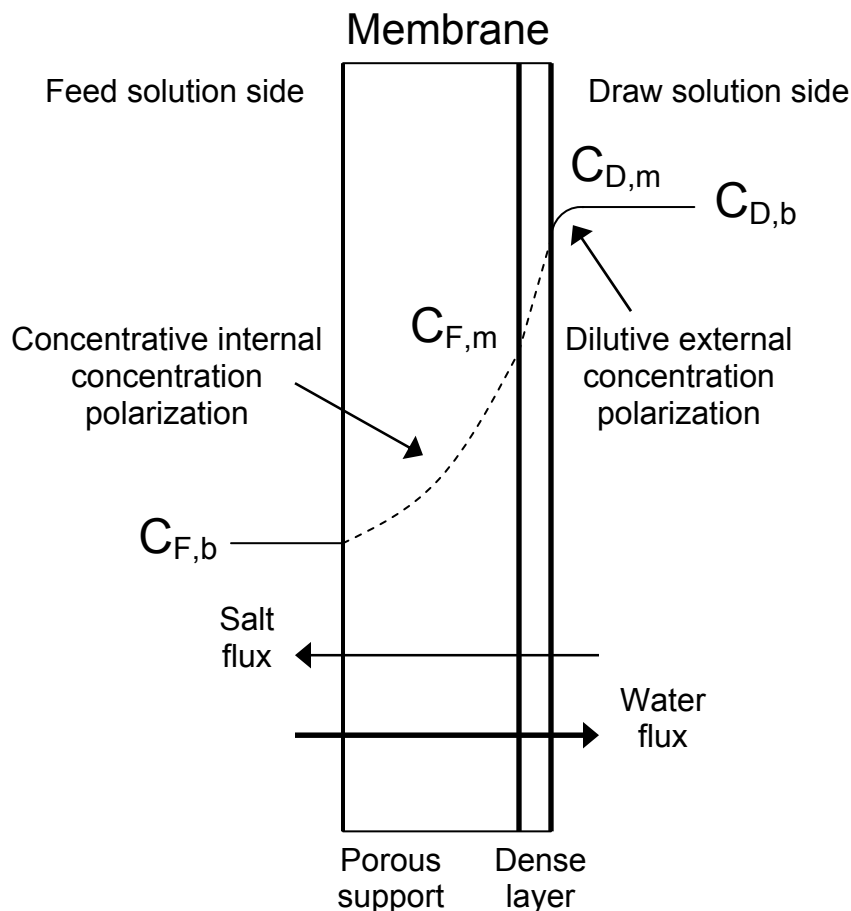


Figure 4.4 Illustration of osmotic driving force profiles for an asymmetric membrane with the dense layer facing the draw solution (PRO mode). Internal and external concentration polarization are also shown.

4.2.4 External concentration polarization in PRO

Dilutive external concentration polarization is concentration polarization that results in the solute being diluted on the draw solution side of the membrane. Dilutive external concentration polarization can be calculated from film theory [19, 24]. The external concentration polarization modulus ($\pi_{D,m} / \pi_{D,b}$) is calculated using:

$$\frac{\pi_{D,m}}{\pi_{D,b}} = \exp\left(-\frac{J_w}{k}\right) \quad (6)$$

where $\pi_{D,m}$ is the osmotic pressure at the membrane surface and $\pi_{D,b}$ is the bulk osmotic pressure of the draw solution. J_w is negative in this equation because the water flux is in the direction of the more concentrated solution and the concentration polarization effect is dilutive ($\pi_{D,m} < \pi_{D,b}$). The mass transfer coefficient (k) in the draw solution is calculated using:

$$k = \frac{Sh D}{d_h} \quad (7)$$

where D is the diffusion coefficient of the solute in the draw solution and d_h is the hydraulic diameter of the flow channel. It has been shown that in spacer-filled flow channels the flow becomes turbulent at relatively low Reynolds numbers (Re) (e.g., $Re < 50$) [25-27]. Under these conditions, the Sherwood number (Sh) is determined using the correlation [27]:

$$Sh = 0.2 Re^{0.57} Sc^{0.40} \quad (8)$$

where Sc is the Schmidt number.

4.2.5 Internal concentration polarization in PRO

Concentrative internal concentration polarization is concentration polarization that results in the solute being concentrated inside the support layer of the membrane. Lee et al. [17] derived an expression to model the effect of internal concentration polarization in PRO applications. J_w is determined by:

$$J_w = A \left[\pi_{D,m} \frac{1 - \frac{C_{F,b}}{C_{D,m}} \exp(J_w K)}{1 + \frac{B}{J_w} [\exp(J_w K) - 1]} - \Delta P \right] \quad (9)$$

where $C_{F,b}$ is the salt concentration of the bulk feed solution and $C_{D,m}$ is the salt concentration of the draw solution at the membrane surface. The solute resistivity for diffusion within the porous support layer (K) is defined by:

$$K = \frac{t\tau}{D\varepsilon} \quad (10)$$

where t , τ , and ε are the thickness, tortuosity, and porosity of the support layer, respectively. Similar to k for external concentration polarization, K can be used to determine the influence of internal concentration polarization on water flux.

4.2.6 Water flux in PRO

In order to consider the effects of both internal and external concentration polarization on water flux in PRO, eq. (9) can be modified by assuming that $C_{F,b} / C_{D,m} = \pi_{F,b} / \pi_{D,m}$ [23], and substituting $\pi_{D,m} = \pi_{D,b} \exp(-J_w/k)$ (from eq. (6)). The resulting equation for water flux in the presence of both internal and external concentration polarization is:

$$J_w = A \left[\pi_{D,b} \exp\left(-\frac{J_w}{k}\right) \frac{1 - \frac{\pi_{F,b}}{\pi_{D,b}} \exp(J_w K) \exp\left(\frac{J_w}{k}\right)}{1 + \frac{B}{J_w} [\exp(J_w K) - 1]} - \Delta P \right] \quad (11)$$

where J_w is a function of the membrane characteristics (A and B), mass transfer coefficient (k), solute resistivity (K), bulk osmotic pressures ($\pi_{F,b}$ and $\pi_{D,b}$), and applied hydraulic pressure (ΔP).

The parameters necessary to calculate water flux in PRO (eq. (11)) are obtained from RO and FO experiments and from calculation. k is calculated using eqs. (6-8). A and B are determined under RO conditions; A is calculated using eq. (1) and measuring J_w and ΔP when $\Delta\pi=0$ and B is calculated using eqs. (4) and (5). K is obtained from FO experiments ($\Delta P = 0$) with deionized (DI) water as the feed and using eq. (9). In this case eq. (9) is rearranged to:

$$K = \frac{1}{J_w} \ln \left(\frac{A \pi_{D,b} \exp\left(-\frac{J_w}{k}\right) - J_w}{B} + 1 \right) \quad (12)$$

4.2.7 Power density in PRO

The power density in PRO is equal to the product of the water flux through the membrane and the hydraulic pressure differential across the membrane (eq. (2)). In the case of current generation membranes (experiencing reverse salt diffusion and concentration polarization), the equation governing the process is:

$$W = J_w \Delta P = A \left[\pi_{D,b} \exp\left(-\frac{J_w}{k}\right) \frac{1 - \frac{\pi_{F,b}}{\pi_{D,b}} \exp(J_w K) \exp\left(\frac{J_w}{k}\right)}{1 + \frac{B}{J_w} [\exp(J_w K) - 1]} - \Delta P \right] \Delta P \quad (13)$$

After eq. (11) is solved numerically to determine J_w , eq. (13) can be solved algebraically to determine W as a function of ΔP .

Qualitatively, J_w and W as functions of ΔP are illustrated in Figure 4.3. Under ideal conditions, as hydraulic pressure increases, water flux decreases until reaching zero at $\Delta P = \Delta\pi$ (the flux reversal point). Simultaneously, power density increases until reaching a maximum when $\Delta P = \Delta\pi/2$ and then decreases to zero at the flux reversal point. As expected, under real conditions, reverse salt diffusion (represented by B) and concentration polarization (represented by k and K) cause the effective osmotic pressure differential ($\Delta\pi$) across the membrane to be lower than the bulk osmotic pressure differential. This phenomenon reduces the attainable J_w and W compared to the ideal membrane case.

4.3 Experimental

4.3.1 Membranes

A flat-sheet cellulose triacetate (CTA) FO membrane (Hydration Technology Innovations, Albany, OR) was used in the experiments. The physical characteristics of this membrane are unique compared to other commercially available semi-permeable membranes and it has been determined to be the best available membrane for most FO applications [22, 28].

4.3.2 Solution chemistries

Certified ACS-grade NaCl (Fisher Scientific, Pittsburg, PA) was used to prepare both feed and draw solutions. Osmotic pressures, viscosities, and densities of all solutions

(Table 4.1) were calculated using software from OLI Systems Inc. (Morris Plains, NJ). Diffusion coefficients were calculated according to Stokes [29] and Mills [30] and are also shown in Table 4.1.

Table 4.1 NaCl aqueous solution characteristics

C g/L NaCl	π kPa	μ mPa \times s	ρ g/L	D 10^{-9} m ² /s
0	0	0.892	997	1.51
2.5	189	0.895	999	1.497
5	380	0.898	1,000	1.485
20	1,550	0.918	1,011	1.472
35	2,763	0.939	1,021	1.490
60	4,882	0.976	1,037	1.556

4.3.3 RO experiments

4.3.3.1 Bench-scale system

A flat-sheet, bench-scale RO test unit was used to determine the membrane coefficients A and B . The test unit had a channel on the feed side of the membrane to allow the feed solution to flow tangential to the membrane. The channel was 75 mm long, 25 mm wide, and 2.5 mm deep; it had an effective membrane area of 18.75 cm². Mesh spacers placed in the feed channel supported the membrane and enhanced the turbulence in the feed stream. The feed solution was contained in a 2-L reservoir. A high-pressure positive displacement pump (Wanner Engineering Inc., Minneapolis, MN) was used to recirculate the feed solution at 0.5 L/min. The permeate was collected in a 1-L graduated cylinder placed on an analytical balance linked to a computer. Flux through the membrane was calculated based on the change of weight of water in the graduated

cylinder. The conductivity of the permeate was monitored (Accumet Basic, Fisher Scientific, Hampton, NH) and recorded.

4.3.3.2 Determination of membrane coefficients

RO tests were conducted with the dense layer of the membrane facing the feed solution. The first set of experiments was performed to determine A following eq. (1) and using DI water as the feed solution. Pressure was increased at 345-kPa (50-psi) increments from 345 to 1,035 kPa (50 to 150 psi) for a duration of 3 h each. A second experiment was performed to determine B following eqs. (4) and (5). These experiments were performed for 12 h with 2 g/L NaCl as the feed solution and a pressure of 1,035 kPa. The conductivity of the permeate was recorded at the end of the experiment. The temperature was held constant at 24 ± 1 °C.

4.3.4 *PRO experiments*

4.3.4.1 Bench-scale system

A schematic drawing of the flat-sheet bench-scale PRO system is shown in Figure 4.5. The custom-made membrane module had symmetric channels on both sides of the membrane. This allowed for both the feed and draw solutions to flow tangential to the membrane. The membrane area and the dimensions of the feed and draw solution channels were the same as those in the bench-scale RO module and mesh spacers were placed in both channels. A variable-speed gear pump (Cole-Palmer, Vernon Hills, IL) was used to recirculate the feed solution at 0.5 L/min. A high-pressure positive

displacement pump (Wanner Engineering Inc., Minneapolis, MN) was used to recirculate the draw solution at 0.5 L/min.

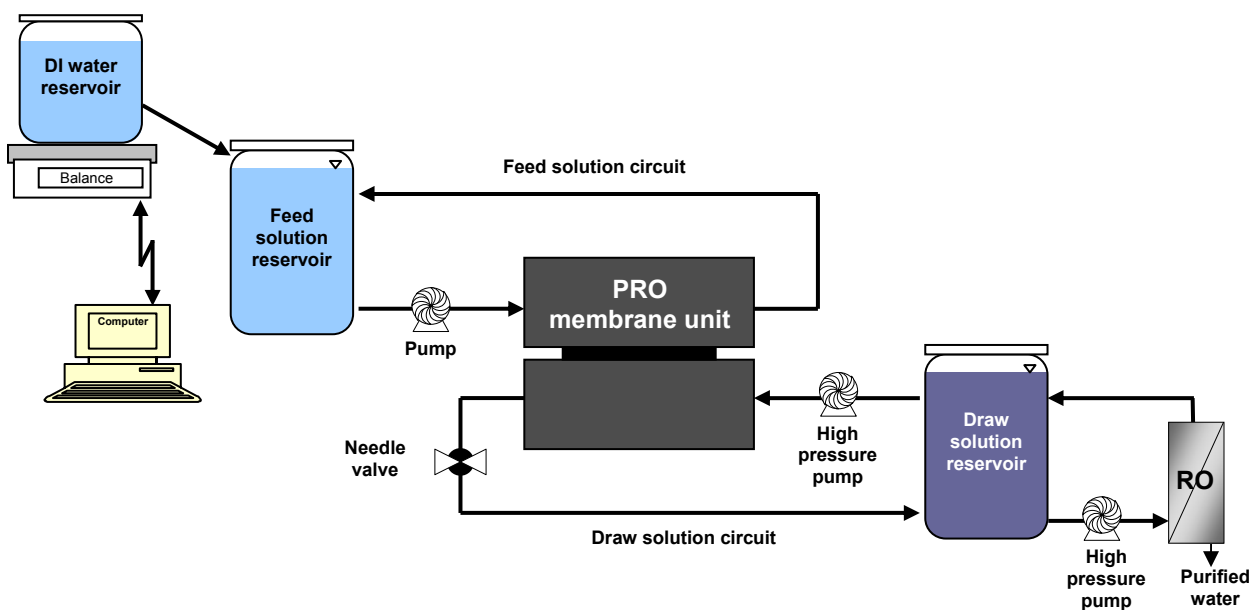


Figure 4.5 Schematic of bench-scale PRO system.

The feed solution was contained in a 5.4-L constant-level reservoir; the volume was kept constant by a float valve and DI water continuously replenished the water that crossed the membrane. The DI water reservoir was placed on an analytical balance linked to a computer that collected data continuously. Flux through the membrane was calculated based on the change of weight of water in the DI water reservoir. Hydraulic pressures on the feed and draw solutions were monitored and recorded. The hydraulic pressure of the draw solution loop was controlled with a needle valve. The draw solution concentration was held constant by continuous reconcentration with a pilot-scale RO subsystem. The RO subsystem (different from the bench-scale RO system used for conducting membrane characteristics tests) is described in a previous publication [31].

4.3.4.2 Determination of mass transport coefficient

Three experiments were performed at $\Delta P=0$ (i.e., in FO mode) and eq. (12) was used to determine K . These experiments were performed for 12 h with DI water as the feed solution and 20, 35, and 60 g/L NaCl as the draw solution. The temperature of the system was held constant at 24 ± 1 °C.

4.3.4.3 PRO performance tests

PRO performance tests were conducted with the dense layer of the membrane facing the draw solution. A matrix of experiments was performed (Table 4.2). Three feed solution concentrations (0, 2.5, and 5 g/L NaCl) and two draw solution concentrations (35 and 60 g/L NaCl) were tested. The hydraulic pressure of the feed solution was 30 kPa and three draw solution hydraulic pressures (340, 680, and 1000 kPa) were tested, resulting in ΔP values of 310, 650, and 970 being tested. Additionally, an FO experiment with both feed and draw solution hydraulic pressures of 30 kPa ($\Delta P=0$) was performed. Each experiment was carried out for 12 h and the temperature of the system was held constant at 24 ± 1 °C.

Table 4.2 PRO experiment conditions

C_{Feed} g/L NaCl	C_{DS} g/L NaCl	ΔP kPa
0	35	0
0	35	310
0	35	650
0	35	970
2.5	35	0
2.5	35	310
2.5	35	650
2.5	35	970
5.0	35	0
5.0	35	310
5.0	35	650
5.0	35	970
0	60	0
0	60	310
0	60	650
0	60	970
2.5	60	0
2.5	60	310
2.5	60	650
2.5	60	970
5.0	60	0
5.0	60	310
5.0	60	650
5.0	60	970

4.4 Results and discussion

4.4.1 Determination of membrane characteristics (*A* and *B*)

Results of the step-increment test performed to determine *A* are illustrated in Figure 4.6. Water flux increased linearly as the hydraulic pressure increased. *A* was calculated to be 1.87×10^{-9} (m/s)/kPa. This is similar to values reported in previous studies using similar membranes [18, 32]. Results of the test performed to determine *B* are illustrated in Figure 4.7. Water flux was constant at an average of 1.14×10^{-6} m/s throughout the experiment. The NaCl rejection of the membrane was calculated to be

94% and B was calculated to be 1.11×10^{-7} m/s. These results are comparable to values reported in a previous study using similar membranes [32].

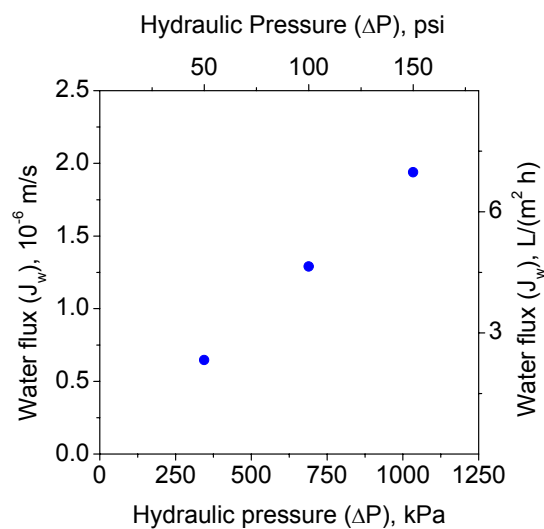


Figure 4.6 Water flux (J_w) as a function of applied hydraulic pressure (ΔP) during the RO experiment performed to determine A . Feed solution was DI water and temperature was 25 °C.

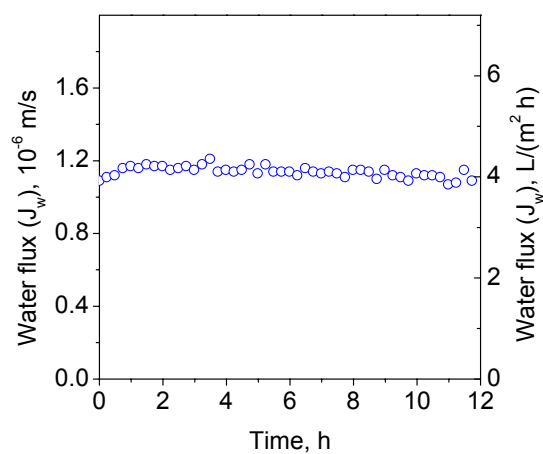


Figure 4.7 Water flux (J_w) as a function of elapsed time during the RO experiment performed to determine B . Feed solution was 2 g/L NaCl, hydraulic pressure was 1,035 kPa, and temperature was 25 °C.

4.4.2 Calculations of mass transport coefficient (k)

k values (Table 4.3) were calculated using eq. (7). For the three draw solution concentrations, eq. (8) was used to calculate the Sh number. The hydraulic diameter (d_h) of the flow channel was 9.46×10^{-4} m, calculated as proposed by [25]. k values increased slightly with draw solution concentration due to increases in density, viscosity, and diffusion coefficient as the solute concentration increases.

Table 4.3 Mass transfer coefficient (k) at various draw solution concentrations

C_{DS} g/L NaCl	Sh	D 10^{-9} m ² /s	d_h m	k m/s
20	52.2	1.472	9.46E-04	8.43E-05
35	53.8	1.490	9.46E-04	8.48E-05
60	52.7	1.556	9.46E-04	8.66E-05

4.4.3 Determination of solute resistivity (K)

A set of FO experiments was performed to evaluate K using eq. (12). The term $t\tau/\varepsilon$ was then calculated for each experimental condition using eq. (10) with a D of 1.51×10^{-9} m²/s, adopted from Mills [30]. The same D was used for all three experiments because the same solution (DI water) was used as the feed stream. The term $t\tau/\varepsilon$ represents the structural characteristic of the membrane support layer, and therefore, should be constant for a given membrane. Results (Table 4.4) reveal that the term $t\tau/\varepsilon$ remains fairly constant under the three different experimental conditions.

Table 4.4 Solute resistivity (K) at various draw solution concentrations with DI water as feed solution

C_{DS} g/L	K s/m	$t\tau/\varepsilon$ m
20	4.68E+05	7.07E-04
35	4.51E+05	6.82E-04
60	4.28E+05	6.46E-04
average		6.78E-04

The resulting average $t\tau/\varepsilon$ was used to calculate K coefficients for different feed solution concentrations. K is expected to change slightly since D is a function of the solute concentration. The calculated K coefficients for the different feed solution concentrations used during the PRO performance tests are summarized in Table 4.5.

Table 4.5 Solute resistivity (K) at various feed solution concentrations

C_{Feed} g/L	average $t\tau/\varepsilon$ m	D $10^{-9} \text{ m}^2/\text{s}$	K s/m
0	6.78E-04	1.51	4.49E+05
2.5	6.78E-04	1.497	4.52E+05
5.0	6.78E-04	1.485	4.55E+05

4.4.4 PRO model results

Theoretical PRO water flux and power density curves as a function of hydraulic pressure for three feed solution concentrations and two draw solution concentrations are illustrated in Figure 4.8. The two draw solution concentrations evaluated were 35 g/L NaCl to simulate sea water and 60 g/L NaCl to simulate concentrate from RO desalination facilities [33]. Water flux values are reported on the primary y-axis while power density values are reported on the secondary y-axis. In both cases, as hydraulic pressure increases, water flux decreases until reaching zero (the flux reversal point).

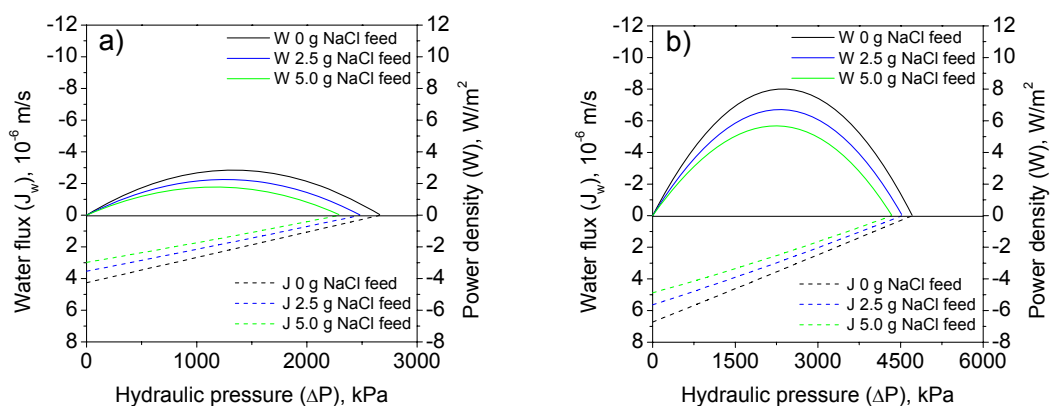


Figure 4.8 Model results for water flux (J_w) and power density (W) as a function of applied hydraulic pressure (ΔP). Draw solution concentrations are (a) 35 g/L NaCl (2,763 kPa) and (b) 60 g/L NaCl (4,882 kPa).

Power density reaches a maximum when the hydraulic pressure is approximately half of the hydraulic pressure of the flux reversal point. For example, in the case of the 35 g/L NaCl draw solution (Figure 4.8a) and 2.5 g/L NaCl feed solution, the flux reversal point occurs at 2,450 kPa and the maximum in power density occurs at 1,280 kPa. As the feed concentration increases, water flux and power density decrease because of the reduced $\Delta\pi$ and likely due to increased concentration polarization and increased salt passage. When comparing Figure 4.8a and b, it can be seen that when the higher draw solution concentration is used (Figure 4.8b), the water fluxes and power densities are much higher. This is simply due to the higher driving force. From the model predictions in Figure 4.8, it is estimated that the maximum power density can be between 1.6 and 2.9 W/m^2 for the 35 g/L NaCl draw solution and between 5.1 and 8.1 W/m^2 for the 60 g/L NaCl draw solution. These ranges are close to (in the case of the 35 g/L NaCl draw

solution), or in excess of (in the case of 60 g/L NaCl draw solution) the 4 W/m² target that has been set for successful development of osmotic power technology [4, 16].

The effects of external concentration polarization, internal concentration polarization, and salt passage on water flux and power density are illustrated in Figure 4.9. In the *ideal* scenario, no external concentration polarization, internal concentration polarization, or salt passage are considered. Theoretical water flux and power density are computed considering a membrane with an A of 1.87×10^{-9} (m/s)/kPa. In the k scenario, the effects of external concentration polarization are introduced. In the K scenario, the effects of internal concentration polarization are introduced by considering a membrane with a support layer. In the K and B scenario, the effects of both internal concentration polarization and salt passage are considered (a B of 1.11×10^{-7} m/s was used). In the *complete* scenario, the combined effects of external concentration polarization, internal concentration polarization, and salt passage are considered.

In Figure 4.9a and d, a K scenario does not exist; when DI water is used as the feed solution and no salt passage is considered, there is no internal concentration polarization because there is no salt on the feed side of the membrane. It is also worth noting that the effect of salt passage alone (i.e., a B scenario) is not considered. Salt passage cannot be isolated from internal concentration polarization because salt passage affects process performance only if the membrane has a support layer, and if the membrane has a support layer, internal concentration polarization must be considered.

As expected, in all six figures, water flux and power density values decrease as the model gets more complex. Concentration polarization and salt passage reduce the

driving force across the membrane; however, their effects vary depending on the feed and draw solution concentrations.

The effects of internal concentration polarization (K scenario) are greater than the effects of external concentration polarization (k scenario). Also, the effects of internal concentration polarization (K scenario) are enhanced by salt passage (K and B scenario). The magnitudes of internal concentration polarization (K scenario) and internal concentration polarization plus salt passage (K and B scenario) increase with increasing feed solution concentrations and with increasing draw solution concentrations while the magnitude of external concentration polarization (k scenario) decreases with increasing feed solution concentrations and increases with increasing draw solution concentrations. Explanations for these trends are given below.

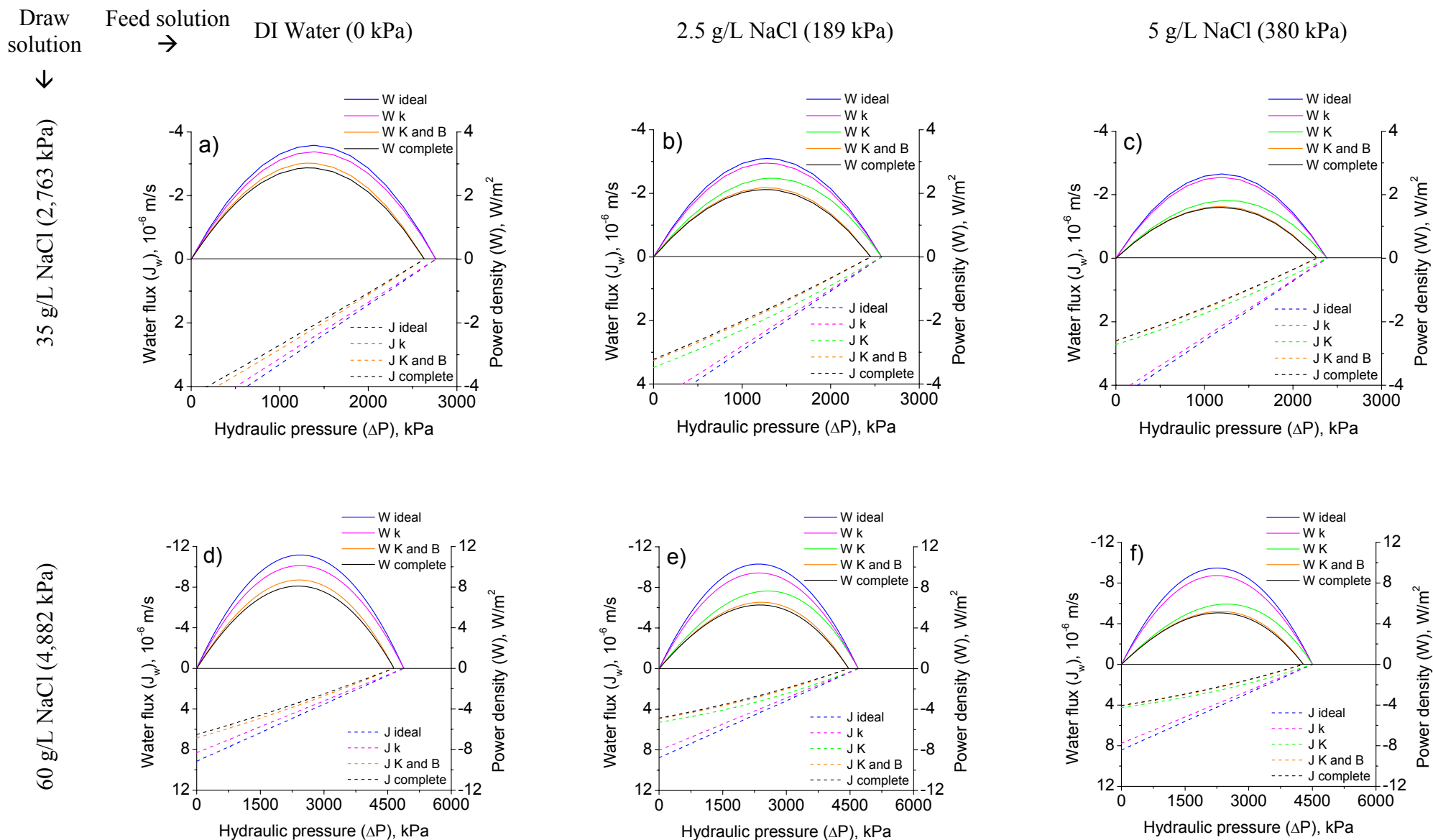


Figure 4.9 Model results for water flux (J_w) and power density (W) as a function of applied hydraulic pressure (ΔP) for different feed and draw solution concentrations.

The external concentration polarization modulus is dependent on flux (eq. 6) and decreases as water flux decreases. Increasing feed solution concentration (0 to 2.5 g/L to 5 g/L) decreases the driving force and subsequently, the attainable water flux. This causes a decrease in the effects of external concentration polarization. This can be seen in Fig. 4.9 by comparing the difference between the *ideal* and *k* scenarios either for Fig. 4.9a and b and c or d and e and f. Similarly, increasing draw solution concentration (35 g/L to 60 g/L) increases the driving force and flux. This causes an increase in the effect of external concentration polarization, which can be seen by comparing the difference between the *ideal* and *k* scenarios either for Fig. 4.9a and d or b and e or c and f.

The analysis of internal concentration polarization is more complex. Its modulus, implicitly contained in eq. (9), depends on both water flux and feed concentration; it decreases as water flux decreases and increases as feed concentration increases. Results show that internal concentration polarization becomes more severe as feed concentration increases (and water flux decreases) (0 to 2.5 g/L to 5 g/L), thus, it appears that internal concentration polarization may be more dependent on feed concentration than on water flux. This can be seen by comparing the difference between the *ideal* and *K* scenarios for Fig. 4.9b and c or e and f. The effect of water flux alone on internal concentration polarization can be isolated by comparing the difference between the *ideal* and *K* scenarios between Fig. 4.9b and e or c and f. When the feed solution is constant, the increased draw solution concentration results in higher water fluxes and increased internal concentration polarization.

It has been shown that internal and external concentration polarization in PRO depend on water flux; when water flux approaches zero (i.e., the hydraulic draw solution

pressure approaches the osmotic pressure differential across the membrane), the contributions of internal and external concentration polarization to water flux reduction also approach zero and fluxes for the k and K scenarios approach that for the ideal scenario. However, the K and B and *complete* scenarios do not follow this behavior. The salt that crosses the membrane increases the salt concentration of the feed solution at the membrane surface ($C_{F,m}$), which reduces the osmotic pressure differential across the dense layer of the membrane, and therefore, reduces the pressure at which the flux reversal point occurs. Reverse salt diffusion is not flux-dependent and is solely responsible for the reduction of the flux reversal point pressure. If reverse salt diffusion could be eliminated, the flux reversal point, and hence W_{\max} , would be greater.

4.4.5 PRO experimental results

Figure 4.10 compares water flux and power density experimental results (symbols) with model results (lines). The maximum hydraulic pressure differential that could be achieved during the experiments was 970 kPa. Larger pressures caused perforation of the membrane because the spacers placed in the feed channels essentially tore the membrane. The experimental data closely follow the model results.

At a pressure of 970 kPa, the water fluxes achieved were between 1.8×10^{-6} and 2.8×10^{-6} m/s for the 35 g/L NaCl draw solution and between 3.6×10^{-6} and 5.2×10^{-6} m/s for the 60 g/L NaCl draw solution, depending on feed solution concentrations. These flux values are well above results previously reported in the literature (Table 4.6), likely due to the improved membrane and membrane module used in the current investigation. Loeb et al. [9], Loeb and Mehta [10], and Mehta and Loeb [11, 12] used hydrophobic

polymeric membranes and hollow-fiber membrane modules not particularly suited for PRO applications. The power densities achieved in the current investigation (Figure 4.10) were up to 2.7 W/m^2 for a 35 g/L NaCl (2,763 kPa) draw solution and up to 5.1 W/m^2 for a 60 g/L NaCl (4,882 kPa) draw solution. In order to compare these values with those previously reported in the literature, a normalized power density value which takes into account the draw solution concentrations and hydraulic pressures used in previous investigations, was calculated ($W/(\Delta\pi-\Delta P)$). From Table 6 (last column) it can be seen that the normalized power density values from the current investigation are well above results previously reported in the literature.

The proposed model provides guidance on how to increase power density in PRO operations. Changing operating conditions (e.g., increasing crossflow on the membrane) can marginally improve power density by decreasing the effect of external concentration polarization. Greater improvement could be achieved by modifying the membrane structure. For example, a substantial improvement in the power density output could be made by optimization of the membrane support layer to reduce the internal concentration polarization that occurs. Specifically, the power density could be increased by up to 70% by reducing internal concentration polarization (seen by comparing the *complete* scenarios with the *k* scenarios in Figure 4.10). Thus, development of new membranes with thinner, less tortuous, and more porous support layers may be a key factor in successful osmotic power development.

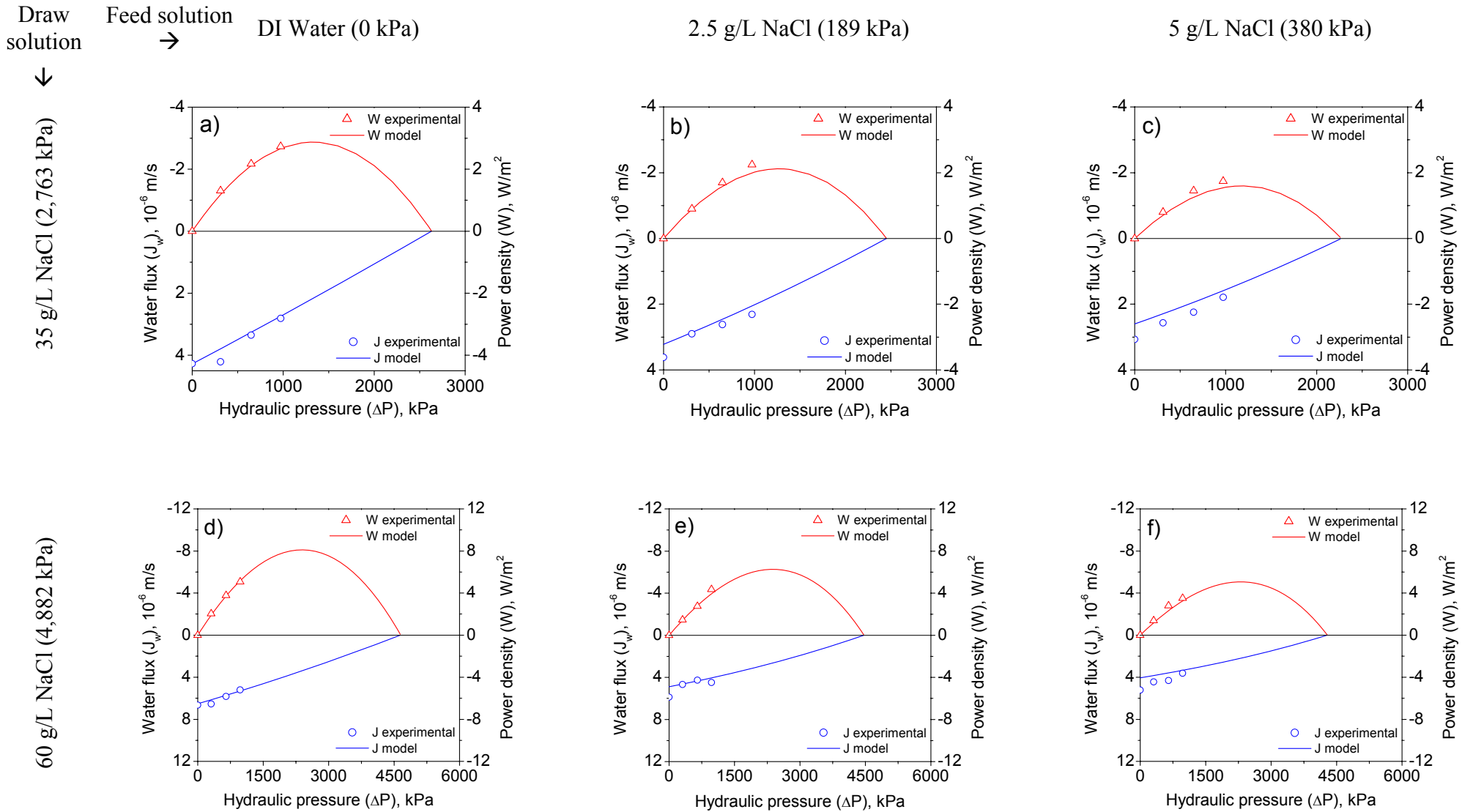


Figure 4.10 Experimental results for water flux (J_w) and power density (W) as a function of applied hydraulic pressure (ΔP) (points) compared with model results (lines) under different feed and draw solution concentrations. Temperature was 25 °C.

Table 4.6 Comparison between power density results from the literature and from the current study

Reference	$\Delta\pi$ kPa	ΔP kPa	J_w 10^{-6} m/s	W W/m ²	$W/(\Delta\pi-\Delta P)$ 10^{-3} W/m ² ×kPa
[9]	2,533	1,216	0.29	0.35	0.27
[10]	10,132	1,925	0.81	1.56	0.19
[11]	8,106	4,053	0.81	3.27	0.81
[12]	7,802	4,053	0.77	3.12	0.83
This study	2,763	972	2.81	2.73	1.52
This study	4,882	972	5.21	5.06	1.30

Furthermore, in the current study, the pressure drop along the membrane module was directly measured and found negligible due to the small size of the module itself. Practically, the pressure drop along the membrane module is a function of the flow hydraulics of the system, and when designing future PRO membrane modules pressure drop should be taken into consideration using appropriate correlations in order to minimize its magnitude.

Figure 4.11 illustrates how the maximum power density would change by varying A , k , and K . This example was constructed using 35 g/L NaCl as the draw solution, DI water as the feed solution, and a ΔP of approximately 1300 kPa. In this example, A was increased up to 10 times from the values determined earlier in this investigation to represent the typical permeability of a nanofiltration membrane. k was increased up to 2.5 times compared to the values determined earlier to represent a mass transfer coefficient with Re equal to 1000, which is the typical upper limit for spacer-filled flow channels [25, 27]. K was reduced up to a tenth of the value determined earlier to simulate a very thin membrane support layer with low tortuosity and high porosity. These values are

extreme and not achievable with current membrane technologies but are used to demonstrate the relative contribution of the three parameters to power density.

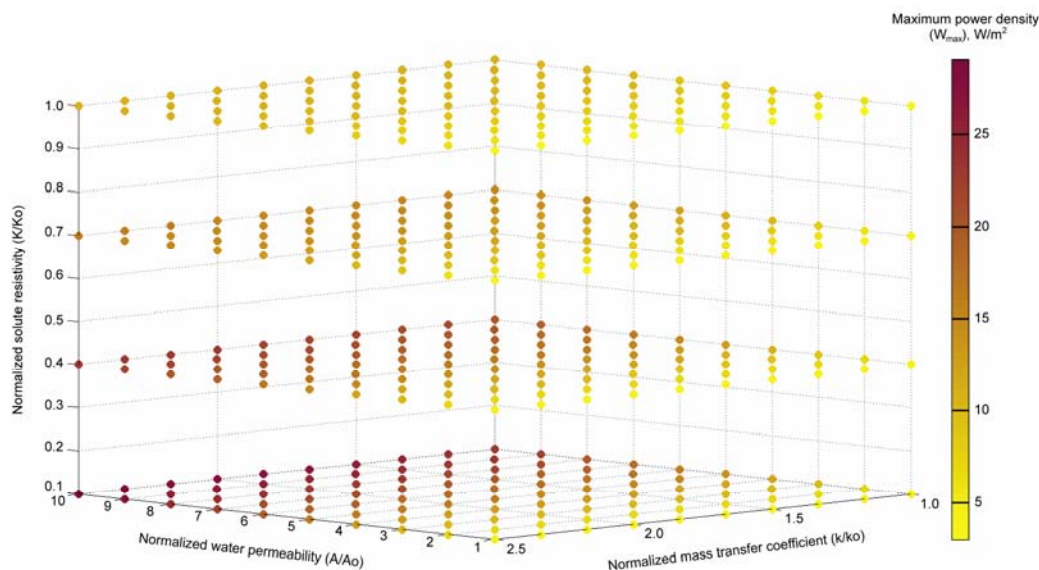


Figure 4.11 Model results for maximum power density (W_{\max}) as a function of water permeability (A), mass transfer coefficient (k), and solute resistivity (K). Results illustrates W_{\max} achievable with DI water feed solution and 35 g/L NaCl draw solution concentration at a hydraulic pressure of 1300 kPa.

Results show that combining the improvements of all three parameters could lead to a power density of over 28 W/m^2 ; this is a ten-fold increase from the earlier experimental PRO results shown in this study. The results also show that A is the parameter that influences W_{\max} the most, closely followed by K . The influence of both K and k on W_{\max} are greater when A is high, due to their dependency on J_w , as explained in the model results section.

4.5 Conclusions

In this investigation, for the first time, experimental PRO results were compared with model predictions. The PRO model was developed to predict water flux and power density under specific experimental conditions. PRO experiments were performed using a bench-scale PRO system utilizing a custom-made cross-flow membrane module. Data collected from the PRO experiments closely matched model predictions. At 970 kPa hydraulic pressure on the draw solution side, the power densities achieved were up to 2.8 W/m² for the 35 g/L NaCl draw solution and up to 5.1 W/m² for the 60 g/L NaCl draw solution. For the asymmetric membrane employed, the power density was substantially reduced due to severe internal concentration polarization and, to a lesser degree, to reverse salt diffusion. External concentration polarization was found to exhibit a relatively small effect on reducing the osmotic driving force.

Using the predictive model, the PRO process can be improved by optimizing operating conditions and system configuration to achieve maximum power density. Output from the model can assist in determining membrane characteristics needed to design and craft new-generation PRO membranes.

Acknowledgments

The authors acknowledge the support of the Department of Energy, Grant No. DE-FG02-05ER64143 and Hydration Technology Innovations (Albany, OR) for donating the FO membrane.

Nomenclature

ΔP	Hydraulic pressure differential (kPa)
$\Delta \pi$	Osmotic pressure differential (kPa)
ε	Porosity
$\pi_{D,b}$	Osmotic pressure of the bulk draw solution (kPa)
$\pi_{D,m}$	Osmotic pressure of the draw solution at the membrane surface (kPa)
$\pi_{F,b}$	Osmotic pressure of the bulk feed solution (kPa)
$\pi_{F,m}$	Osmotic pressure of the feed solution at the membrane surface (kPa)
τ	Tortuosity
A	Water permeability coefficient ((m/s)/kPa)
B	Salt permeability coefficient (m/s)
$C_{D,b}$	Salt concentration of the bulk draw solution (g/L)
$C_{D,m}$	Salt concentration of the draw solution at the membrane surface (g/L)
$C_{F,b}$	Salt concentration of the bulk feed solution (g/L)
$C_{F,m}$	Salt concentration of the feed solution at the membrane surface (g/L)
C_F	Salt concentration in the feed solution (g/L)
C_P	Salt concentration in the permeate solution (g/L)
D	Salt diffusion coefficient (m ² /s)
d_h	Hydraulic diameter (m)
J_w	Water flux (m/s)
k	External concentration polarization mass transfer coefficient (m/s)
K	Internal concentration polarization mass transfer coefficient (s/m)
L	Length of channel (m)

<i>R</i>	Salt rejection
<i>Re</i>	Reynolds number
<i>Sc</i>	Schmidt number
<i>Sh</i>	Sherwood number
<i>t</i>	Thickness (m)
<i>W</i>	Power density (W/m ²)

References

- [1] S. Loeb and R.S. Norman, Osmotic power plants, *Science*, 189 (1975) 654-655.
- [2] S. Loeb, Production of energy from concentrated brines by pressure-retarded osmosis, I. Preliminary technical and economic correlations, *Journal of Membrane Science*, 1 (1976) 49-63.
- [3] S. Loeb, Large-scale power production by pressure-retarded osmosis, using river water and sea water passing through spiral modules, *Desalination*, 143 (2002) 115-122.
- [4] R.J. Aaberg, Osmotic Power. A new and powerful renewable energy source?, *Refocus*, 4 (2003) 48-50.
- [5] The Energy Information Administration, <http://www.eia.doe.gov/>
- [6] R.E. Pattle, Production of electric power by mixing fresh and salt water in the hydroelectric pile, *Nature*, 174 (1954) 660.
- [7] R.S. Norman, Water salination: a source of energy, *Science*, 186 (1974) 350-352.
- [8] O. Levenspiel and N. de Nevers, The osmotic pump, *Science*, 183 (1974) 157-160.
- [9] S. Loeb, F. Van Hessen and D. Shahaf, Production of energy from concentrated brines by pressure-retarded osmosis, II. Experimental results and projected energy costs, *Journal of Membrane Science*, 1 (1976) 249-269.
- [10] S. Loeb and G.D Mehta, A Two coefficient water transport equation for pressure-retarded osmosis, *Journal of Membrane Science*, 4 (1979) 351-362.

- [11] G.D Mehta and S. Loeb, Performance of permasep B-9 and B-10 membranes in various osmotic regions and at high osmotic pressures, *Journal of Membrane Science*, 4 (1979) 335-349.
- [12] G.D. Mehta and S. Loeb, Internal polarization in the porous substructure of a semipermeable membrane under pressure-retarded osmosis, *Journal of Membrane Science*, 4 (1978) 261-265.
- [13] H.H. Jellinek and H. Masuda, Osmo-power. Theory and performance of an osmo-power pilot plant, *Ocean Engineering*, 8 (1981) 103-128.
- [14] J.R. McCutcheon and M. Elimelech, Influence of membrane support layer hydrophobicity on water flux in osmotically driven membrane processes, *Journal of Membrane Science*, 318 (2008) 458-466.
- [15] J.R. McCutcheon and M. Elimelech, Influence of concentrative and dilutive internal concentration polarization on flux behavior in forward osmosis, *Journal of Membrane Science*, 284 (2006) 237-247.
- [16] K. Gerstandt, K.-V. Peinemann, S.E. Skilhagen, T. Thorsen and T. Holt, Membrane processes in energy supply for an osmotic power plant, *Desalination*, 224 (2008) 64-70.
- [17] K.L. Lee, R.W. Baker and H.K. Lonsdale, Membrane for power generation by pressure retarded osmosis, *Journal of Membrane Science*, 8 (1981) 141-171.
- [18] J.R. McCutcheon, R.L. McGinnis and M. Elimelech, Desalination by ammonia-carbon dioxide forward osmosis: Influence of draw and feed solution concentrations on process performance, *Journal of Membrane Science*, 278 (2006) 114-123.
- [19] M. Elimelech and S. Bhattacharjee, A novel approach for modeling concentration polarization in crossflow membrane filtration based on the equivalence of osmotic pressure model and filtration theory, *Journal of Membrane Science*, 145 (1998) 223-241.
- [20] S.S. Sablani, M.F.A. Goosen, R. Al-Belushi and M. Wilf, Concentration polarization in ultrafiltration and reverse osmosis: a critical review, *Desalination*, 141 (2001) 269-289.
- [21] A. Achilli, T.Y. Cath, E.A. Marchand and A.E. Childress, The forward osmosis membrane bioreactor: A low fouling alternative to MBR processes, *Desalination*, 239 (2009) 10-21.

- [22] T.Y. Cath, A.E. Childress and M. Elimelech, Forward osmosis: Principles, applications, and recent developments, *Journal of Membrane Science*, 281 (2006) 70-87.
- [23] S. Loeb, L. Titelman, E. Korngold and J. Freiman, Effect of porous support fabric on osmosis through a Loeb-Sourirajan type asymmetric membrane, *Journal of Membrane Science*, 129 (1997)
- [24] V. Gekas and B. Hallstrom, Mass transfer in the membrane concentration polarization layer under turbulent cross flow. I. Critical literature review and adaptation of existing Sherwood correlations to membrane operations, *Journal of Membrane Science*, 30 (1987) 153-170.
- [25] G. Schock and A. Miguel, Mass transfer and pressure loss in spiral wound modules, *Desalination*, 64 (1987) 339-352.
- [26] C.P. Koutsou, S.G. Yiantsios and A.J. Karabelas, Direct numerical simulation of flow in spacer-filled channels: Effect of spacer geometrical characteristics, *Journal of Membrane Science*, 291 (2007) 53-69.
- [27] C.P. Koutsou, S.G. Yiantsios and A.J. Karabelas, A numerical and experimental study of mass transfer in spacer-filled channels: Effects of spacer geometrical characteristics and Schmidt number, *Journal of Membrane Science*, 326 (2009) 234-251.
- [28] R.W. Holloway, A.E. Childress, K. E. Dennett and T.Y. Cath, Forward osmosis for concentration of anaerobic digester centrate, *Water Research*, 41 (2007) 4005-4014.
- [29] R.H. Stokes, The diffusion coefficients of eight uni-equivalent electrolytes in aqueous solution at 25°, *Journal of the American Chemical Society*, 72 (1950) 2243-2247.
- [30] R. Mills, The effect of the ionization of water on diffusional behavior in dilute aqueous electrolytes, *Journal of Physical Chemistry*, 66 (1962) 2716-2718.
- [31] T.Y. Cath, S. Gormly, E.G. Beaudry, M.T. Flynn, V.D. Adams and A.E. Childress, Membrane contactor processes for wastewater reclamation in space. I. Direct osmotic concentration as pretreatment for reverse osmosis, *Journal of Membrane Science*, 257 (2005) 85-98.
- [32] G.T. Gray, J.R. McCutcheon and M. Elimelech, Internal concentration polarization in forward osmosis: role of membrane orientation, *Desalination*, 197 (2006) 1-8.

- [33] C. Fritzmann, J. Lowenberg, T. Wintgens and T. Melin, State-of-the-art of reverse osmosis desalination, *Desalination*, 216 (2007) 1-76.

Chapter 5

5 CONCLUSIONS

5.1 Research Synopsis

This dissertation represents several investigations into the evaluation of osmotically-driven membrane processes for water reuse and energy production. These investigations include: 1) the evaluation of combining biological processes and FO in a single integrated process (the OMBR), 2) the evaluation of several inorganic-based draw solutions for FO applications, and 3) the evaluation of PRO to produce renewable energy.

5.2 Summary of evaluation of OMBR

A novel submerged OMBR system was presented. The system utilizes an FO membrane module inside a bioreactor. Through osmosis, water is transported from the mixed liquor across a semi-permeable membrane, and into a draw solution with a higher osmotic pressure. To produce potable water, the diluted draw solution is treated in an RO unit; the byproduct is a reconcentrated draw solution for reuse in the FO process. Results from experiments conducted with a flat-sheet cellulose triacetate FO membrane demonstrated high sustainable flux and relatively low reverse diffusion of solutes from the draw solution into the mixed liquor. Long-term water fluxes for experiments with activated sludge operated at a solids concentration of 5.5 g MLSS/L were only 18% lower than water fluxes for experiments using DI water. Most of the reduction in water flux was due to membrane fouling; only a small part was due to increased salt concentration inside the bioreactor resulting from reverse salt diffusion.

Osmotic backwashing was conducted once per week to restore water flux to approximately 90% of the initial water flux. Compared to a conventional MBR, this system required substantially less backwashing. OMBR process removal efficiencies for TOC and NH_4^+ -N were greater than 99% and 98%, respectively, suggesting a better compatibility of the OMBR with downstream RO systems than conventional MBRs.

5.3 Summary of evaluation of inorganic-based draw solutions for forward osmosis applications

More than 500 inorganic compounds were screened by taking into consideration water solubility, phase, hazard, osmotic pressure, and cost. The screening process revealed 14 draw solutions suitable for FO applications. The selected draw solutions were then investigated experimentally under FO conditions and theoretically under RO reconcentration conditions. FO experiments were performed to quantify the water flux and reverse salt diffusion. RO modeling was performed to evaluate RO reconcentration of the draw solution and permeate water quality. The replenishment cost of the draw solution due to reverse salt diffusion through the FO membrane and solute passage through the RO membrane was also calculated. The large draw solution matrix in terms of both constituents and concentrations enabled insight into the role of membrane characteristics and solution characteristics on water flux and reverse salt diffusion. Internal concentration polarization influences water flux and was found to be strongly dependent on the diffusion coefficient of the draw solution. Also, internal concentration polarization influences the rate of reverse salt diffusion by lowering the draw solute concentration at the interface between the support and the dense layer of the membrane.

The most suitable draw solution depends on the specific FO application and membrane used; however, a small group of draw solutes (CaCl_2 , KHCO_3 , MgCl_2 , MgSO_4 , NaCl , NaHCO_3 , and Na_2SO_4) appeared to be the most suitable to be employed in FO processes with currently available FO membranes. From the literature, the most widely employed draw solutions are CaCl_2 , $\text{Ca}(\text{NO}_3)_2$, NaCl , and a proprietary draw solution based on ammonium and carbon dioxide, similar to NH_4HCO_3 . From this investigation it is apparent that a broader range of draw solutes should be considered for future FO applications.

5.4 Summary of evaluation of pressure retarded osmosis to produce renewable energy

PRO was investigated as a viable source of renewable energy. In PRO, water from a low salinity feed solution permeates through a membrane into a pressurized, high salinity draw solution; power is obtained by depressurizing the permeate through a hydroturbine. In this investigation, for the first time, experimental PRO results were compared with model predictions. The PRO model was developed to predict water flux and power density under specific experimental conditions. The model relies on experimental determination of the membrane water permeability coefficient, the membrane salt permeability coefficient, and the solute resistivity. Membrane water permeability coefficient and salt permeability coefficient were determined under RO conditions, while the solute resistivity was determined under FO conditions. Previous investigations of PRO were unable to verify model predictions due to the lack of suitable membranes and membrane modules. In this investigation, the use of a custom-made

laboratory-scale membrane module enabled the collection of experimental PRO data. Results obtained with a flat-sheet asymmetric cellulose triacetate FO membrane and NaCl feed and draw solutions closely matched model predictions. At 970 kPa hydraulic pressure on the draw solution side, the power densities achieved were up to 2.8 W/m² for the 35 g/L NaCl draw solution and up to 5.1 W/m² for the 60 g/L NaCl draw solution, depending on feed concentrations. For the asymmetric membrane employed, the power density was substantially reduced due to severe internal concentration polarization and, to a lesser degree, to reverse salt diffusion. External concentration polarization was found to exhibit a relatively small effect on reducing the osmotic driving force. Using the predictive model, the PRO process can be improved by optimizing operating conditions and system configuration to achieve maximum power density. Output from the model can assist in determining membrane characteristics needed to design and craft new-generation PRO membranes.

5.5 Environmental significance

Innovative applications of osmotically-driven membrane processes were evaluated in this dissertation. The novel OMBR system for water reuse was presented. This system combines biological treatment and membrane separation, and represents a high-quality, multiple-barrier treatment for wastewater reuse. The FO membrane provides high rejection of the solute contaminants in the wastewater stream. The diluted draw solution is sent to a RO process which reconcentrates the draw solution and provides a high-quality product water. In certain coastal situations, seawater or concentrated brine from a desalination facility could be employed as the draw solution

(Figure 5.1). In this open-loop configuration, the diluted seawater or brine would be mixed with treated wastewater and discharged to the ocean. This process would likely be a cost effective treatment in areas where reuse is not a key concern but high-quality coastal water is desired.

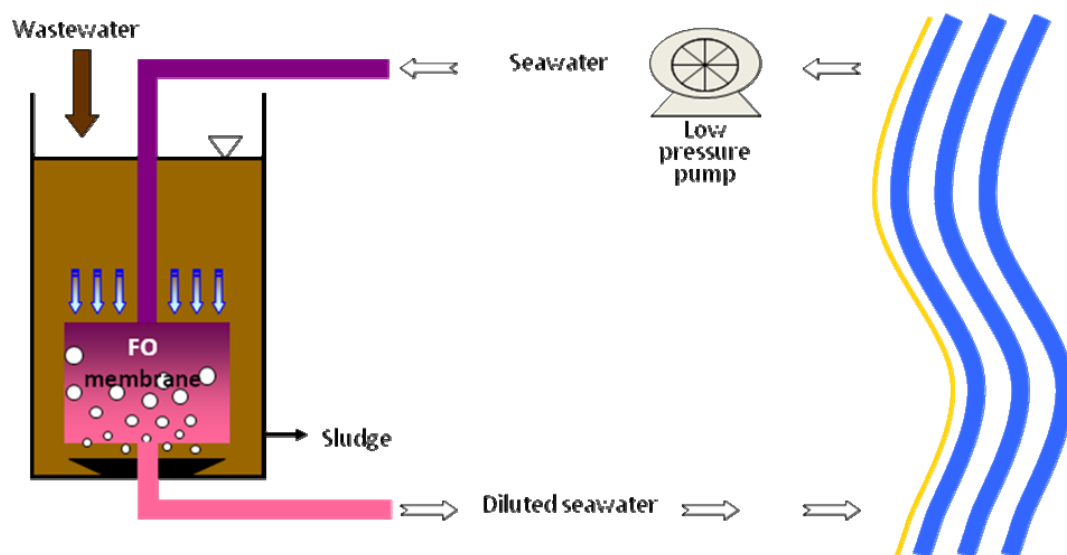


Figure 5.1 Schematic diagram of an open-loop OMBR system.

Another application of osmotically-driven membrane processes is PRO. In a PRO system, water from a low salinity feed solution (e.g., fresh water) permeates through a membrane into a pressurized, high salinity brine/draw solution (e.g., seawater); power is obtained by depressurizing a portion of the diluted seawater through a hydro turbine. The source of feed water can be a fresh water stream, or impaired water. In the case of impaired water, the PRO process could be combined with the OMBR (Figure 5.2) to achieve energy recovery and water treatment at the same time, this process could be referred to as the pressure retarded OMBR (ProMBR).

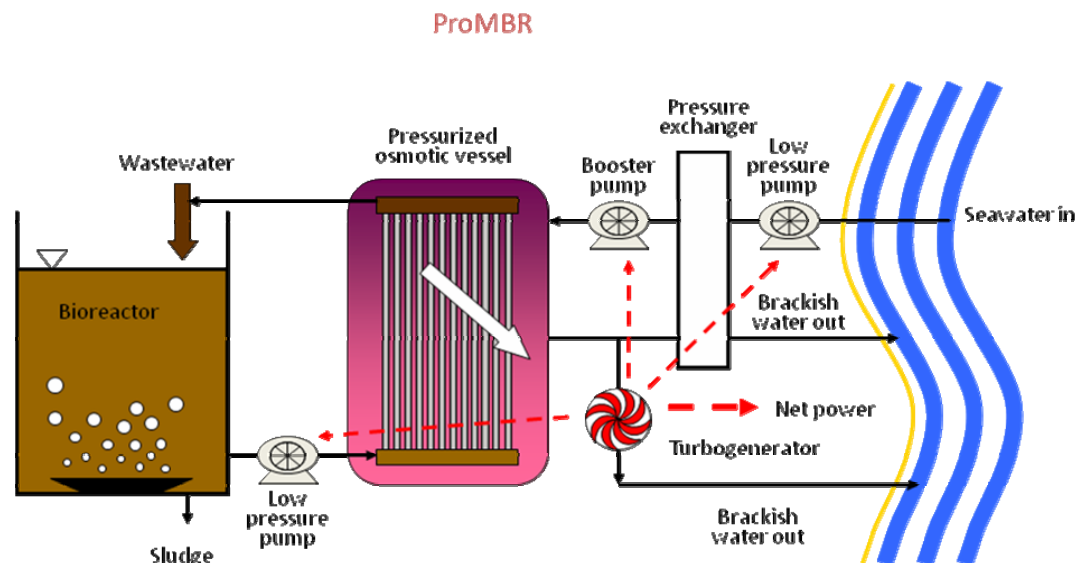


Figure 5.2 Schematic diagram of a ProMBR system.

Preliminary experimental results for the ProMBR process are illustrated in Figure 5.3. Experiments were performed with 35 g NaCl/L draw solution concentration and with activated sludge at a concentration of 5.5 g MLSS/L feed solution. The maximum power density obtained was 2.3 W/m² at a hydraulic pressure of 970 kPa, about 17% less than experimental results obtained with DI water feed solution (Table 4.6). The power density reduction is due to the lower water flux recorded in the activated sludge experiments (Figure 5.4). As expected, water flux decreases as hydraulic pressure increases due to the lower driving force across the membrane. Water fluxes achieved with activated sludge feed solution are lower than those achieved with DI water feed solution. This is also the case when there is not hydraulic pressure in the draw solution, likely due to reduced driving force (i.e., solutes contained in activated sludge) and membrane fouling. During the limited duration of the experiments (18 h), however, water flux was relatively

constant over time, suggesting that fouling could be reasonably small during ProMBR operation.

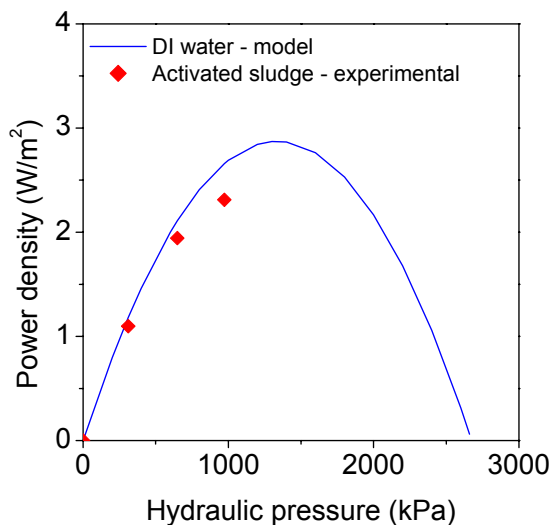


Figure 5.3 Experimental results for power density as a function of applied hydraulic pressure with activated sludge feed solution (points) compared with model results (line) with DI water feed solution. Draw solution concentration was 35 g/L NaCl. Activated sludge feed concentration was 5.5 g MLSS/L. Temperature was 25 °C.

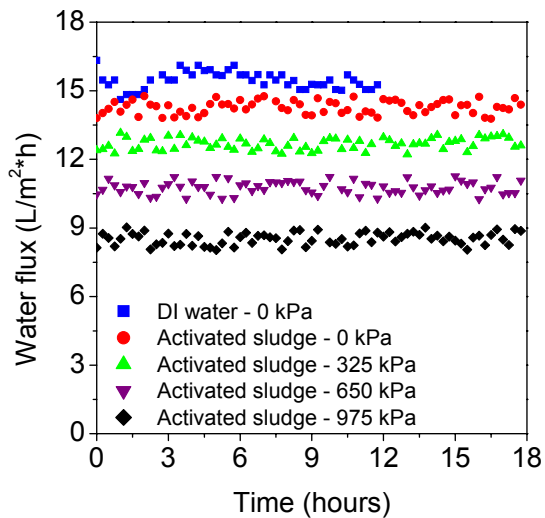


Figure 5.4 Experimental results for water flux as a function of time. Draw solution concentration was 35 g/L NaCl. Activated sludge feed concentration was 5.5 g MLSS/L. Temperature was 25 °C.

In certain situations, when there is also a need for fresh water through seawater desalination, an integrated RO/ProMBR system could be employed. In the RO/ProMBR system (Figure 5.5) the concentrated brine stream of the RO process is used as the draw solution. This is advantageous because concentrated RO brines typically have double the osmotic pressure of seawater and would enable the ProMBR process to work at higher hydraulic pressure and higher water flux. Higher fluxes translate to increased power production and decreased membrane requirements.

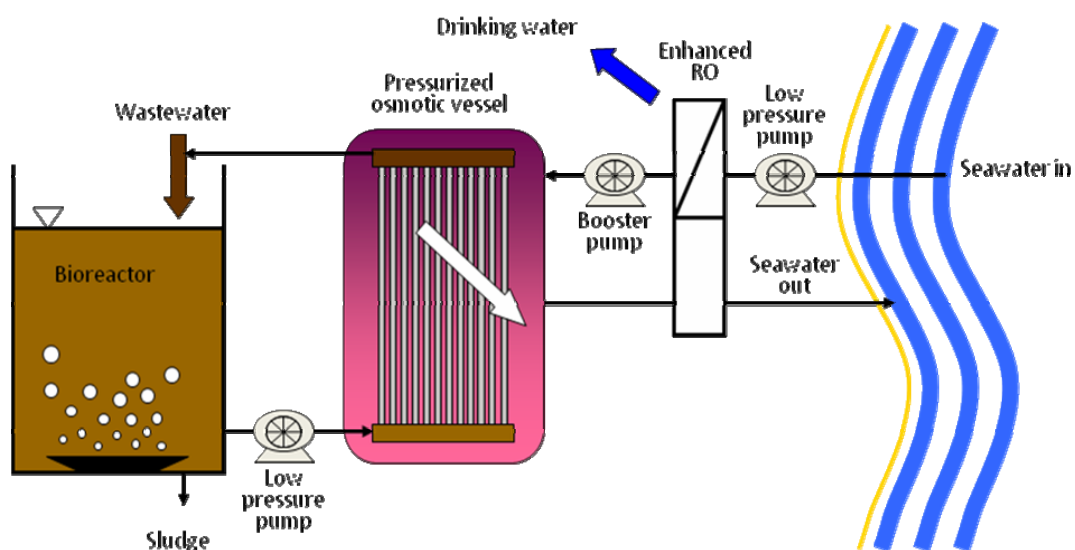


Figure 5.5 Schematic diagram of an RO/ProMBR system.

These novel hybrid systems can be tailored to the specific water demands and energy availability of individual locations. They offer improvements to centralized

systems and insight into the development of decentralized systems. They represent substantial progress towards greater water and energy sustainability.